Advanced Engineering Research

Theoretical and scientific-partical journal

Vol. 20
no. 4
2020

ISSN 2687-1653

1. Mechanics
2. Machine Building and Machine Science
3. Information Technology, Computer Science, and Management

DOI 10.23947/2687-1653

vestnik-donstu.ru

Advanced Engineering Research

Vol. 20, no. 4

Theoretical and scientific-practical journal

Published since 1999

4 issues a year
October-December 2020

ISSN 2687-1653
DOI: 10.23947/2687-1653

Founder and publisher – Federal State Budgetary Educational Institution of Higher Education Don State Technical University (DSTU)

The journal was known as Vestnik of Don State Technical University (until August 2020)

Included in the list of peer-reviewed scientific editions where the basic research results of doctoral, candidate's theses should be published (State Commission for Academic Degrees and Titles List) in the following research areas:

01.02.01 – Analytical Mechanics (Engineering Sciences)
01.02.04 – Deformable Solid Mechanics (Engineering Sciences)
01.02.04 – Deformable Solid Mechanics (Physicomathematical Sciences)
01.02.06 – Dynamics, Strength of Machines, Gear, and Equipment (Engineering Sciences)
05.02.02 – Engineering Science, Drive Systems and Machine Parts (Engineering Sciences)
05.02.04 – Machine Friction and Wrear (Engineering Sciences)
05.02.07 – Technology and Equipment of Mechanical and Physicotechnical Processing (Engineering Sciences)
05.02.08 – Engineering Technology (Engineering Sciences)
05.02.10 – Welding, Allied Processes and Technologies (Engineering Sciences)
05.02.11 – Testing Methods and Diagnosis in Machine Building (Engineering Sciences)
05.13.11 – Software and Mathematical Support of Machines, Complexes and Computer Networks (Engineering Sciences)
05.13.17 – Foundations of Information Science (Engineering Sciences)
05.13.18 – Mathematical Simulation, Numerical Methods and Program Systems (Engineering Sciences)

The journal is indexed and archived in the Russian Science Citation Index (RSCI), and in EBSCO International Database

The journal is a member of Directory of Open Access Journals (DOAJ), Association of Science Editors and Publishers (ASEP) and Cross Ref

Certificate of mass media registration ЭЛ № ФС 77 – 78854 of 07.08.2020 is issued by the Federal Service for Supervision of Communications, Information Technology, and Mass Media

The issue is prepared by:

Inna V. Boyko, Gennady I. Rassokhin, Marina P. Smirnova (English version)

Founder's, Publisher's and Printery Address:

Gagarin Sq. 1, Rostov-on-Don, 344003, Russia. Phone: +7 (863) 2-738-372

E-mail: vestnik@donstu.ru http://vestnik-donstu.ru/

CONTENTS

MECHANICS

UDC 539.3 https://doi.org/10.23947/2687-1653-2020-20-4-350-359

Mechanical and finite element models of corneal keratoprostheses

A. N. Soloviev[1], N. I. Glushko[1], A. N. Epikhin[2], M. Swain[3], O. N. Lesnyak[1], A. E. Ivanov[1]
[1] Don State Technical University (Rostov-on-Don, Russian Federation)
[2] Rostov State Medical University (Rostov-on-Don, Russian Federation)
[3] Sydney University (Sydney, Australia)

Introduction. When developing ocular prostheses, a number of problems arise, one of which is the construction of the connection between the hard optical part and the soft corneal tissue. Their Young's modules can differ by three orders of magnitude. In this case, the problem arises of creating an intermediate layer, possibly with gradient properties, whose purpose is to exclude injury to soft biological tissues. Two types of keratoprostheses are considered: the first type with a support plate and the second type with an intermediate functionally gradient layer. The stress-strain state of the prosthesis is calculated for the first type. For the second type, analytical and finite element modeling of the interaction of a cylindrical optical prosthesis, an intermediate inhomogeneous layer, and the cornea was carried out in the elastic media. Two versions are considered: discounting the curvature (circular plate or plate) and with account of the curvature (spherical dome or shell). The work objective is to study the stress-strain state of the keraprosthesis and cornea in the contact area.
Materials and Methods. Mathematical models of the structures under consideration are the boundary value problems of the linear elasticity theory. The analytical solution is constructed for a simplified model in the form of a composite circular plate. Spatial three-dimensional problems and axisymmetric problems are solved by the finite element method. Finite element modeling of the considered structures was performed in the CAE package ANSYS and ACELAN.
Results. CAD models of keratoprostheses with conditions of fixing and loading are constructed. The load acting on the keraprosthesis under the effect of intraocular pressure was determined. The stress-strain state of the keratoprosthesis and cornea elements was calculated. Special attention was paid to the area of its contact with the keratoprosthesis.
Discussion and Conclusions. The results of calculating the axial displacements and mechanical stresses in the first type of keratoprosthesis show that the selected geometric parameters meet the kinematic and strength requirements. The proposed models of the deformed state of soft biological tissues provide assessing their injury when using a keratoprosthesis of the second type, as well as selecting the geometric parameters and gradient properties of the intermediate layer.

***Keywords**:* ocular prosthesis, inhomogeneous elastic properties, plate, shell, finite element method.

For citation: A. N. Soloviev, N. I. Glushko, A. N. Epikhin, et al. Mechanical and finite element models of corneal keratoprostheses. Advanced Engineering Research, 2020, vol.20, no. 4, pp. 350–359. https://doi.org/10.23947/2687-1653-2020-20-4-350-359

Funding information: the research is supported by the Government of the Russian Federation (grant no. 14.Z50.31.0046).

Introduction. A keratoprosthesis (KPro) is a cell-free artificial implant designed so that a cylindrical frame holds the optics. Keratoprosthesis replaces the removed part of the cornea. Previously, corneal transplants had high rates of infection and rejection. In the late 1980s, the “core-skirt” design (a bio-integrated “skirt” surrounds the optics) was the most widespread one. Not only the sizes, but also the location of the pores in the porous skirt were important. Keratoprostheses, such as AlphaCor (formerly known as Chirila), were polymethylmethacrylate devices with a central optical region fused to the surrounding porous skirt.

Modern keratoprostheses consist of an optical element and a supporting plate. The optical transparent element has the shape of a cylinder or lens. The supporting plate connected to the optical element can have various shapes: a ring with holes, a spoked wheel, ears, or amoeboid legs. The book by S. N. Fedorov [1] describes various types and

forms of keratoprostheses and fasteners. The main complication after keratoprosthetics is aseptic necrosis of the cornea which develops in front of the supporting attachment of the implant. This complication often causes rejection of the keratoprosthesis [1]. The major cause of aseptic necrosis is blocking the flow of vital substances into the layers of the cornea, which are located above the keratoprosthesis support. In this regard, for the manufacture of the supporting plate, it is required to use a biocompatible material that will allow corneal tissues to grow through the supporting mount.

American researchers have described a microporous support plate[1] for keratoprosthesis made of stretched polytetrafluoroethylene (PTFE). Its structure has a configuration in the form of polymer nodes, which are connected by fibrils 7-8 μm long. Too small pores prevent the corneal tissue from ingrowth. Therefore, it is required to additionally penetrate the prosthesis with pores perpendicular to the surfaces of the supporting plate with a diameter of 20-150 μm (preferably 50 μm). The thickness of the supporting plate should be about 0.2 μm, but not more than 0.3 μm.

In the model with a ring-shaped[2] supporting attachment, the optical element is made of a transparent substance such as polymethylmethacrylate (PMMA), the attachment is made of a hydrophilic porous material with fibrous structure through which corneal tissue can ingrow. A supporting plate with a thickness of 0.15–0.30 μm is formed from this fiber. A ring with an external diameter of about 9.5 mm is placed on the optical element. Its front part is cylindrical, the back has a conoid, whose larger section is directed inward. The supporting plate has elastic characteristics required to prevent rejection of the keratoprosthesis and necrosis due to the pressure of the surrounding eye tissues.

In another design[3], the supporting plate consists of two parallel shells spaced 0.4–0.7 μm apart. The optimal distance is 0.3±0.02 mm. Conical shells are attached to a cylindrical optical element. The material of the supporting plates should be bio-populated; therefore, it is assumed that its porosity is 50% or higher, the pores should be open, and their diameter is about 20–100 μm.

Elements of the keratoprosthesis[4] proposed by Russian scientists (Fig. 1) are as follows:

— supporting plate — 1 (radius of curvature is 7–10 mm, external diameter is 7–12 mm);

— optical part — 2 (optical element in the form of a cylinder with rounded ends that serve to select diopters);

— cylindrical surface of the optical threaded element — 3;

— connecting washer — 4 (rigidly attached to the supporting plate).

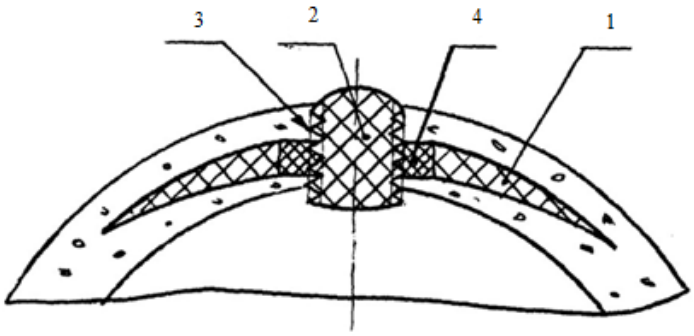

Fig. 1. Scheme of keratoprosthesis

The keratoprosthesis is implanted in the intralamellar corneal pocket. The supporting plate is located inside the cornea, and the optical element penetrates the entire cornea.

The implant for strengthening the cornea[5] is a plate — round, oval, in the form of a shamrock, chamomile, or convex-concave lens with a curve radius of 7–10 mm. There may be a cylindrical hole in the center of the lens. In the structure of the implant material, the volume void rating is 15–40 %, their specific surface area is 0.25–0.55 $mm^2/\mu m^3$, the average distance between voids is 25–50 μm, and the mean volume chord is 8–25 μm. The implant is a convex-concave lens whose curve radius corresponds to the curve radius of the patient's cornea. In the central part, the implant thickness is 0.3–0.7 mm, and it is 0.01 mm at the edges.

In another modification of the keratoprosthesis[6], in contrast to the one described above, the supporting block is made of porous titanium nickelide, the curvature of the plate coincides with the curvature of the cornea. The supporting plate is installed on the surface of the cornea and is retentively fixed with a sclera allograft. The cylindrical optical element is connected to the supporting plate by a tight fit method. This approach enables to treat leukomata more effective-

[1] US Patent no. 5713956, M. cl. 7 A 61 F 2/14, 1998.
[2] US Patent no. 5489301, M. cl. 6 A 61 F 2/14, 1996.
[3] US Patent no. 6106552, M. cl. 7 A 61 F 2/14, 2000.
[4] Keratoprosthesis. RF Patent no. 2270643, 2006. (In Russ.)
[5] Implant to strengthen the cornea. RF Patent no. 2270642, 2006. (In Russ.)
[6] Keratoprosthesis and method of surgical treatment with its help. RF Patent no. 2367379, 2009. (In Russ.)

ly, thanks to the rapid and successful integration of the porous implant (base) with the surrounding tissues and mechanically strong fixation of the optical element, which reduces the risk of keratoprosthesis reposition.

The developer of the combined keratoprosthesis[1] notes that the supporting part of the implant should maximally resist pushing pressure of the intraocular fluid on the optical part of the keratoprosthesis and minimally deform the appropriate tissues. The material of the supporting part should not only be biocompatible, but also structured so as to provide the fusion of the above and below layers of the cornea, which are separated during the implantation of the keratoprosthesis. Keratoprostheses with an optical element made of a transparent substance (for example, PMMA) and a supporting plate in the form of a ring made of hydrophilic porous material PTFE or polyethylene[2] were fore-mentioned. Their use provides fusion of the above and underneath layers of the cornea due to the high porosity of the material (from 50 %) and the pore diameter up to 100 μm. The main disadvantages of such structures are excessive flexibility and low mechanical strength. These characteristics do not provide reliable retention and fixation of the installed keratoprosthesis with large optics for a long time.

The optical part of the combined keratoprosthesis is made of a transparent elastic polymer saturated with UV adsorbent. In shape, it is a removable bolt with a diameter of 5–6 mm. The front end is fungiform, while the others are spherical (aspherical). The haptic part is a supporting disk with an outer diameter of 8–12 mm and a thickness of 0.3–0.9 mm. Its side surface is threaded. For this part, a porous (perforated) solid (elastic) areactive polymer (metal) with a volume void rating of no more than 50 % is used. The front part of the haptic is made of biological materials, the back part is made of artificial biocompatible materials. The supporting disk of the back part is flat and connects perpendicularly to the supporting hollow cylinder located in the center. The connection is provided by a groove and / or flange on the outer rear of the cylinder. The profile and diameter of the internal thread of the cylinder correspond to the thread of the optical bolt. The support disk can pass into a sleeve that wraps around the supporting cylinder from the outside. The supporting plate is connected at the front with a round biodisc, which is cut out of freshly removed or preserved sterile biological materials. They are multi-layered combinations of biological tissues. Before joining, parts of the keratoprosthesis are sterilized. The connection is carried out under sterile conditions. Assembly is performed immediately before prosthetics or in advance (in this case, the implant is stored until the surgery). The external diameter of the biodisc should be greater than the external diameter of the supporting disk by 0.3–1 mm. In the center of the biodisc, a coaxial bore is made with a diameter corresponding to the outer diameter of the cover sleeve or the supporting cylinder.

For penetrating keratoplasty, models are developed using various materials, structures, and surgical methods [2]. However, the problem is not completely resolved. This is confirmed by cases of corneal blindness in patients with repeated graft failure or severe damage to the eye surface [3–6]. The issues of keratoprosthetics in diseases of the cornea and ocular surface are considered in [7]. Review on the application of Boston KPro is presented in [8]. In [9], complications with wide consequences in the use of keratoprostheses are discussed.

In this paper, we consider two types of keratoprostheses with a cylindrical optical element. The diagram of the first type is shown in Fig. 1. In the second type, there is some intermediate layer with non-uniform mechanical properties on the cylindrical surface. Fig. 2 shows a diagram of the half-axial section of the second-type KPro disregarding the curvature (a) and with account for the cornea curve (b). The layer with functionally gradient properties is greyed out. It is needed for non-traumatic contact of the optics with the soft tissue of the cornea.

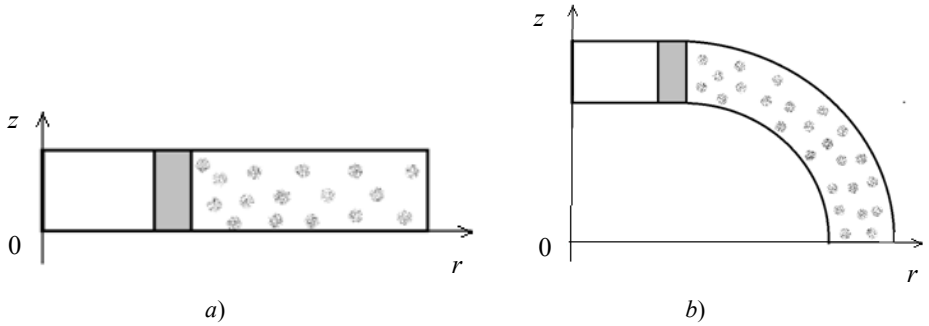

a) *b*)

Fig. 2. KPro half axial section: plate model (a), dome model (b)

Analytical and numerical models of keratoprosthesis implantation in the cornea are constructed using the finite element method. The stress-strain state of the cornea in the contact area is studied. This defines the objectives of this work. For the first-type KPro, they include investigations on its stress-strain state under the action of intraocular pressure, assuming that the outer edge of the supporting plate is fixed. The objectives for the second-type KPro are to study

[1] Combined keratoprosthesis. RF Patent no. 2707646, 2019. (In Russ.)
[2] US Patents no.5489301, no. 6106552.

the stress-strain state of the cornea in the vicinity of the contact with the keratoprosthesis, whose outer layer is a structure that reduces soft tissue injury. This intermediate (interface) layer is modeled as a hollow cylinder with functionally gradient mechanical properties.

Three models are considered in the paper.

I. Analytical — for an implanted prosthesis based on the bending of a composite circular plate.

II. Finite element — for an implanted prosthesis based on a composite circular plate.

III. Finite element model — for an implanted prosthesis based on a composite spherical dome.

Modeling problems are solved for:

— keratoprosthesis of the first type (A),

— keratoprosthesis of the second type (B).

Materials and Methods. The continual formulation of the tasks. The general mathematical formulation of the problem under study (for problems A and B) is a static boundary value problem of elasticity theory for a composite isotropic body.

For the unknown $\vec{u} = (u_1, u_2, u_3)$ of the displacement vector component, the system of differential equations has the form [10]:

$$\sigma_{ij,j} = 0\,,\ \varepsilon_{kl} = \frac{1}{2}(u_{k,l} + u_{l,k})\,, \tag{1}$$

where σ_{ij}, c_{ijkl}, ε_{kl} are components of stress tensors, elastic constants, and deformations, respectively.

Boundary conditions are set for the displacement and stress vectors on the corresponding surfaces S_u and S_t:

$$u_i\,|_{S_u} = u_i^0(\overline{x}, t),\ \ \overline{x} \in S_u\,, \tag{2}$$

$$t_i\,|_{S_t} = \sigma_{ij} n_j\,|_{S_t} = q(\overline{x}, t),\ \ \overline{x} \in S_t\,, \tag{3}$$

where n_j are coordinates of the outer normal unit vector.

In addition, for problem B (see Fig. 2) subbodies have different properties, namely:

— two of them (cylindrical optical prosthesis and cornea) are homogeneous, with elastic moduli Er_1 and Er_3;

— functionally gradient elasticity modulus of the interface layer — $Er_2 = Er_2(r)$.

The right side is fixed, and the left side has symmetry conditions. The lower boundary is affected by uniform pressure, which corresponds to excessive intraocular pressure compared to atmospheric pressure. On the interface boundaries, continuity conditions are set.

To study the model (I), the boundary value problem (1) – (3) is reduced to a system of ordinary differential equations (4), (5), and (6) for the first, second, and third sections, respectively, relative to the angle of rotation of the normal with a power-law dependence on the radius of the elastic modulus of the second section [11]:

$$\left(\frac{d^2}{dr^2}\theta(r)\right)r^2 + \left(\frac{d}{dr}\theta(r)\right)r - \theta(r) = \tfrac{1}{2}Klqr^3, \tag{4}$$

$$\left(\frac{d^2}{dr^2}\theta(r)\right)r^2 + a\left(\frac{d}{dr}\theta(r)\right)r + a\vartheta_2\theta(r) + \left(\frac{d}{dr}\theta(r)\right)r - \theta(r) = \tfrac{1}{2}\frac{K_2 q(r^2 - r_1^2)r^{2-a}}{r}, \tag{5}$$

$$\left(\frac{d^2}{dr^2}\theta(r)\right)r^2 + \left(\frac{d}{dr}\theta(r)\right)r - \theta(r) = \tfrac{1}{2}K3q(r^2 - r_2^2)r, \tag{6}$$

where $K = 1/D$, D is cylindrical stiffness.

Research Results

Analytical solution

General solution to the system (4) – (6) is presented below.

The first section:

$$\theta(r) = rC_2 + \tfrac{1}{16}Klqr^3 + \tfrac{C_1}{r}.$$

The third section:

$$\theta(r) = \tfrac{C_1}{r} + rC_2 - \tfrac{1}{16}K3q(4\ln(r)r_2^2 - r^2)r. \tag{7}$$

The second section:

$$\theta(r) = r^{-\frac{1}{2}a + \frac{1}{2}\sqrt{a^2 - 4a\vartheta_2 + 4}}C_2 + r^{-\frac{1}{2}a + \frac{1}{2}\sqrt{a^2 - 4a\vartheta_2 + 4}}C_1 + \\ + \frac{1}{2}\frac{K_2 q r^{1-a}\left(((r^2 - r_1^2)\vartheta_2 - r^2 + 3rl^2)a - 8rl^2\right)}{(8 + (\vartheta_2 - 3)a)a(\vartheta_2 - 1)}$$

at

$$Er_2 = Er_1\left(\frac{r_1}{r}\right)^a;\ D_2 = \frac{Er_2 h_2^3}{12(1-\vartheta_2^2)},\ a = \frac{\ln(\frac{Er_1}{Er_2})}{\ln(\frac{r_2}{r_1})}$$

Arbitrary constants C_i of the general solution (7) are determined from the boundary conditions at the right end and the blending conditions, and $C_1 = 0$ for the first section.

Finite element solution

Numerical simulation was performed in finite element packages ANSYS and ACELAN [12, 13].

Numerical results for KPro of the first type. Fig. 3 shows a CAD model of the keratoprosthesis with the conditions of fixing and loading.

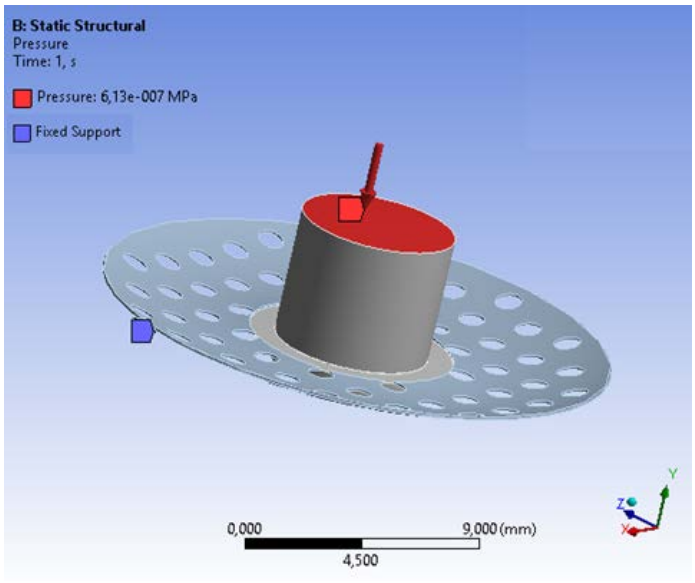

Fig. 3. Geometric model with fixing and loading conditions

The outer edge of the supporting plate is fixed, and the optical element is affected by distributed pressure. Normal intraocular pressure is between 12 and 21 mm/Hg. The pressure of 45 mm/Hg is critical. In this case, an operation can still save the eye. With higher pressure, it is almost impossible to save the eye. The current keratoprosthesis has actual load of 46 mm/Hg.

Fig. 4 shows the distribution of the axial displacement (*a*) and von Mises stress (*b*) on the finite element grid of the model.

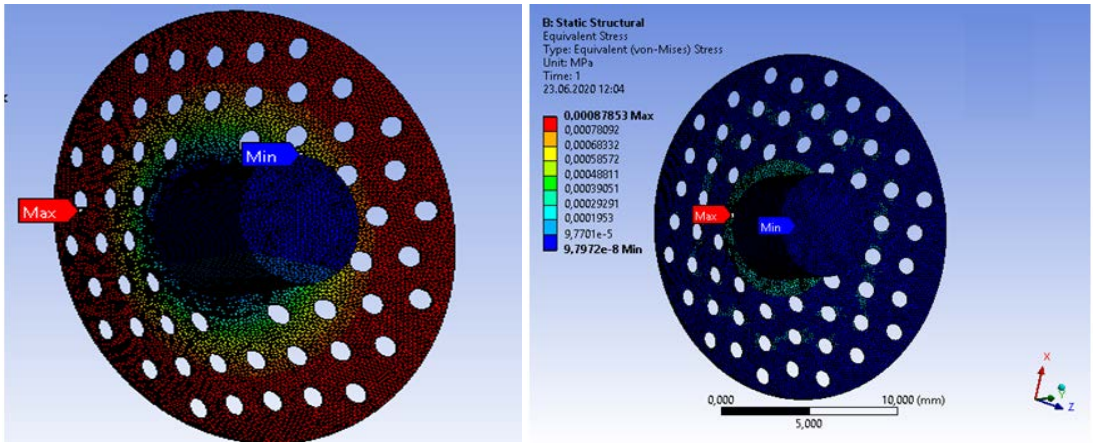

a) *b*)

Fig. 4. Distribution of the stress-strain state characteristics on the finite element model: axial displacement (*a*) and stresses according to von Mises (*b*)

Maximum stresses occur at the junction of the optical element and the supporting plate, but their values do not exceed the strength limit of the selected material.

Next, we consider the calculation results for problem B in the axisymmetric formulation. So, Fig. 5–7 show the components of the stress-strain state (II).

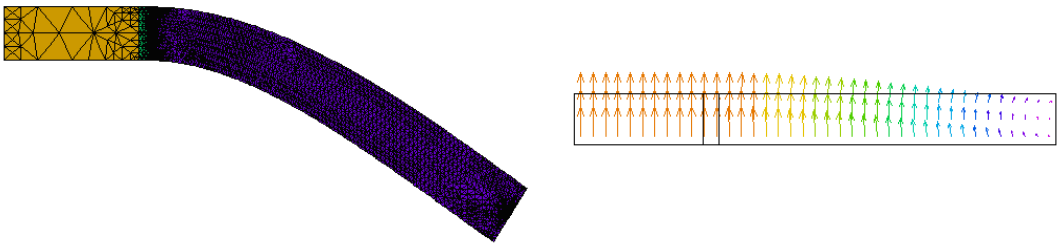

a) *b*)

Fig. 5. Calculation of displacements: finite element grid on a deformed structure (*a*), distribution of the displacement vector (*b*)

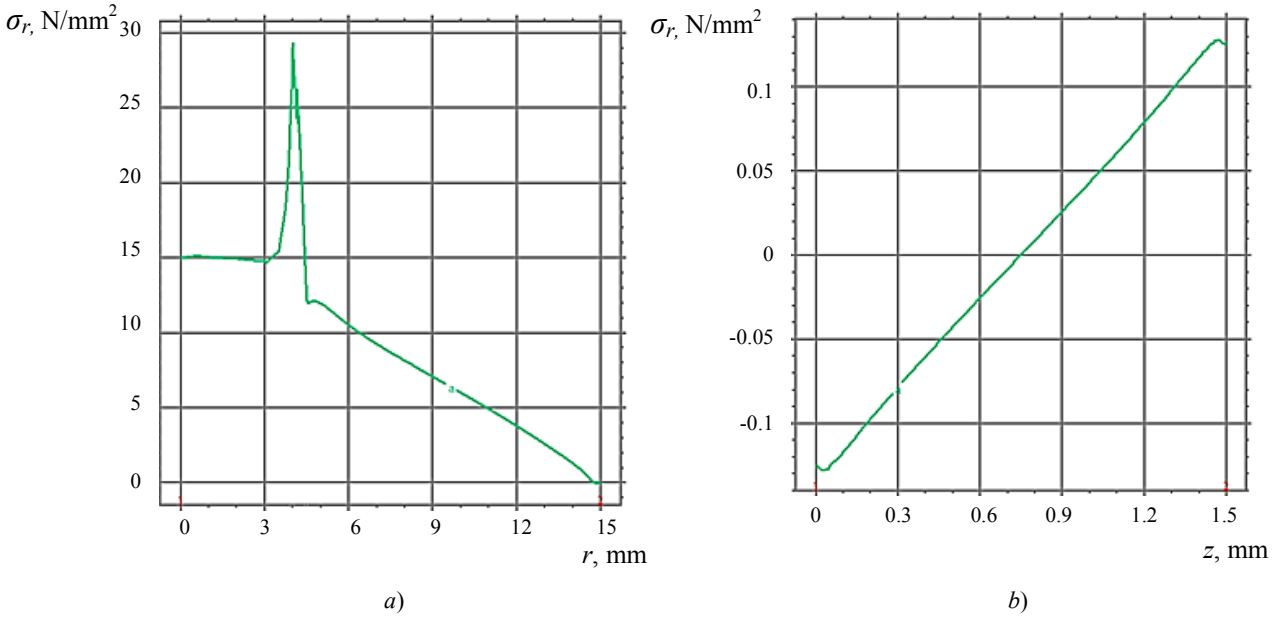

a) *b*)

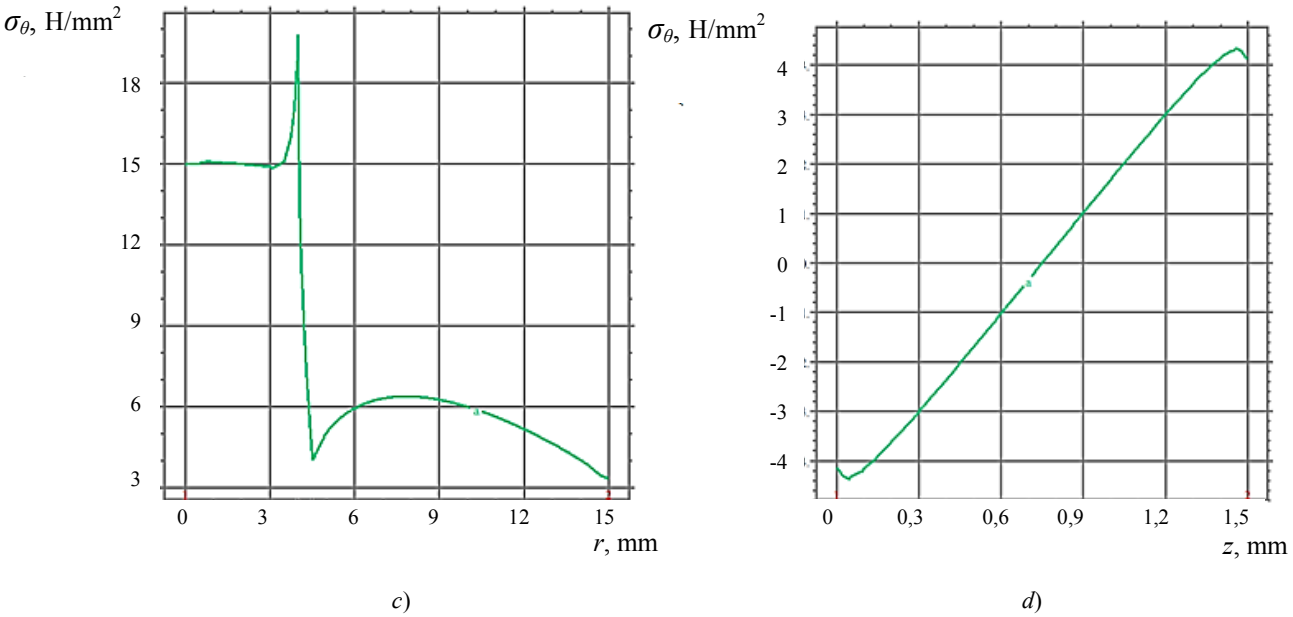

c) *d*)

Fig. 6. Calculation of stress tensor components. Dependence on radius: radial stresses at the upper boundary (*a*), at the interface boundary with the cornea (*b*), angular stresses at the upper boundary (*c*), at the interface boundary with the cornea (*d*) N/mm^2

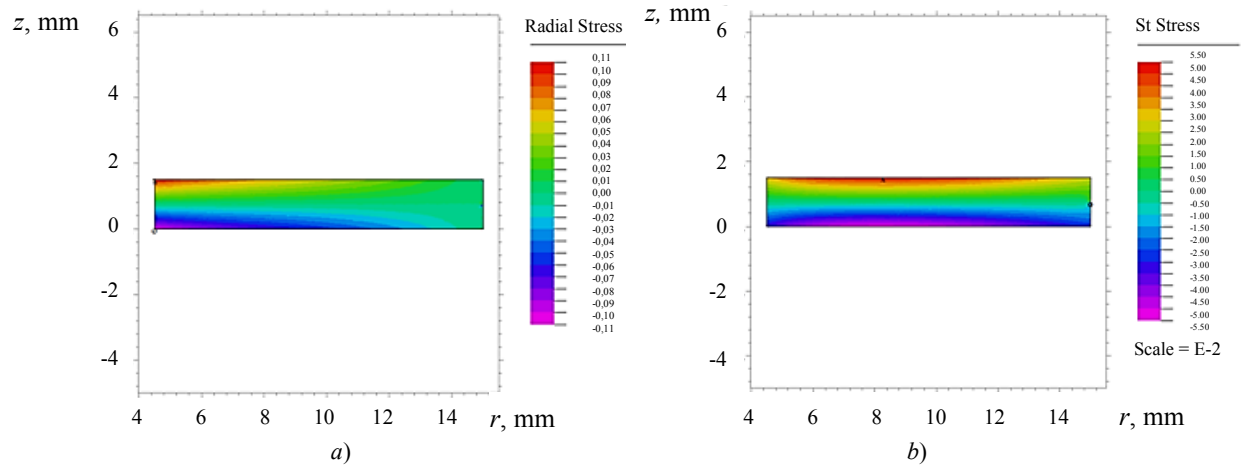

Fig. 7. Distribution of components of stresses inside the area: radial stresses (a), angular stresses (b)

The stress-strain state characteristics of model III are shown in Fig. 8–11

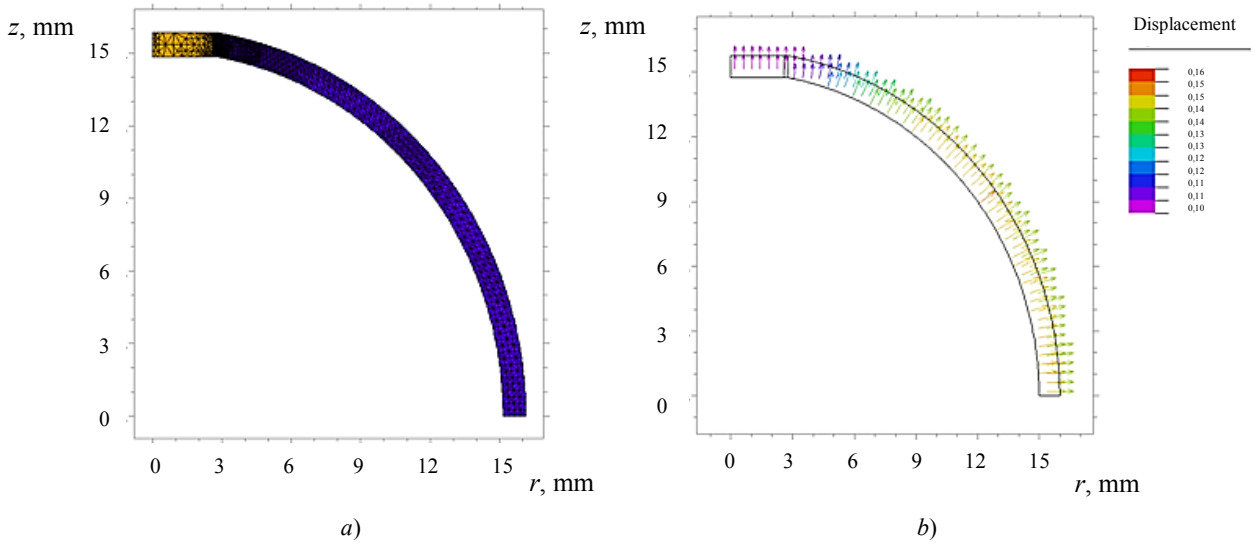

Fig. 8. Calculation of dome displacements: finite element grid on deformed structure (*a*), distribution of the displacement vector (*b*)

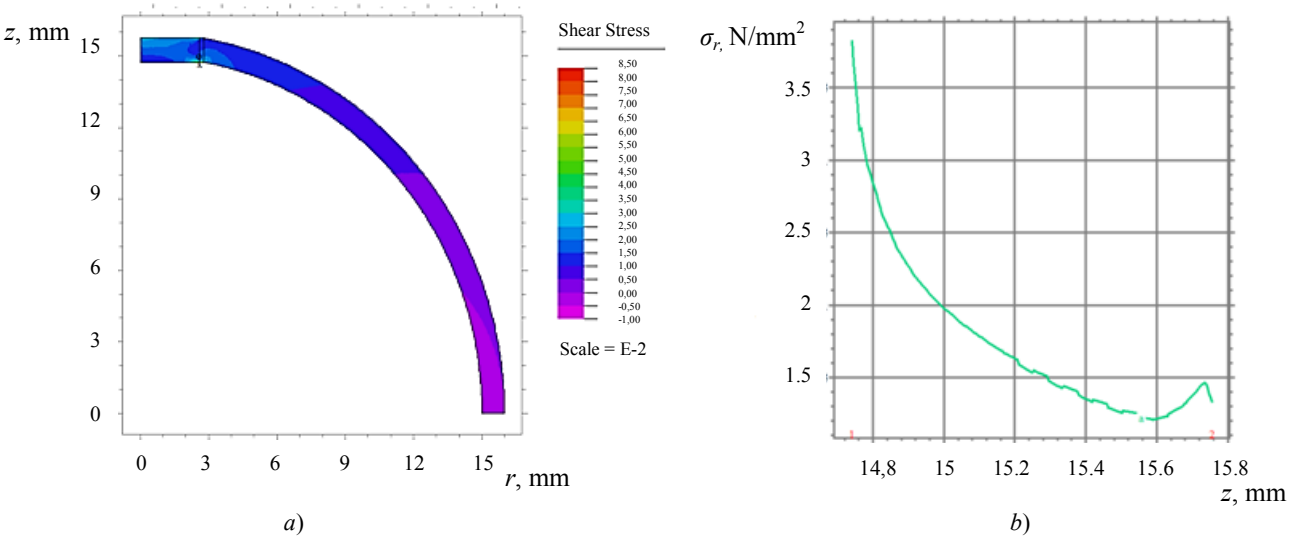

Fig. 9. Calculation of radial stresses: distribution in the region (*a*), at the interface border with the cornea (*b*)

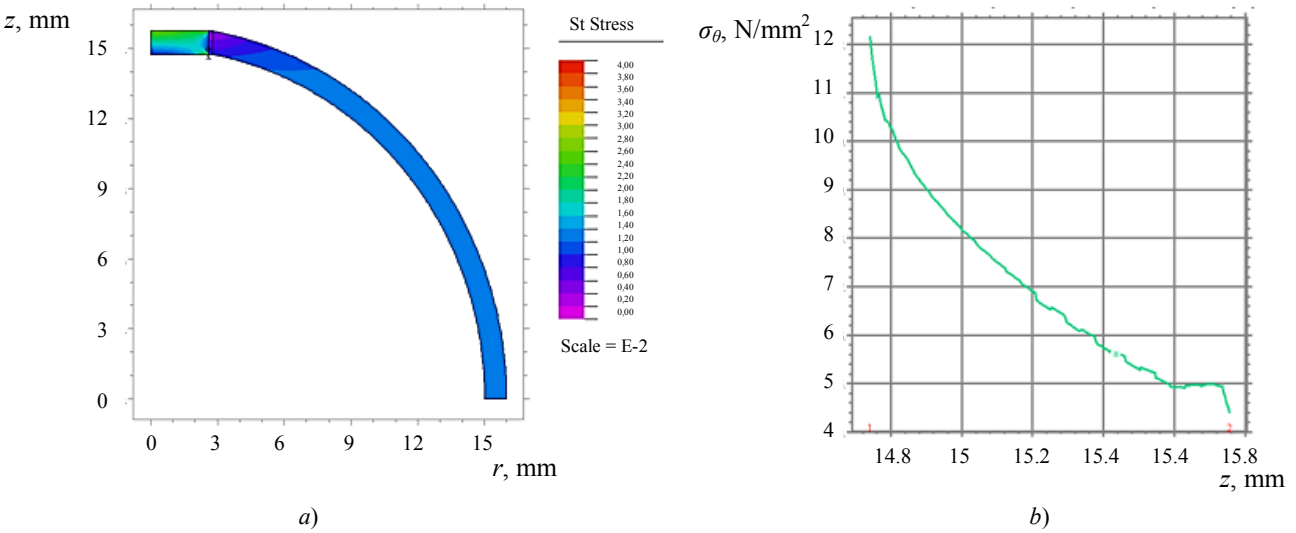

a) *b*)

Fig. 10. Calculation of angular stresses: distribution in the region (*a*), at the interface border with the cornea (*b*)

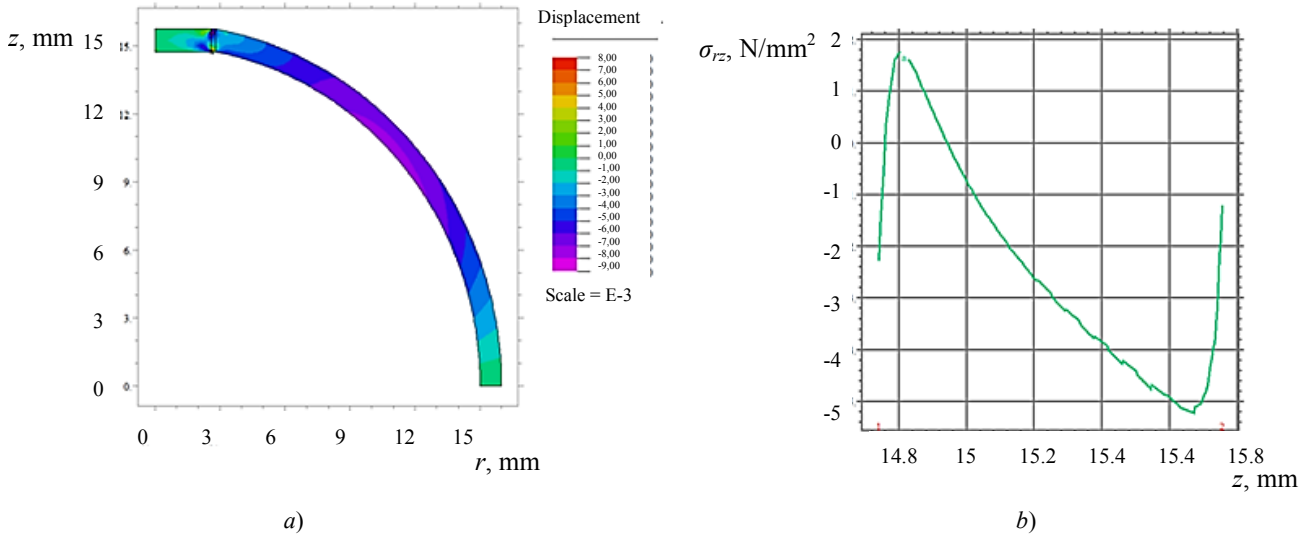

a) *b*)

Fig. 11. Calculation of shear stresses: distribution in the region (*a*), at the interface border with the cornea (*b*)

Discussion and Conclusions. Two types of keratoprostheses are considered, and their mechanical and mathematical models are constructed. For the first type of KPro with a supporting plate, its stress-strain state was studied, and a finite element model was created in ANSYS. It is shown that at maximum eye pressure, the resulting maximum stresses do not exceed the strength limits of the selected materials. For the second type of KPro, an analytical solution disregarding curvature and a finite element solution in the ACELAN package with corneal curve are constructed. The characteristics of the stress-strain state, including those at the interface border with the cornea, are calculated. This provides evaluating its injury and selecting geometric parameters and gradient properties of the intermediate layer.

References

1. Fedorov SN, Moroz ZI, Zuev VK. Keratoprotezirovanie [Keratoprosthesis]. Moscow: Meditsina; 1982. 144 p. (In Russ.)

2. Keeler R, Singh AD, Dua HS. Guillaume Pellier de Quengsy: a bold eye surgeon. British Journal of Ophthalmology. 2014;98(5):576–578. DOI: 10.1136/bjophthalmol-2014-305269

3. External Disease Panel. Preferred Practice Pattern® Guidelines. Corneal Ectasia. American Academy of Ophthalmology Cornea. San Francisco: American Academy of Ophthalmology. 2019;126(1):171–215.

4. Belin MW, Guell JL, Grabner G. Suggested guidelines for reporting keratoprosthesis results. National Center for Biotechnology Information. 2016;35(2):143–144.

5. Charoenrook V, Michael R, de la Paz MF, et al. Comparison of long-term results between osteo-odonto-keratoprosthesis and tibial bone keratoprosthesis. The Ocular Surface. 2018;16:259–264.

6. Khandekar R, Sudhan A, Jain BK, et al. Impact of Cataract Surgery in Reducing Visual Impairment: A Review. Middle East African Journal of Ophthalmology. 2015;22(1):80–85. DOI: 10.4103/0974-9233.148354

7. Sánchez Ferreiro AV, Muñoz Bellido L. Keratoprosthesis in cornea and ocular surface diseases. Archivos de la Sociedad Española de Oftalmología (English Edition). 2013;88(8):327–328.

8. Cortina MS, Karas FI, Bouchard Ch, et al. Staged ocular fornix reconstruction for glaucoma drainage device under neoconjunctiva at the time of Boston type 1 Keratoprosthesis implantation. The Ocular Surface. 2019;17(2):336–340.

9. Park J, Phrueksaudomchai P, Soledad Cortina M. Retroprosthetic membrane: A complication of keratoprosthesis with broad consequences. The Ocular Surface. 2020;18(4):893–900.

10. Novatskii V. Teoriya uprugosti [The theory of elasticity]. Moscow: Mir; 1975. 872 p. (In Russ.)

11. Boyarshinov SV. Osnovy stroitel'noi mekhaniki [Fundamentals of construction mechanics]. Moscow: Mashinostroenie; 1973. 456 p. (In Russ.)

12. Belokon AV, Eremeyev VA, Nasedkin AV, et al. Partitioned schemes of the finite-element method for dynamic problems of acoustoelectroelasticity. Journal of Applied Mathematics and Mechanics. 2000;64(3):367–377.

13. Belokon AV, Nasedkin AV, Solov'yev AN. New schemes for the finite-element dynamic analysis of piezoelectric devices. Journal of Applied Mathematics and Mechanics. 2002;66(3):481–490.

Submitted 01.07.2020
Scheduled in the issue 05.09.2020

About the Authors:

Soloviev, Arkady N., Head of the Theoretical and Applied Mechanics Department, Don State Technical University (1, Gagarin sq., Rostov-on-Don, 344003, RF), Dr.Sci. (Phys.-Math.), ResearcherID H-7906-2016, ScopusID 55389991900, ORCID: http://orcid.org/0000-0001-8465-5554, Solovievarc@gmail.com

Glushko, Nadezhda I., teaching assistant of the Theoretical and Applied Mechanics Department, Don State Technical University (1, Gagarin sq., Rostov-on-Don, 344003, RF), ORCID: http://orcid.org/0000-0003-2482-8710, leksa_n@list.ru

Epikhin, Alexander N., Head of the Ophthalmology Department, Rostov State Medical University (105 "O", Voroshilovsky Pr., Rostov-on-Don, 344010, RF), Cand.Sci. (Medicine), associate professor, ORCID: https://orcid.org/0000-0002-9514-5039, kgb1rostgmu@yandex.ru

Michael Swain, professor at the Dental School, Sydney University (C24-Westmead Hospital, The University of Sydney, NSW 2006, Australia), ORCID: http://orcid.org/0000-0002-8801-8656, michael.swain@sydney.edu.au

Lesnyak, Olga N., associate professor of the Theoretical and Applied Mechanics Department, Don State Technical University (1, Gagarin sq., Rostov-on-Don, 344003, RF), Cand.Sci. (Eng.), ORCID: http://orcid.org/0000-0001-7410-0061, lesniak.olga@yandex.ru

Ivanov, Andrey E., graduate student of the Theoretical and Applied Mechanics Department, Don State Technical University (1, Gagarin sq., Rostov-on-Don, 344003, RF), ORCID: http://orcid.org/0000-0002-0001-1469, al.drobotow@yandex.ru

Claimed contributorship

A. N. Soloviev: general statement of tasks; selection of research methods and programs; analysis of results. N. I. Glushko: conducting a review; building an approximate solution, finite element models in ACELAN; computational analysis. A. N. Epikhin: description of the keratoprostheses designs. Michael Swain: general statement of tasks. O. N. Lesnyak: building finite element models in ACELAN; computational analysis; correction of the text. A. E. Ivanov: building finite element models in ACELAN; computational analysis.

All authors have read and approved the final manuscript.

MECHANICS

UDC 519.71, 681.5, 303.732.4, 62.752; 621.534; 629.4.015 https://doi.org/10.23947/2687-1653-2020-20-4-360-369

Frequency function and damping function in assessment of dynamic processes in mechanical oscillatory systems with symmetry

A. V. Eliseev
Irkutsk State Railway Transport University (Irkutsk, Russian Federation)

Introduction. A new approach to the formation of the methodological basis of system analysis in the application to the problems on mechanical oscillatory structure dynamics is considered. The study objective is to develop a method for evaluating properties of the mechanical oscillatory systems with account for viscous friction forces based on frequency functions and damping functions that depend on the so-called coefficient of connection forms, which is the ratio of characteristics of generalized coordinates.
Materials and Methods. The graphoanalytical methods used for evaluating the dynamic properties of mechanical oscillatory two-degree-of-freedom systems are based on determining the extreme values of the frequency functions and the damping function, which are determined from the relations between the kinetic, potential energy and the values of the energy dissipation function. Mathematical models are based on Lagrange formalism, matrix methods, and elements of the theory of functions of a complex variable.
Results. A method is proposed for constructing frequency functions and damping functions for a class of mechanical oscillatory two-degree-of-freedom systems based on the analytical expressions that reflect features of the ratio of the potential and kinetic energy of the system considering viscous friction forces represented by the dissipative function. General analytical expressions for the frequency function and the damping function are derived. Graphoanalytical analysis of extreme properties of the corresponding frequency functions and damping functions is performed for mechanical vibrational systems with elastic-damping elements with symmetry properties. The results of numerical experiments are presented. A criterion for classifying frequency functions and damping functions based on the topological features of the graphs of the corresponding functions is proposed.
Discussion and Conclusions. The developed method for constructing frequency functions and damping functions can be used to display the dynamic features of mechanical oscillatory systems. The proposed matrix method for constructing a frequency-damping function for a two-degree-of-freedom system can be extended to the mechanical vibrational systems considered in different coordinate systems.

Keywords: mechanical system, dynamic connections, frequency function, damping function, connectivity of movement, extreme properties, oscillation, viscous friction.

For citation: A. V. Eliseev. Frequency function and damping function in assessment of dynamic processes in mechanical oscillatory systems with symmetry. Advanced Engineering Research, 2020, vol. 20, no. 4, pp. 360–369. https://doi.org/10.23947/2687-1653-2020-20-4-360-369

Introduction. Considerable attention is paid to the methods of using mechanical vibration systems as calculation schemes in the problems on evaluating the dynamic properties of technical objects operating under intense vibration loads [1–9]. Methods based on extreme properties of the ratio of potential and kinetic energy can be considered as common approaches to evaluating the dynamic properties of mechanical oscillatory systems [10, 11]. Methods based on energy relations have been developed in the use of the frequency function as a function of the coefficient of connection forms of the mechanical system coordinates to evaluate the dynamics of mechanical oscillatory systems disregarding friction forces [12–15].

At the same time, methods for evaluating the dynamic properties of mechanical oscillatory systems, with account for the viscous friction forces based on the frequency function, require detailed representations depending on

the viscous friction value. In particular, this is due to the fact that for systems with aperiodic motion, the concept of oscillation frequency may lose its meaning.

The proposed work is devoted to the creation of a method for evaluating the properties of mechanical movements based on the development of the concept of the frequency function, when an additional damping function reflecting the features considering viscous friction forces depending on the coefficients of connection forms, is introduced.

Materials and Methods. Free motions of a mechanical elastic-dissipative system with concentrated two-degree-of-freedom parameters are considered. The schematic diagram of the system is shown in Fig. 1.

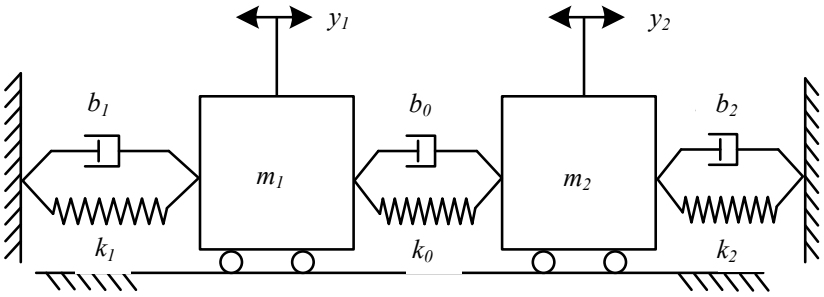

Fig. 1. Mechanical oscillating system with account for viscous friction

Generalized coordinates y_1, y_2 denote the displacement of mass-inertial elements m_1, m_2 relative to the static equilibrium position. Kinetic energy T, potential energy Π and scattering function F have the form:

$$T = \frac{1}{2}m_1\dot{y}_1^2 + \frac{1}{2}m_2\dot{y}_2^2, \tag{1}$$

$$\Pi = \frac{1}{2}k_1y_1^2 + \frac{1}{2}k_2y_2^2 + \frac{1}{2}k_0(y_2 - y_1)^2, \tag{2}$$

$$F = \frac{1}{2}b_1\dot{y}_1^2 + \frac{1}{2}b_0(\dot{y}_2 - \dot{y}_1)^2 + \frac{1}{2}b_2\dot{y}_2^2. \tag{3}$$

The system of Lagrange equations of the second kind has the form:

$$\begin{cases} \frac{d}{dt}\frac{\partial T}{\partial \dot{y}_1} + \frac{\partial \Pi}{\partial y_1} + \frac{\partial F}{\partial \dot{y}_1} = 0; \\ \frac{d}{dt}\frac{\partial T}{\partial \dot{y}_2} + \frac{\partial \Pi}{\partial y_2} + \frac{\partial F}{\partial \dot{y}_2} = 0. \end{cases} \tag{4}$$

After substituting expressions T, Π, F, the system of differential equations (4) takes the form:

$$\begin{cases} m_1\ddot{y}_1 + (b_0 + b_1)\dot{y}_1 - b_0\dot{y}_2 + (k_0 + k_1)y_1 - k_0y_2 = 0; \\ m_2\ddot{y}_2 + (b_0 + b_2)\dot{y}_2 - b_0\dot{y}_1 + (k_0 + k_2)y_2 - k_0y_1 = 0. \end{cases} \tag{5}$$

The forms of free motions of the presented system (5) are generally determined by the eigenvalues of the characteristic equation, taking into account their multiplicity. The case of simple roots is considered. Thus, let the solution $y_1 = y_1(t)$, $y_1 = y_2(t)$ of the system (5) be represented as:

$$\vec{y} = \vec{Y}e^{pt}, \tag{6}$$

where $\vec{y} = \begin{bmatrix} y_1 \\ y_2 \end{bmatrix}$ is the solution vector, $\vec{Y} = \begin{bmatrix} Y_1 \\ Y_2 \end{bmatrix}$ is the numeric vector, $p = \sigma + j\omega$ is the complex parameter, t is the time variable. It is assumed that the initial conditions are consistent with the type of solution you are looking for (6).

The task is to construct and evaluate the extreme properties of functions that display the characteristics of the proper motions of the system with account for the viscous friction forces.

Research Results

1. Construction of the frequency function and the dissipation function based on the energy ratio. The system (5) in the notation (6) has the form:

$$\begin{bmatrix} m_1p^2 + (b_0 + b_1)p + k_0 + k_1 & -b_0p - k_0 \\ -b_0p - k_0 & m_2p^2 + (b_0 + b_2)p + k_0 + k_2 \end{bmatrix} \begin{bmatrix} Y_1 \\ Y_2 \end{bmatrix} = 0. \tag{7}$$

We introduce the notations:

$$A=\begin{bmatrix} m_1 & 0 \\ 0 & m_2 \end{bmatrix},\ B=\begin{bmatrix} b_0+b_1 & -b_0 \\ -b_0 & b_0+b_2 \end{bmatrix},\ C=\begin{bmatrix} k_0+k_1 & -k_0 \\ -k_0 & k_0+k_2 \end{bmatrix}. \quad (8)$$

Considering (8), the matrix relation (5) takes the form:

$$(p^2A+pB+C)\vec{Y}=0. \quad (9)$$

On the basis of the matrix relation (9), various scalar equations can be obtained. With account for their extreme properties, in turn, the properties of the solution p of the equation (9) can be determined. In particular, scalar multiplication of the left and right parts of the equation (9) by vector $\vec{Y}$ results in the scalar expression:

$$p^2\left\langle A\vec{Y},\vec{Y}\right\rangle+p\left\langle B\vec{Y},\vec{Y}\right\rangle+\left\langle C\vec{Y},\vec{Y}\right\rangle=0. \quad (10)$$

Using substitution $p=\sigma+j\omega$, we can write (10) as:

$$(\sigma^2-\omega^2+2j\sigma\omega)\left\langle A\vec{Y},\vec{Y}\right\rangle+(\sigma+j\omega)\left\langle B\vec{Y},\vec{Y}\right\rangle+\left\langle C\vec{Y},\vec{Y}\right\rangle=0, \quad (11)$$

Let the following relation be fulfilled for the coordinates of vector $\vec{Y}$:

$$Y_2=\alpha Y_1, \quad (12)$$

where α is the coefficient of the connection form. In this case, vector $\vec{Y}$ can be presented as:

$$\vec{Y}=Y_1\vec{\alpha}, \quad (13)$$

where $\vec{\alpha}=\begin{bmatrix}1\\ \alpha\end{bmatrix}$ is vector defined by the connectivity coefficient α. After substituting (13), the expression (11) takes the form:

$$(\sigma^2-\omega^2+2j\sigma\omega)A_\alpha+(\sigma+j\omega)B_\alpha+C_\alpha=0, \quad (14)$$

where $A_\alpha=\left\langle A\vec{\alpha},\vec{\alpha}\right\rangle$, $B_\alpha=\left\langle B\vec{\alpha},\vec{\alpha}\right\rangle$, $B_\alpha=\left\langle B\vec{\alpha},\vec{\alpha}\right\rangle$ are scalar functions of the coefficient of the connection form α. The equation (14) can be presented in the equivalent form:

$$\begin{cases}\omega^2A_\alpha=\sigma^2A_\alpha+\sigma B_\alpha+C_\alpha;\\ 2\sigma\omega A_\alpha+\omega B_\alpha=0.\end{cases} \quad (15)$$

We find the solution to the system (15) with respect to σ,ω, as functions α. Function $\omega(\alpha)$ is considered as a frequency function, $\sigma(\alpha)$ is the damping function. Features of the solution to the system are determined by the sign of the expression $\sigma^2A_\alpha+\sigma B_\alpha+C_\alpha$.

Considering dissipation. The level of energy dissipation can be characterized by discriminant $B_\alpha{}^2-4A_\alpha C_\alpha$. Under the following condition:

$$B_\alpha{}^2<4A_\alpha C_\alpha, \quad (16)$$

which is understood as a small amount of friction, the solution (15) can be presented as:

$$\begin{cases}\omega^2=\dfrac{C_\alpha}{A_\alpha}-\left(\dfrac{B_\alpha}{2A_\alpha}\right)^2;\\ \sigma=-\dfrac{B_\alpha}{2A_\alpha}.\end{cases} \quad (17)$$

It should be noted that when the conditions of smallness of the viscous friction forces (16) are met, the equation is performed:

$$\omega^2+\sigma^2=\frac{C_\alpha}{A_\alpha}. \quad (18)$$

Under the condition of "large viscous friction forces":

$$B_\alpha{}^2>4A_\alpha C_\alpha, \quad (19)$$

the solution (15) can be presented as:

$$\omega=0,\ (20)\ \sigma_1(\alpha)=-\frac{B_\alpha}{2A_\alpha}-\sqrt{\left(\frac{B_\alpha}{2A_\alpha}\right)^2-\frac{C_\alpha}{A_\alpha}},\ \sigma_2(\alpha)=-\frac{B_\alpha}{2A_\alpha}+\sqrt{\left(\frac{B_\alpha}{2A_\alpha}\right)^2-\frac{C_\alpha}{A_\alpha}}. \quad (21)$$

The damping function has two components $\sigma_1(\alpha)$, $\sigma_2(\alpha)$, such that:

$$\sigma_1(\alpha)+\sigma_2(\alpha)=-\frac{B_\alpha}{A_\alpha},\ \sigma_1(\alpha)\cdot\sigma_2(\alpha)=\frac{C_\alpha}{A_\alpha}. \quad (22)$$

Thus, depending on the level of viscous friction forces, different types of presentation of the frequency function and the damping function are possible. If $B_\alpha^{\,2} - 4A_\alpha C_\alpha < 0$, then the frequency function $\omega^2(\alpha)$ and one component of the damping function $\sigma(\alpha)$ are defined. If $B_\alpha^{\,2} - 4A_\alpha C_\alpha > 0$, then it is assumed that the frequency function $\omega^2(\alpha)$ takes zero values, and the damping function has two different negative components $\sigma_1(\alpha)$, $\sigma_2(\alpha)$.

As for the condition $B_\alpha^{\,2} - 4A_\alpha C_\alpha = 0$, it requires a separate analysis. However, the condition $B_\alpha^{\,2} - 4A_\alpha C_\alpha = 0$ can be interpreted as a boundary between two different modes of motion of a mechanical system.

The presented analytical expressions of the frequency function, the damping function, and the conditions of "small" and "large" viscous friction forces can be detailed when considering specific options of mechanical oscillatory systems obtained on the basis of a two-degree-of-freedom system.

2. Frequency function and damping function for a mechanical two-degree-of-freedom system. Parameter options for the mechanical system shown in Fig.1 are considered. It is supposed that a set of boundary parameters separating the modes of motion for small and large forces of viscous friction is determined from the equation:

$$B_\alpha^{\,2} = 4A_\alpha C_\alpha, \tag{23}$$

where:

$$A_\alpha = m_1 + m_2\alpha^2, \tag{24}$$

$$B_\alpha = (b_0 + b_2)\alpha^2 - 2\alpha b_0 + b_0 + b_1, \tag{25}$$

$$C_\alpha = (k_0 + k_2)\alpha^2 - 2\alpha k_0 + k_0 + k_1. \tag{26}$$

The conditions of smallness of viscous friction forces have the form:

$$B_\alpha^{\,2} < 4A_\alpha C_\alpha. \tag{27}$$

In this case, frequency function $\omega^2(\alpha)$ and damping function $\sigma(\alpha)$:

$$\begin{cases} \omega^2(\alpha) = \dfrac{(k_0 + k_2)\alpha^2 - 2\alpha k_0 + k_0 + k_1}{m_1 + m_2\alpha^2} - \left(\dfrac{1}{2}\dfrac{(b_0 + b_2)\alpha^2 - 2\alpha b_0 + b_0 + b_1}{m_1 + m_2\alpha^2}\right)^2 \\ \sigma(\alpha) = -\dfrac{1}{2}\dfrac{(b_0 + b_2)\alpha^2 - 2\alpha b_0 + b_0 + b_1}{m_1 + m_2\alpha^2} \end{cases}. \tag{28}$$

The conditions of large viscous friction forces have the form:

$$B_\alpha^{\,2} > 4A_\alpha C_\alpha. \tag{29}$$

Under the conditions (29), functions ω^2 and $\sigma(\alpha)$ have the form:

$$\begin{cases} \omega^2 = 0; \\ \sigma_1(\alpha) = -\dfrac{1}{2}\dfrac{(b_0 + b_2)\alpha^2 - 2\alpha b_0 + b_0 + b_1}{m_1 + m_2\alpha^2} - \\ -\sqrt{\left(\dfrac{1}{2}\dfrac{(b_0 + b_2)\alpha^2 - 2\alpha b_0 + b_0 + b_1}{m_1 + m_2\alpha^2}\right)^2 - \dfrac{(k_0 + k_2)\alpha^2 - 2\alpha k_0 + k_0 + k_1}{m_1 + m_2\alpha^2}}; \\ \sigma_2(\alpha) = -\dfrac{1}{2}\dfrac{(b_0 + b_2)\alpha^2 - 2\alpha b_0 + b_0 + b_1}{m_1 + m_2\alpha^2} + \\ +\sqrt{\left(\dfrac{1}{2}\dfrac{(b_0 + b_2)\alpha^2 - 2\alpha b_0 + b_0 + b_1}{m_1 + m_2\alpha^2}\right)^2 - \dfrac{(k_0 + k_2)\alpha^2 - 2\alpha k_0 + k_0 + k_1}{m_1 + m_2\alpha^2}}. \end{cases} \tag{30}$$

The presented expressions reflect motions in the form of exponential decrease in the absence of fluctuations.

3. Features of frequency functions and damping functions for symmetric mechanical oscillatory systems. We consider a mechanical oscillating system with elastic damping elements, whose parameter values are imposed by symmetry conditions in the form $b_1 = b_2 = b_0 = b$, $k_1 = k_2 = k_0 = k$. The schematic diagram is shown in Fig. 2.

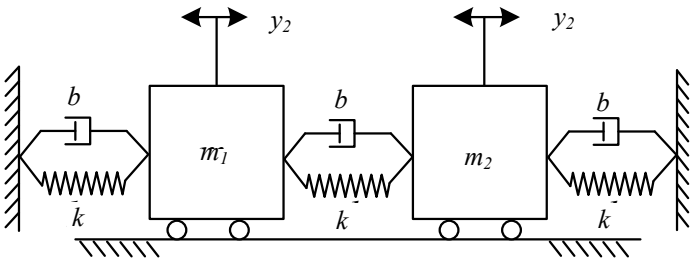

Fig. 2. “Symmetrical” mechanical system

The system of differential equations (5) has the form:

$$\begin{cases} m\ddot{y}_1 + 2b\dot{y}_1 - b\dot{y}_2 + 2ky_1 - ky_2 = 0; \\ m\ddot{y}_2 + 2b\dot{y}_2 - b\dot{y}_1 + 2ky_2 - ky_1 = 0. \end{cases} \quad (31)$$

Functions A_α, B_α, C_α can be presented by the expressions:

$$A_\alpha = m_1 + m_2\alpha^2, \quad (32)$$

$$B_\alpha = 2b(\alpha^2 - \alpha + 1), \quad (33)$$

$$C_\alpha = 2k(\alpha^2 - \alpha + 1). \quad (34)$$

On the basis of the presented components, frequency function and damping function can be constructed, and the conditions for the smallness of the viscous friction forces can be formulated.

Accounting for viscous friction forces. The condition of smallness of the friction forces can be presented from the inequality:

$$\left(\frac{B_\alpha}{2A_\alpha}\right)^2 < \frac{C_\alpha}{A_\alpha}. \quad (35)$$

After substituting the functions (32) – (34), the condition of smallness of the friction forces (35) can be written as:

$$\gamma_0 < M(\alpha), \quad (36)$$

where $\gamma_0 = \frac{b^2}{4k}$ is a generalized viscoelastic parameter, $M(\alpha) = \frac{1}{2} \cdot \frac{m_1 + m_2\alpha^2}{\alpha^2 - \alpha + 1}$ is a generalized mass-inertia coefficient that depends on the shape coefficient α. The graph of function M_α for each fixed γ_0 defines a set of values for α, at which the condition of smallness of the friction forces is satisfied.

As an example, Fig. 3 shows a graph of the parameterizing function $M(\alpha)$. Function $M(\alpha)$ has global minimum M_1 and maximum M_2 at $\alpha \to \infty$ $M(\alpha) \to \frac{m_2}{2}$.

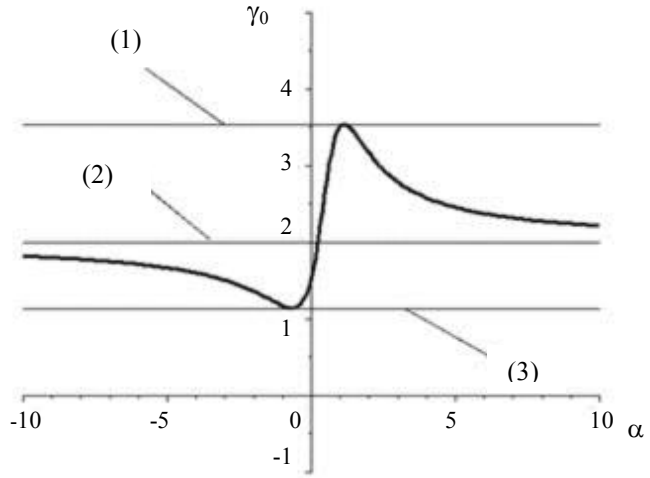

Fig. 3. Parameterizing function $M(\alpha)$: 1 — global maximum level M_2, 3 — global minimum level M_1, 2 — level of horizontal asymptote $\frac{m_2}{2}$

The change in parameter γ_0 in the intervals $(0, M_1), (M_1, \frac{m_2}{2}), (\frac{m_2}{2}, M_2), (M_2, \infty)$ determines the characteristic intervals of the shape coefficient α, under which the conditions for low friction forces are met.

For low friction forces, frequency function and damping function have the form:

$$\begin{cases} \omega^2(\alpha) = \dfrac{2k(\alpha^2 - \alpha + 1)}{m_1 + m_2\alpha^2} - \left(\dfrac{b(\alpha^2 - \alpha + 1)}{m_1 + m_2\alpha^2}\right)^2; \\ \sigma(\alpha) = -\dfrac{b(\alpha^2 - \alpha + 1)}{m_1 + m_2\alpha^2}. \end{cases} \tag{37}$$

For high friction forces, at which the aperiodic motion of the system is realized, the frequency function is zero, and the damping function has two components:

$$\begin{cases} \omega^2 = 0; \\ \sigma_1(\alpha) = -\dfrac{b(\alpha^2 - \alpha + 1)}{m_1 + m_2\alpha^2} - \sqrt{\left(\dfrac{b(\alpha^2 - \alpha + 1)}{m_1 + m_2\alpha^2}\right)^2 - \dfrac{2k(\alpha^2 - \alpha + 1)}{m_1 + m_2\alpha^2}}; \\ \sigma_2(\alpha) = -\dfrac{b(\alpha^2 - \alpha + 1)}{m_1 + m_2\alpha^2} + \sqrt{\left(\dfrac{b(\alpha^2 - \alpha + 1)}{m_1 + m_2\alpha^2}\right)^2 - \dfrac{2k(\alpha^2 - \alpha + 1)}{m_1 + m_2\alpha^2}}. \end{cases} \tag{38}$$

On the basis of analytical representations of the frequency function and the damping function, characteristic variants and features of the extreme properties of the corresponding functions can be determined, taking into account the viscous friction forces.

Discussion and Conclusion. Of interest are the characteristic variants of frequency functions and damping functions depending on the conditions of low viscous friction forces. Variants of value γ_0, that determine the characteristic intervals of the shape coefficient α, under which the conditions of smallness of the viscous friction forces are met, are considered.

1. Let $\gamma_0 \in (0, M_1)$. The example $\gamma_0 \approx 0.1$ is considered. In this case, the conditions for low friction forces for any shape coefficient $\alpha \in (-\infty..\infty)$ are met. Fig. 4 and 5 show the frequency function $\omega^2(\alpha)$ and damping function $\sigma(\alpha)$ for the mechanical elastic-dissipative system with parameters $b = 1$, $m_1 = 3$, $m_2 = 4$, $k = 3$.

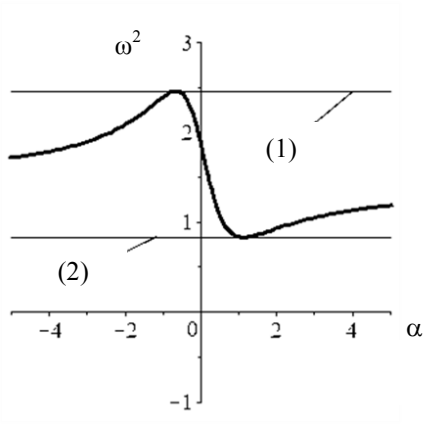

Fig. 4. Frequency functions $\omega^2(\alpha)$:
(1) and (2) are extreme levels

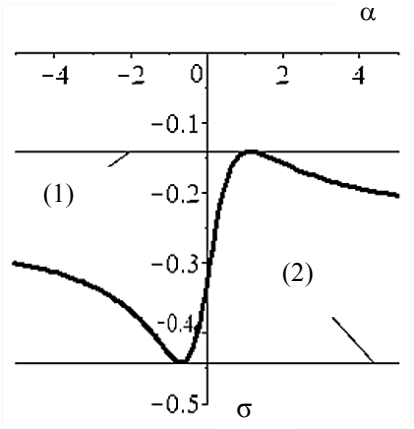

Fig. 5. Damping function $\sigma(\alpha)$:
(1) and (2) are extreme levels

Roots of the equation that is equal to zero of the corresponding determinant

$$\left|Ap^2 + Bp + C\right| = 0, \tag{39}$$

are $p_i = \omega_i + j\sigma_i$, $i = 1..4$, where $\omega_1 \approx 0.91$; $\omega_2 \approx 1.56$; $\omega_3 \approx -1.56$; $\omega_4 \approx -0.91$; $\sigma_1 \approx -0.14$; $\sigma_2 \approx -0.44$; $\sigma_3 \approx -0.44$;

In Fig. 4, the frequency function reaches extreme values equal to the squares of the frequencies $\omega_2^2 \approx 2.46$ and $\omega_1^2 \approx 0.82$. In Fig. 5, the damping function reaches extreme values that are $\sigma_3 \approx -0.44$ and $\sigma_4 \approx -0.14$. The

frequency function and the damping function reach their extreme values when the form coefficients are $\alpha_1^* = -0,65$ and $\alpha_2^* = 1.15$.

2.Let $\gamma_0 \in (M_1, \frac{m_2}{2})$. We consider a mechanical system with parameters $b = 4$, $\gamma_0 \approx 1.33$. Fig. 6 and 7 show the corresponding frequency function and damping function. The set of coefficients of forms for which the condition of low friction forces is satisfied is: $(-\infty, \alpha_1) \cup (\alpha_2, \infty)$, where α_i are the roots of the equation $M(\alpha) = \gamma_0$. For parameters $b = 4$, $m_1 = 3$, $m_2 = 4$, $k = 3$ the roots of the characteristic equation (39) have real parts representing the dissipation coefficients, $\sigma_1 \approx -0.57$; $\sigma_2 \approx -1.08$; $\sigma_3 \approx -2.46$; $\sigma_4 \approx -0.57$ and imaginary parts representing the frequencies $\omega_1 \approx 0.73$; $\omega_2 \approx 0$; $\omega_3 \approx 0$; $\omega_4 \approx -0.73$. In Fig. 6, the frequency function has a local minimum $\omega_4^2 \approx 0.53$ in the interval $(-\infty, \alpha_1) \cup (\alpha_2, \infty)$.

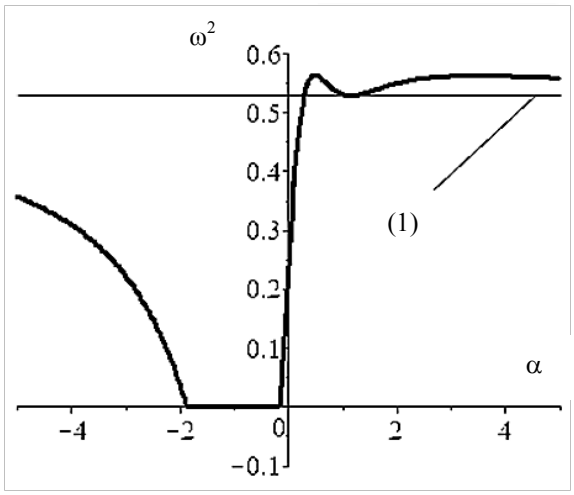

Fig. 6. Frequency function:
(1) is extreme level at point α_2^*

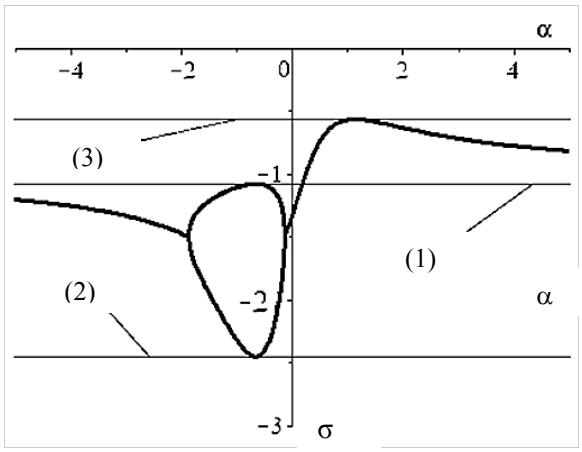

Fig. 7. Damping function:
(3) is extreme level at point α_2^*; (1), (2) are extreme levels at point α_1^* on the two-valued interval

On the interval (α_1, α_2), the frequency function is zero. In turn, in Fig. 7, the damping function in the interval (α_1, α_2) is double-valued and reaches simultaneously two extreme values $\sigma_2 \approx -1.08$ and $\sigma_3 \approx -2.46$ at point α_2^*. In the domain $(-\infty, \alpha_1) \cup (\alpha_2, \infty)$, the damping function is single-valued and has one local extremum $\sigma_1 \approx -0.57$ at point α_2^*.

3. Let $\gamma_0 \in (\frac{m_2}{2}, M_2)$. We consider a mechanical system with parameters $b = 6$; $m_1 = 3$; $m_2 = 4$; $k = 3$. The roots of the characteristic equation (39) have real $\sigma_1 \approx -0.85$; $\sigma_2 \approx -0.56$; $\sigma_3 \approx -4.74$; $\sigma_4 \approx -0.85$ and imaginary parts $\omega_1 \approx 0.36$; $\omega_2 \approx 0$; $\omega_3 \approx 0$; $\omega_4 \approx -0.36$. The conditions for low friction forces are met in the interval (α_1, α_2), where $\alpha_1 \approx 0.63$; $\alpha_2 \approx 2.37$. In Fig. 8, the corresponding frequency function is positive only on the interval (α_1, α_2). The local extremum of the frequency function is $\omega_4^2 \approx 0.13$. Outside the interval (α_1, α_2), the frequency function is zero.

In Fig. 9, the damping function is double-valued in the interval $(-\infty, \alpha_1)$ and reaches simultaneously two extreme values at point α_1^*, which are $\sigma_3 \approx -4.74$ and $\sigma_2 \approx -0.56$. In the interval (α_2, ∞) the damping function is also double-valued. In the interval (α_1, α_2), the damping function is single-valued and has one local extremum $\sigma_1 \approx -0.85$ at point α_2^*.

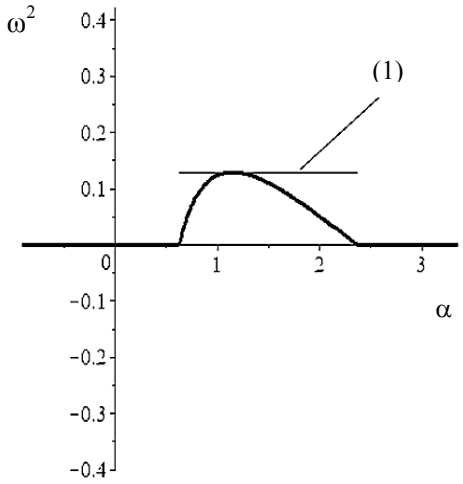

Fig. 8. Frequency function:
(1) is extreme level at point α_2^*

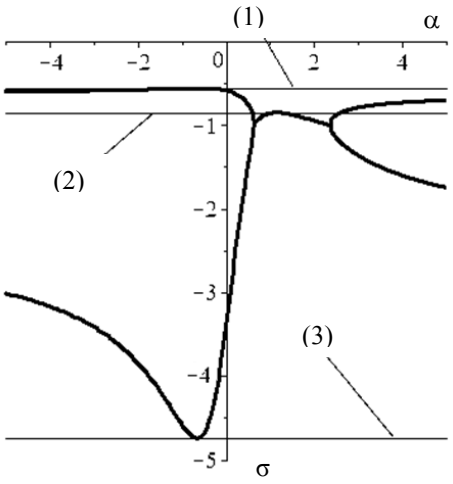

Fig. 9. Damping function: (1), (3) are extreme levels at point α_1^* on the two-valued interval, (2) is extreme level at point α_2^*

4. Let $\gamma_0 \in (M_2,\infty)$. For parameters $b = 6.52$; $m_1 = 3$; $m_2 = 4$; $k = 3$, the characteristic equation (39) has only real roots $\sigma_1 \approx -0.50$; $\sigma_2 \approx -0.88$; $\sigma_3 \approx -0.96$; $\sigma_4 \approx -5.26$. The corresponding frequency function and damping function are shown in Fig. 10 and 11. The interval of fulfillment of the conditions of smallness of the friction forces degenerates into an empty set.

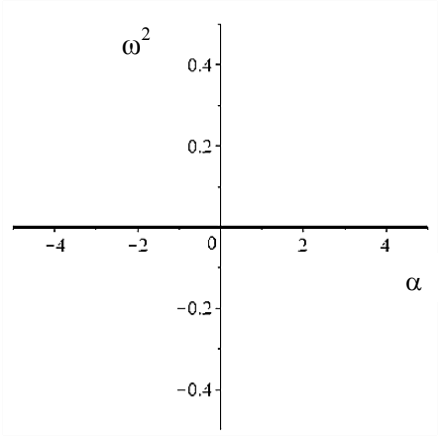

Fig. 10. Frequency function:
case of degeneracy

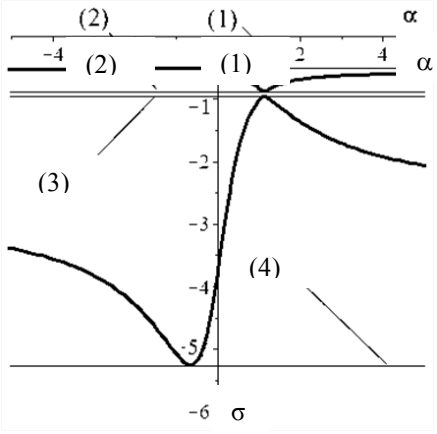

Fig. 11. Damping function, formed by two branches: (1), (2) are extreme levels of the "upper" branch at points α_1^* and α_2^*; (3), (4) are extreme levels of the "lower" branch at points α_1^* and α_2^*

In Fig. 10, the frequency function is zero on the whole number axis. In Fig. 11, the corresponding damping function is double-valued on the entire numeric axis and has 4 local extrema $\sigma_1 \approx -0.50$; $\sigma_2 \approx -0.88$; $\sigma_3 \approx -0.96$; $\sigma_4 \approx -5.26$ at points α_1^* and α_2^*.

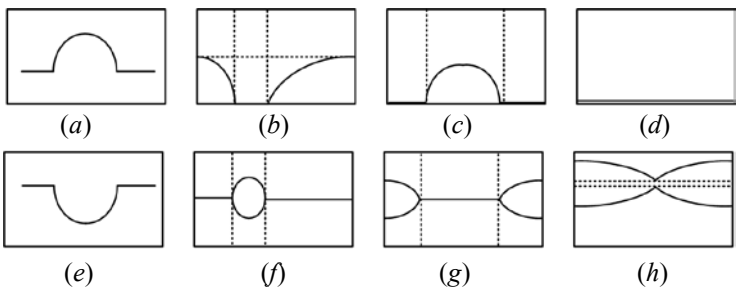

Fig. 12. Pictograms of topological features of frequency function and damping function graphs: (a)-(d) are pictograms associated with graphs of frequency functions shown in Fig. 4, 6, 8, 10, respectively; (e)-(h) are pictograms associated with damping functions in Fig. 5, 7, 9, 11, respectively

The pictograms shown in Fig. 12, compared to the function graphs in Fig. 4–11, reflect a number of topological features of the frequency function and damping function graphs. These features include the shape of the graph as a single curve, the presence of bifurcation points on the graph of one curve into two, the presence of two nonintersecting curves or a "ring".

Thus, the achieved extreme values of the frequency function and the damping function are related to the dynamic characteristics of the mechanical oscillatory system taking into account the friction forces. In particular, the extreme values of the constructed frequency function and damping function are related to the proper frequencies and dissipative coefficients of damped oscillations. In this case, the issue on the existence of extreme values of the frequency function and the damping function that do not coincide with the squares of the proper oscillation frequencies requires additional consideration. At the same time, it can be assumed that the forms of frequency functions and damping functions that determine the modes of free motions of mechanical oscillatory systems with friction are of interest for evaluating a wider range of dynamic properties.

In terms of practical implementation of the possible control of oscillatory modes of mechanical systems based on the connectivity coefficient, there are no fundamental obstacles. For example, possible dynamic state control systems may include sensors of vibration amplitudes at control points of a vibrating process machine or vehicle. However, the construction of such systems requires detailed consideration of a wide range of features related to the technical object.

In conclusion, the following points can be noted as the conclusions of the presented studies.

1. For the mechanical vibrating system considering forces of viscous friction, a method of constructing frequency function and damping function that are dependent on the connection form coefficient of the free motion coordinates, is developed. It is shown that the set of extreme values of the frequency function and the damping function displays the proper characteristics of an elastic-dissipative mechanical oscillatory system.

2. It is shown that the frequency function and damping functions for a mechanical oscillatory two-degree-of-freedom system with account for viscous friction, can be represented in two variants determined by the conditions for the value of the viscous friction forces for a fixed connection form coefficient; for the conditions of low viscous friction forces, the values of the frequency function take positive values, and the damping function has one negative component; if the conditions of high viscous friction forces are met, the frequency function takes zero values, and the damping function has two negative components.

3. A method is proposed for constructing possible variants of frequency functions and damping functions for various values of system parameters based on a parameterizing function that allows determining the regions of values of the connection form coefficient in which the condition of smallness of viscous friction forces is met. A criterion for classifying frequency functions and damping functions depending on the topological features of their graphs is proposed.

4. The matrix method for constructing the frequency-damping function for a two-degree-of-freedom system can be extended to mechanical oscillatory systems considered in different coordinate systems.

5. As a physical interpretation of the connection coefficient used in the frequency function and the damping function, we can consider the linkage in the form of a gear ratio expressed from the ratio of the amplitudes of the partial block coordinate oscillations. The ratio under consideration, along with the static state, can be determined for steady-state and damped oscillation modes. Thus, a concept is developed in which the starting point for the analysis of a mechanical system is the linkage.

References

1. Clarence W. de Silva. Vibration: Fundamentals and Practice. Boca Raton, London, New York, Washington, D.C.: CRC Press; 2000. 957 p.

2. Iwnicki S. Handbook of railway vehicle dynamics. Boca Raton: CRC Press; 2006. 552 p. DOI: https://doi.org/10.1201/9781420004892

3. Banakh L, Kempner M. Vibrations of Mechanical Systems with Regular Structure. Berlin; Heidelberg: Springer; 2010. 262 p. DOI: 10.1007/978-3-642-03126-7

4. Karnovsky IA, Lebed E. Theory of Vibration Protection. Switzerland: Springer International Publishing; 2016. 708 p.

5. Eliseev SV, Eliseev AV. Theory of Oscillations: Structural Mathematical Modeling in Problems of Dynamics of Technical Objects. Springer International Publishing, Cham; 2020. 521 p.

6. Eliseev SV, Lukyanov AV, Reznik YuN, et al. Dynamics of mechanical systems with additional ties. Irkutsk: Irkutsk State University; 2006. 316 p.

7. Rocard Y. General Dynamics of Vibrations. Paris: Masson; 1949. 458 p.

8. Eliseev AV, Kuznetsov NK, Moskovskikh AO. Dinamika mashin. Sistemnye predstavleniya, strukturnye skhemy i svyazi elementov: monografiya. Moscow: Innovatsionnoe mashinostroenie; 2019. 381 p. (In Russ.)

9. Eliseev SV, Artyunin AI. Prikladnaya teoriya kolebanii v zadachakh dinamiki lineinykh mekhanicheskikh system [Applied theory of vibrations in problems on dynamics of linear mechanical systems]. Novosibirsk: Nauka; 2016. 459 p. (In Russ.)

10. Strutt JW. Teoriya zvuka [The theory of sound]. Moscow: GITTL; 1955. Vol. 1. 503 p. (In Russ.)

11. Eliseev SV. Artyunin AI (ed.). Prikladnoi sistemnyi analiz i strukturnoe matematicheskoe modelirovanie (dinamika transportnykh i tekhnologicheskikh mashin: svyaznost' dvizhenii, vibratsionnye vzaimodeistviya, rychazhnye svyazi): monografiya [Applied system analysis and structural mathematical modeling (dynamics of transport and technological machines: connectivity of movements, vibration interactions, lever connections): monograph]. Irkutsk: IrGUPS; 2018. 692 p. (In Russ.)

12. Khomenko AP, Eliseev SV. Razvitie energeticheskogo metoda opredeleniya chastot svobodnykh kolebanii mekhanicheskikh system [Development of mechanical systems of free oscillations of frequencies of identification of energetic method]. Modern Technologies. System Analysis. Modeling. 2016;1(49):8–19. (In Russ.)

13. Eliseev SV, Kuznetsov NK, Bolshakov RS, et al. O vozmozhnostyakh ispol'zovaniya dopolnitel'nykh svyazei inertsionnogo tipa v zadachakh dinamiki tekhnicheskikh sistem [On applicability of additional ties of inertial type in the problems of engineering systems dynamics]. Proceedings of Irkutsk State Technical University. 2016;5(112):19–36. (In Russ.)

14. Eliseev SV, Bolshakov RS, Nguyen Duc Huynh, et al. Opredelenie chastot sobstvennykh kolebanii mekhanicheskikh kolebatel'nykh system: osobennosti ispol'zovaniya chastotnoi energeticheskoi funktsii. Chast' I [Identification of mechanical oscillation system eigen frequencies: features of using the frequency energy function. Part I]. Proceedings of Irkutsk State Technical University. 2016;6(113):26–33. (In Russ.)

15. Eliseev SV, Bolshakov RS, Nguyen Duc Huynh, et al. Opredelenie chastot sobstvennykh kolebanii mekhanicheskikh kolebatel'nykh system: osobennosti ispol'zovaniya chastotnoi energeticheskoi funktsii. Chast' II [Identification of mechanical oscillation system eigen frequencies: features of using the frequency energy function. Part II]. Proceedings of Irkutsk State Technical University. 2016;7(114):10–23. (In Russ.)

Submitted 06.11.2020
Scheduled in the issue 19.11.2020

About the Author:

Eliseev, Andrey V., associate professor of the Mathematics Department, Irkutsk State Railway Transport Engineering University (15, ul. Chernyshevskogo, Irkutsk, 664074, RF), Cand.Sci. (Eng.), ResearcherID: N-9357-2016, ScopusID: 57191957568, ORCID: https://orcid.org/0000-0003-0222-2507, eavsh@ya.ru

The author has read and approved the final manuscript.

MECHANICS

UDC 539.3 https://doi.org/10.23947/2687-1653-2020-20-4-370-381

Infinite plate loaded with normal force moving along a complex path

A. V. Galaburdin
Don State Technical University (Rostov-on-Don, Russian Federation)

Introduction. A technique of solving the problem on an infinite plate lying on an elastic base and periodically loaded with a force that moves along an arbitrary closed trajectory and according to an arbitrary law, is considered.

Materials and Methods. An original method for solving problems on the elasticity theory for plates loaded with a force moving arbitrarily along a closed trajectory of arbitrary shape is considered. The problem on an infinite plate lying on an elastic foundation is investigated. The plate is loaded with a normal force moving at a variable speed. The load is decomposed into a Fourier series on a time interval whose length is equal to the time of its passage along the trajectory. The solution to this problem is realized through a superposition of solutions to the problems corresponding to the load defined by the summands of the specified Fourier series. The final problem solution is presented in the form of a segment of the Fourier series, each summand of which corresponds to the solution to the problem on the action on an infinite plate of the load distributed along a closed trajectory of the force motion. The fundamental solution to the vibration equation of an infinite plate lying on an elastic foundation is used to construct these solutions.

Results. A solution to the problem of an infinite plane, along which a concentrated force moves at a variable speed, is presented. A smooth closed curve consisting of arcs of circles was considered as a trajectory. The behavior of displacements and stresses near the moving force is investigated; and the process of the elastic wave energy propagation is also studied. For this purpose, a change in the Umov-Poynting vector is considered.

Discussion and Conclusions. The results obtained can be used in calculations for road design. The study of the propagation of the energy of elastic waves from moving vehicles will provide the assessment of the impact of these waves on buildings located near the road. Analysis of the behavior of displacements and stresses near the moving force will allow assessing the wear of the road surface.

Keywords: infinite plate, moving load, arbitrary closed trajectory, variable speed, elastic wave energy.

For citation: A. V. Galaburdin. Infinite plate loaded with normal force moving along a complex path. Advanced Engineering Research, 2020, vol. 20, no. 4, pp. 370–381. https://doi.org/10.23947/2687-1653-2020-20-4-370-381

Introduction. In many areas of science and technology, problems related to the propagation of elastic waves arise. This work objection is to study laws of the propagation of elastic waves that occur under the action of a moving load. Problems of this kind were previously investigated by various authors in a number of papers, which considered a variety of problem statements with a moving load and proposed various solution methods.

Often, when solving such problems, a mobile coordinate system is introduced [1−5], or a quasi-static statement of the problem is considered [6−12] to exclude time from the number of independent variables. A number of papers use the finite element method [11−13]. Interesting results can be obtained using variational [14−16] or direct techniques

[17−19]. Methods based on the application of fundamental solutions to the corresponding differential equations were used in [20−22] under solving problems on the elasticity theory about a force moving at a constant speed.

Problem Setting. Consider a differential equation describing vibration of an infinite plate lying on an elastic base under the action of vertical force *P*:

$$\Delta^2 U + c^{-2}\partial_t^2 U + kU = \frac{P}{D}, \tag{1}$$

where *U* is deflection of the plate; $D = \frac{Ed^3}{12(1-\mu^2)}$; *E* is Young's modulus; μ is Poisson's ratio; *d* is thickness of the plate; $c^{-2} = \frac{\rho d}{D}$; ρ is density of the plate material; $k = \frac{K}{D}$; *K* is coefficient of rigidity of the elastic base.

We will consider a solution for which the energy flow is directed from the sources of elastic wave excitation to infinity, and assume that force *P* moves along a closed trajectory γ in an arbitrary way. In addition, we assume that $P = P(s(t))$, where *s* is the arc coordinate counted from some fixed point of the curve γ. Obviously, $P = P(s(t))$ will be a periodic function over *t* with period T, if $s(t)$ is also a periodic function over *t* with period T.

Materials and Methods. Consider the fundamental solution to the equation (1). It can be obtained from the expression:

$$\Delta^2 W + c^{-2}\partial_t^2 W + kW = \frac{1}{D}\delta(x-x_o)\delta(y-y_o)\delta_T(t-\tau), \tag{2}$$

where $\delta_T(t-\tau) = \sum_{n=-\infty}^{\infty}\delta(t-\tau-nT)$.

The solution to the equation (2) can be obtained by traditional methods, using the limiting absorption principle, and presented as a series:

$$W(x,x_0,y,y_0,t-\tau) = \sum_{k=-\infty}^{\infty} w_k(x,x_0,y,y_0,\omega_k)e^{-i\omega_k(t-\tau)}, \tag{3}$$

where $w_k(x,x_0,y,y_0,\omega_k)$ satisfies the equation:

$$\Delta^2 w_k - c^{-2}\omega_k^2 w_k + kw_k = \frac{1}{D}\delta(x-x_o)\delta(y-y_o)e^{i\omega_k\tau}.$$

It is known that the solution to the equation (1) can be presented as:

$$U(x,y,t) = \frac{1}{T}\int_{-T/2}^{T/2}\iint_{R^2} W(x,x_o,y,y_o,t-\tau)P(x_o,y_o,\tau)dx_o dy_o d\tau.$$

If the moving force is a single concentrated force, which is described by the function:

$$P(s(t)) = \delta(x-x_1(s(t)))\delta(y-y_1(s(t))),$$

the solution in this case will look like:

$$U(x,y,t) = \frac{1}{T}\int_{-T/2}^{T/2} W(x,x_1(s(\tau)),y,y_1(s(\tau)),t-\tau)d\tau. \tag{4}$$

Once defined $U(x,y,t)$, it is possible to calculate displacements and stresses at any point of the plate.

If the expression $\omega_k = \frac{2k\pi}{T}$ is large enough, it is required to calculate integrals of rapidly oscillating functions (3). For this purpose, the quadrature formula was used [23, 24]:

$$\int_a^b e^{i\omega x} f(x)dx \approx \int_a^b e^{i\omega x} S(x)dx \approx -\frac{1}{\omega^4}\sum_{j=1}^{N-1}\frac{e^{i\omega x_{j+1}} - e^{i\omega x_j}}{h_j}\left(M_{j+1} - M_j\right),$$

where h_j are the lengths of elementary segments into which the interval $[a; b]$ is divided; $S(x)$ is approximation of $f(x)$ by cubic spline $M_j = S''(x_j)$.

Research Results. The calculations were performed for an infinite plate loaded with a normal force that moved along a closed curve (Fig. 1).

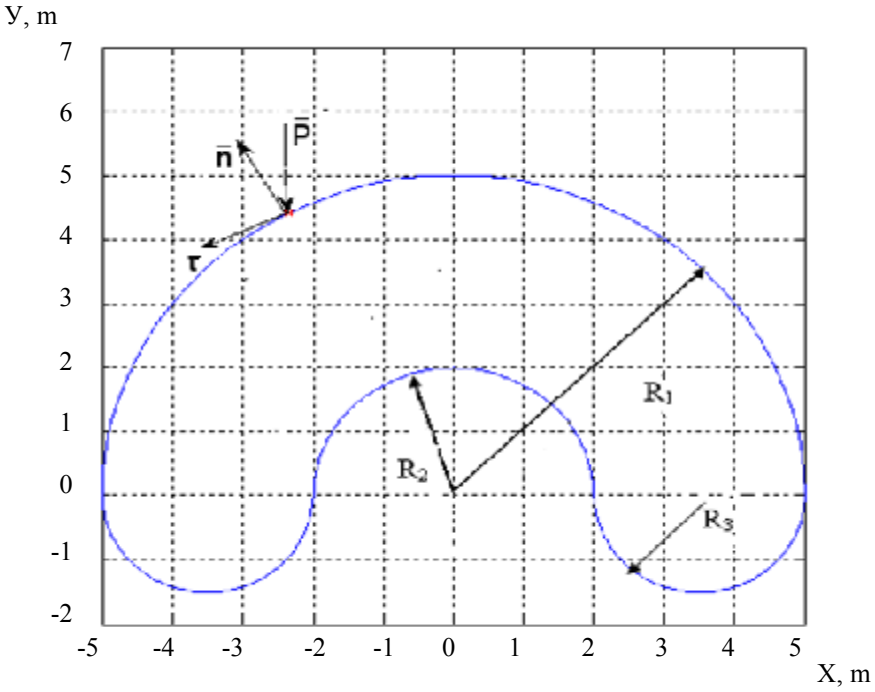

Fig. 1. Trajectory of the concentrated force

During the calculations, it was assumed that the plate thickness was d = 0.25 m, parameter c = 221 m/s, young's modulus of the plate material E = 232469 H/m^2, Poisson's ratio μ = 0.36, elastic base compliance coefficient K=1.864 m^{-4}. The radii that determine the shape of the force trajectory were assumed to be equal to: R_1 = 5 m, R_2 = 3 m, R_3 = 1 m. The formula (3) held 120 terms of the Fourier series, and, when calculating the integral (4), the integration interval was divided into 120 equal subintervals.

The law of force motion along the trajectory was described by the function:

$$s(t) = \frac{L\cdot\sin(\alpha(t - T/2))}{2\sin(\alpha T/2)} + \frac{L}{2}, \text{ где } \alpha = \frac{\pi}{T},\ t \in [0:T].$$

We considered the instant of time $t = \frac{T}{2}$, when the moving force was at the same point of the trajectory for any T. When the parameter T is changed, the speed rate of the concentrated force along the trajectory changes.

To analyze the stress-strain state of the plate, displacements and stresses were calculated in a rectangular coordinate system associated with a moving concentrated force. In this case, the axis τ of this system was directed tangentially to the trajectory $\bar{\tau}$, and n axis coincided in the direction of the external normal to the area bounded by the trajectory $\bar{n}$ (Fig. 1).

In this coordinate system, the displacement vector and stress tensor can be presented as:

$$\bar{U} = Ut\cdot\bar{\tau} + Un\cdot\bar{n} + W\cdot\bar{k},$$

$$\overline{\overline{S}} = St \cdot \overline{\tau}\overline{\tau} + Sn \cdot \overline{n}\overline{n} + Stn \cdot \left(\overline{\tau}\overline{n} + \overline{n}\overline{\tau}\right),$$

where $\overline{k}$ is the normal to the plate.

Fig. 2 shows the variation of the components of the displacement vector Wt, Utt, Unt, the stress tensor $Stt, Snt, Stnt$ (second and third graphs) in the axis τ, and the change in the same values along the axis n — Wn, Utn, Unn and $Stn, Snn, Stnn$ (first and fourth graphs) at $z = h/2$, the speed of the force v = 49.3480 m/s, acceleration along the trajectory w_t = 0 m/s^2, and normal acceleration $w_n = v^2/R_1 = 487.045$ m/s^2 (the position of the force on the trajectory is marked with a red dot in Fig. 1).

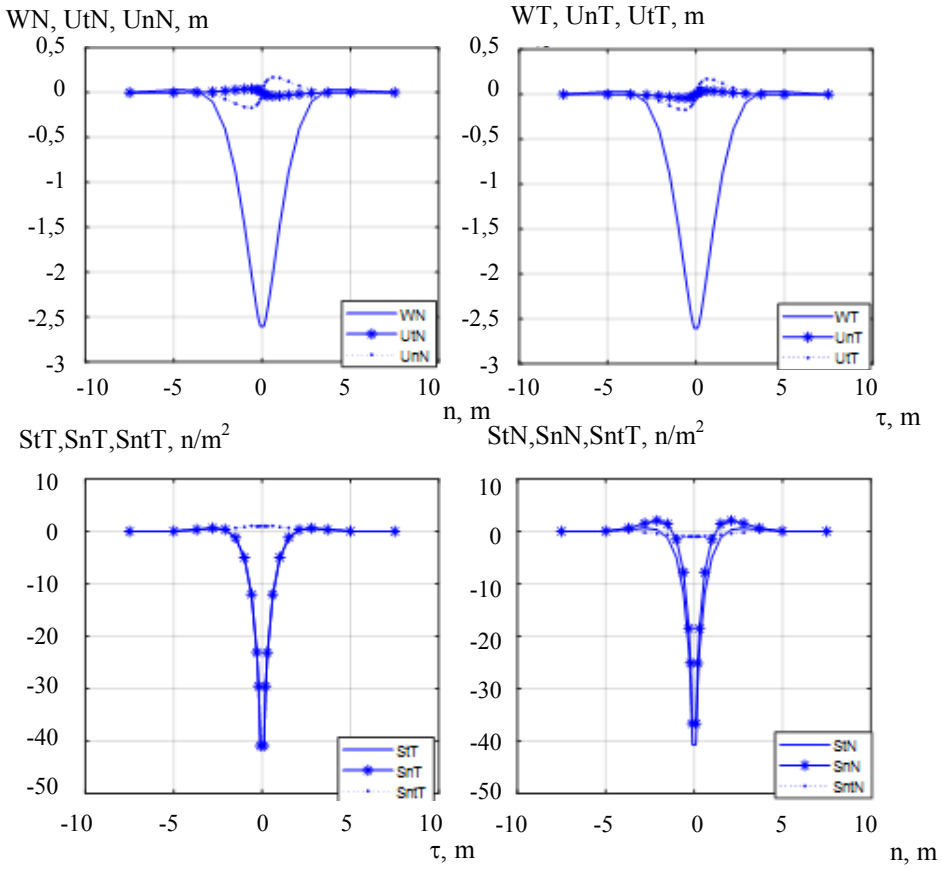

Fig. 2. Variation of displacements and stresses (v = 49.3480 m/s)

When studying the energy propagation of elastic waves, the energy flux vector was calculated:

$$\vec{P} = -(s_{11}\dot{u}_1 + s_{12}\dot{u}_2)\vec{i} - (s_{12}\dot{u}_1 + s_{22}\dot{u}_2)\vec{j},$$

where s_{ij} are components of the stress tensor; $\dot{u}_i$ is time derivative of the coordinates of the displacement vector.

Fig. 3 shows the propagation of elastic wave energy near a concentrated force whose position on the trajectory is indicated with a red dot. The length of the vector shown corresponds to the amount of energy passing through a given point in space per unit of time, and the direction of the vector indicates the direction of energy transfer.

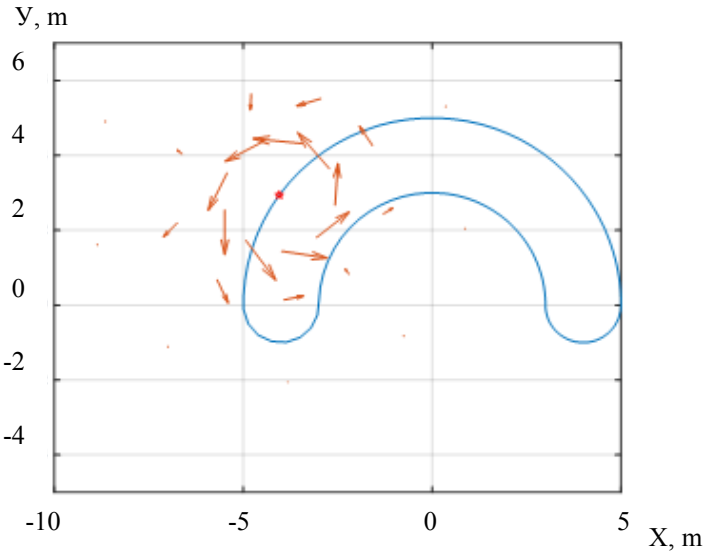

Fig. 3 Energy flux vector (v = 49.3480 m/s)

The calculations have shown that with an increase in the force motion speed, the behavior of displacements and stresses, as well as the nature of the elastic wave energy propagation, changes slightly. Fig. 4 and 5 show the calculation results for speed v = 246.7401 m/s, which exceeds the elastic wave velocity in the plate — c = 221 m/s. The effect of the concentrated force speed on the distribution of vertical displacements W is shown in Fig. 6, 7.

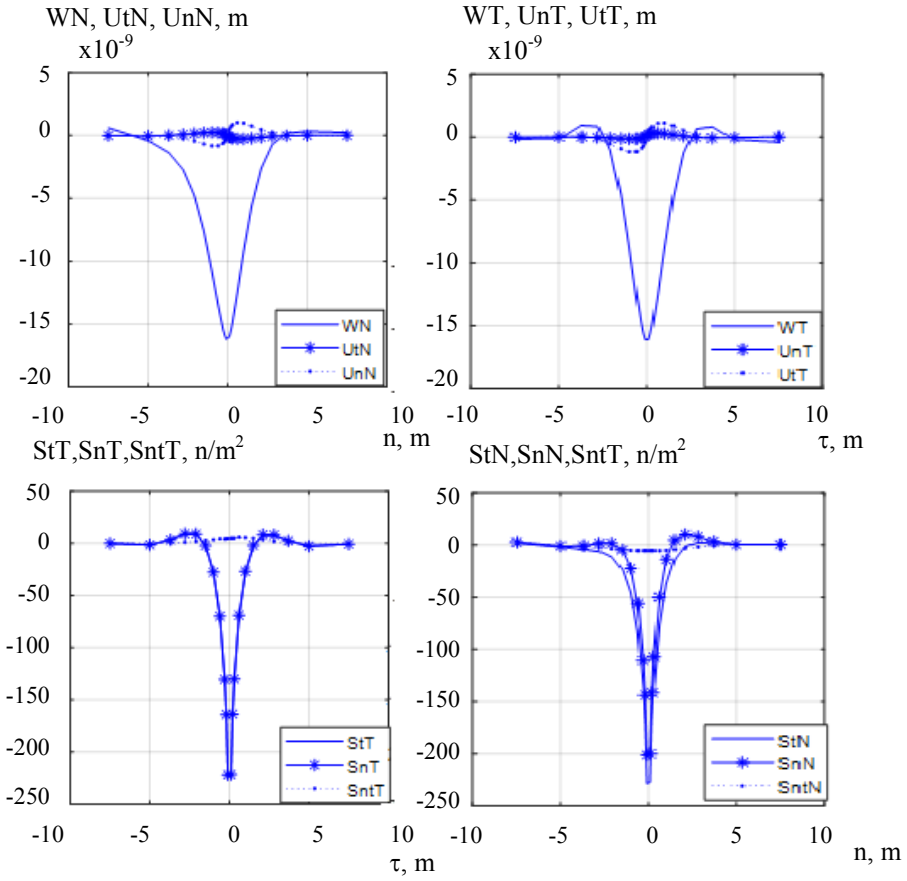

Fig. 4. Variation of displacements and stresses (v =246.7401 m/s)

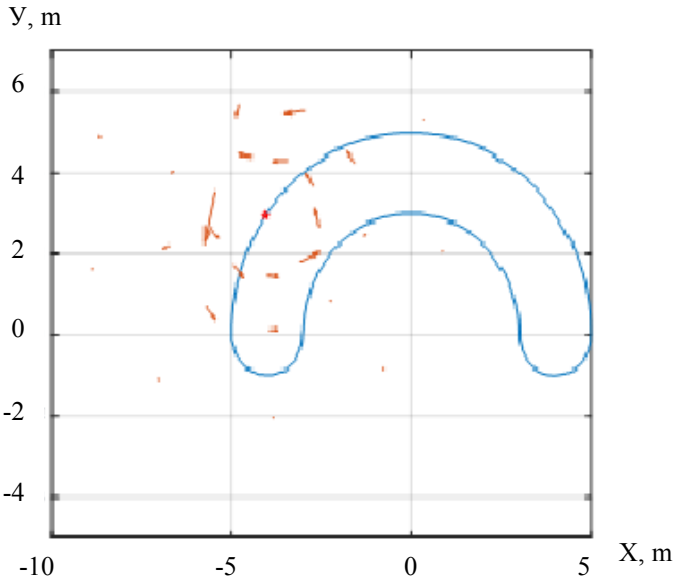

Fig. 5. Energy flux vector (v = 246.7401 m/s)

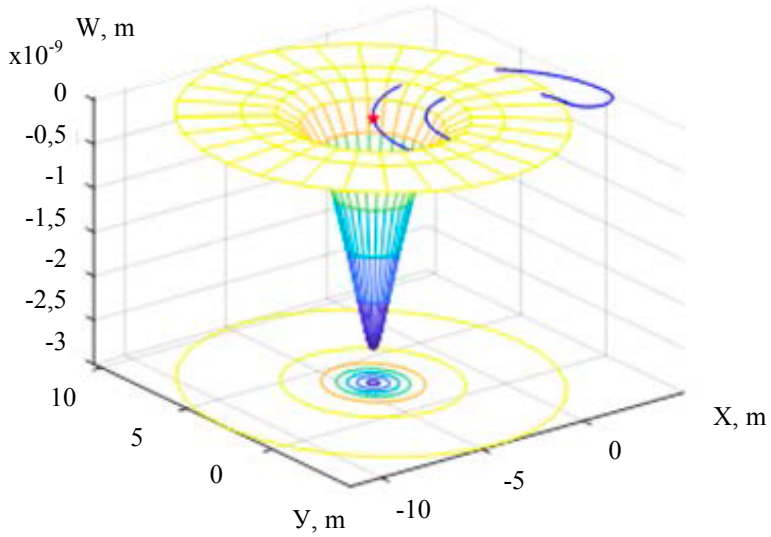

Fig. 6. Variation of vertical displacements at speed v = 49.3480 m/s

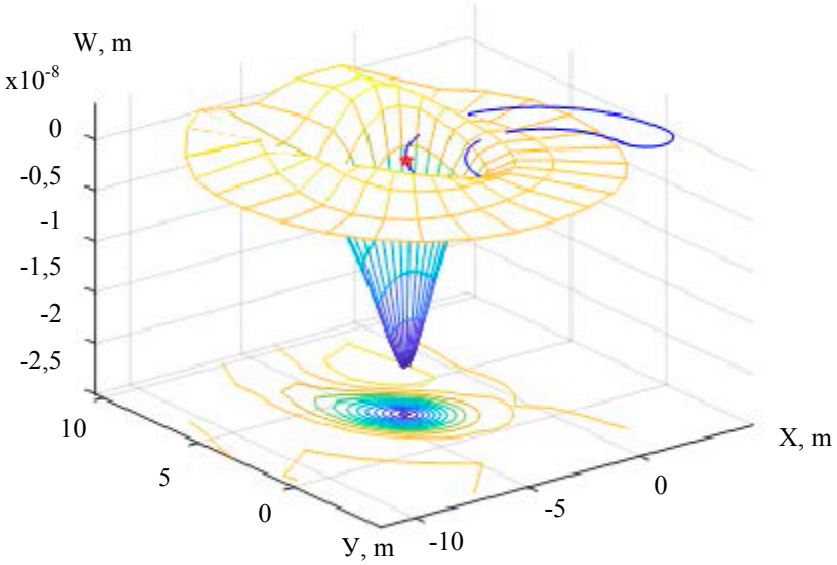

Fig. 7. Variation of vertical displacements at speed v = 493.480 m/s

Fig. 8 and 9 show peak value graphs of displacements and stresses depending on the concentrated force motion speed. The position of the force on the trajectory at the time under consideration is marked with a dot in Fig. 3 and 5.

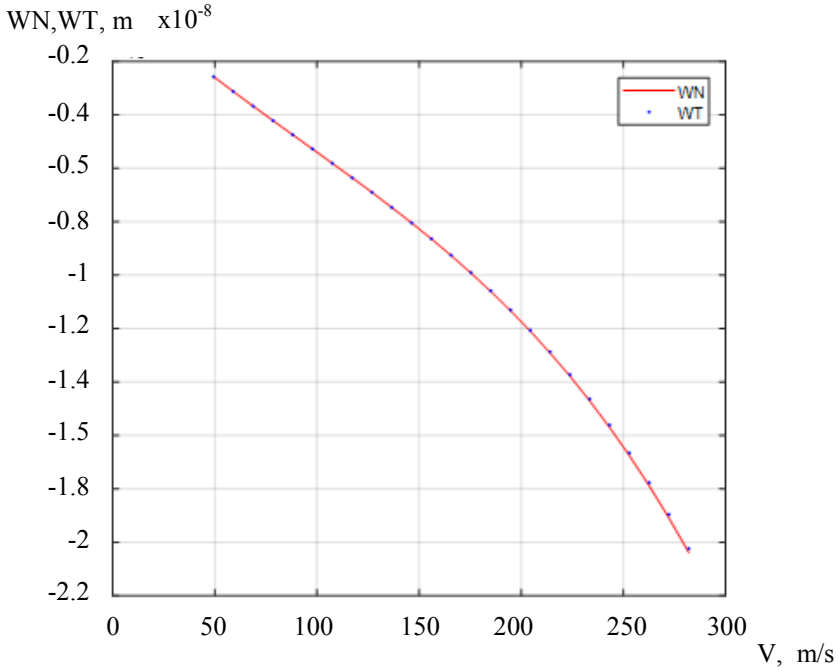

Fig. 8. Change in maximum displacements depending on the concentrated force motion speed

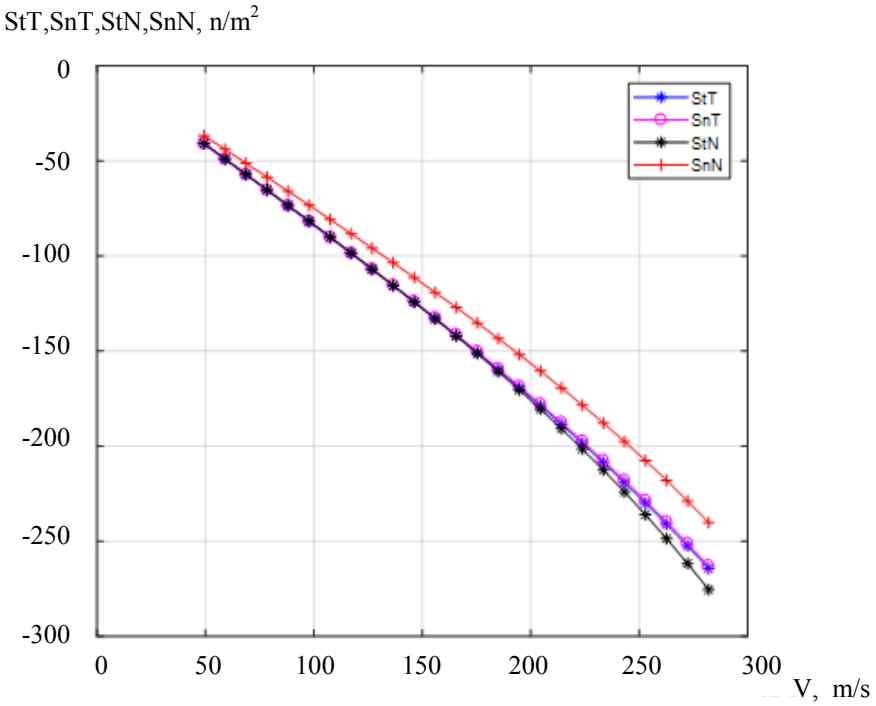

Fig. 9. Change in maximum voltage values depending on the concentrated force speed

Fig. 10 shows the elastic wave energy propagation near a moving concentrated force. The tangential acceleration of the moving force at this moment was equal $w_t = 1.5503$ m/s^2. The calculations are performed for the instant of time $t = T$ with the same law of force motion along the trajectory as in the previous case, hence with the same law of change in the speed and acceleration of the force motion.

At this instant in time, the force was at the point of the trajectory shown in Fig. 10, and its speed was zero. Fig. 11 shows the variation of components of the displacement vector Wt, Utt, Unt and the stress tensor $Stt, Snt, Stnt$ in t axis.

An increase in the force acceleration also caused changes in displacements and stresses and affected the nature of elastic wave energy propagation. Fig. 12 and 13 show the calculation results for the case $w_t = -155.0314$ m/s^2.

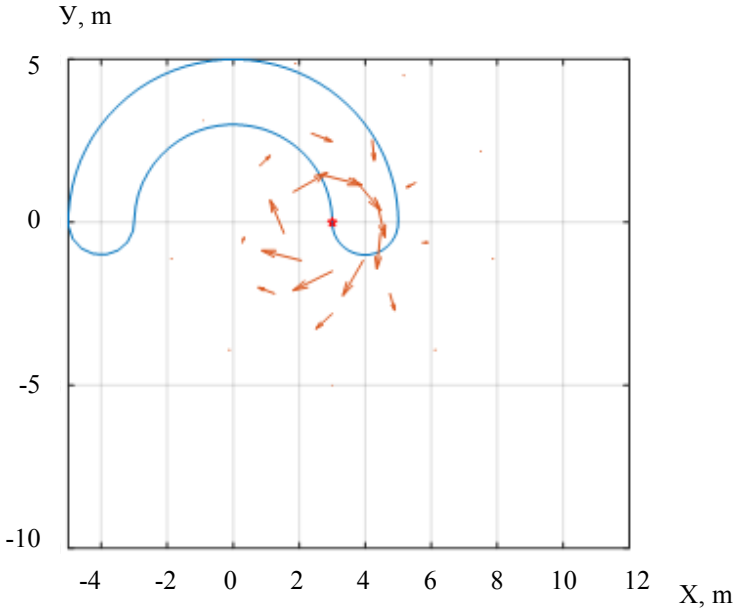

Fig.10 Energy flux vector (w_t = 1.5503 m/s^2)

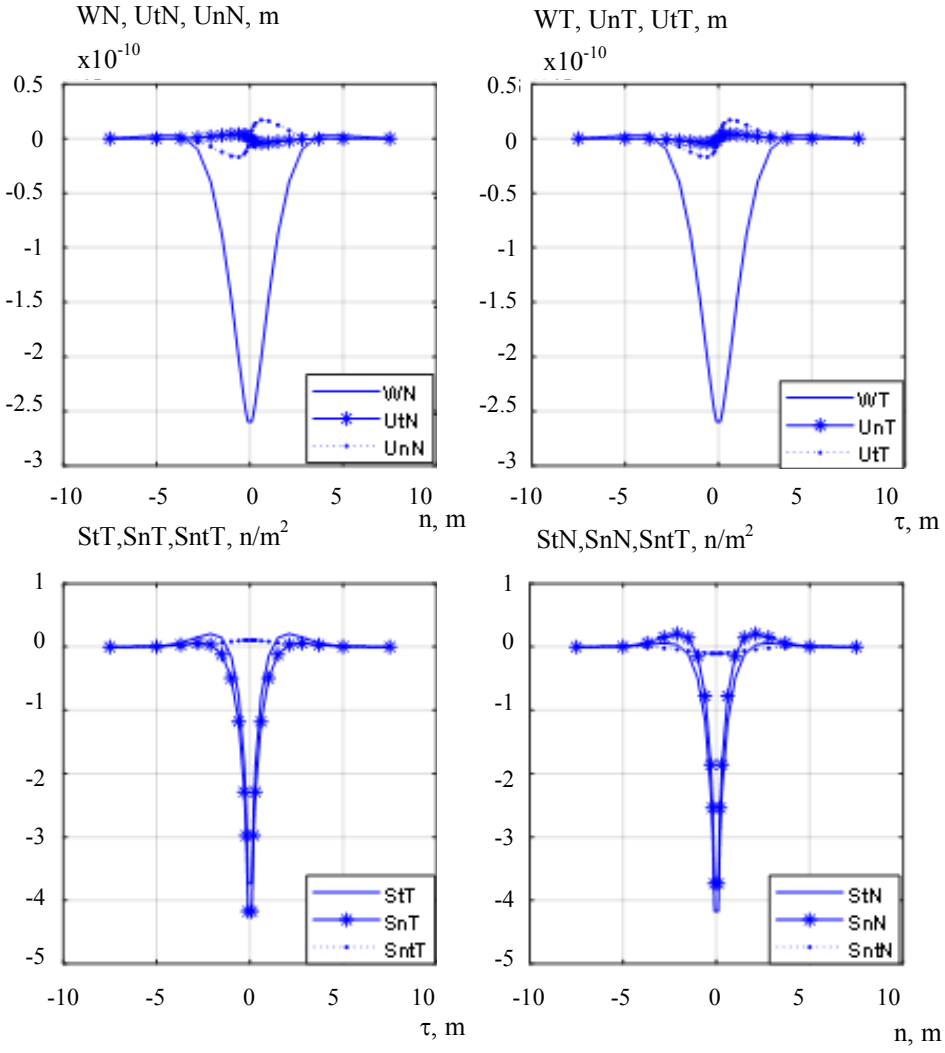

Fig. 11. Variation of displacements and stresses (w_t =1.5503 m/s^2)

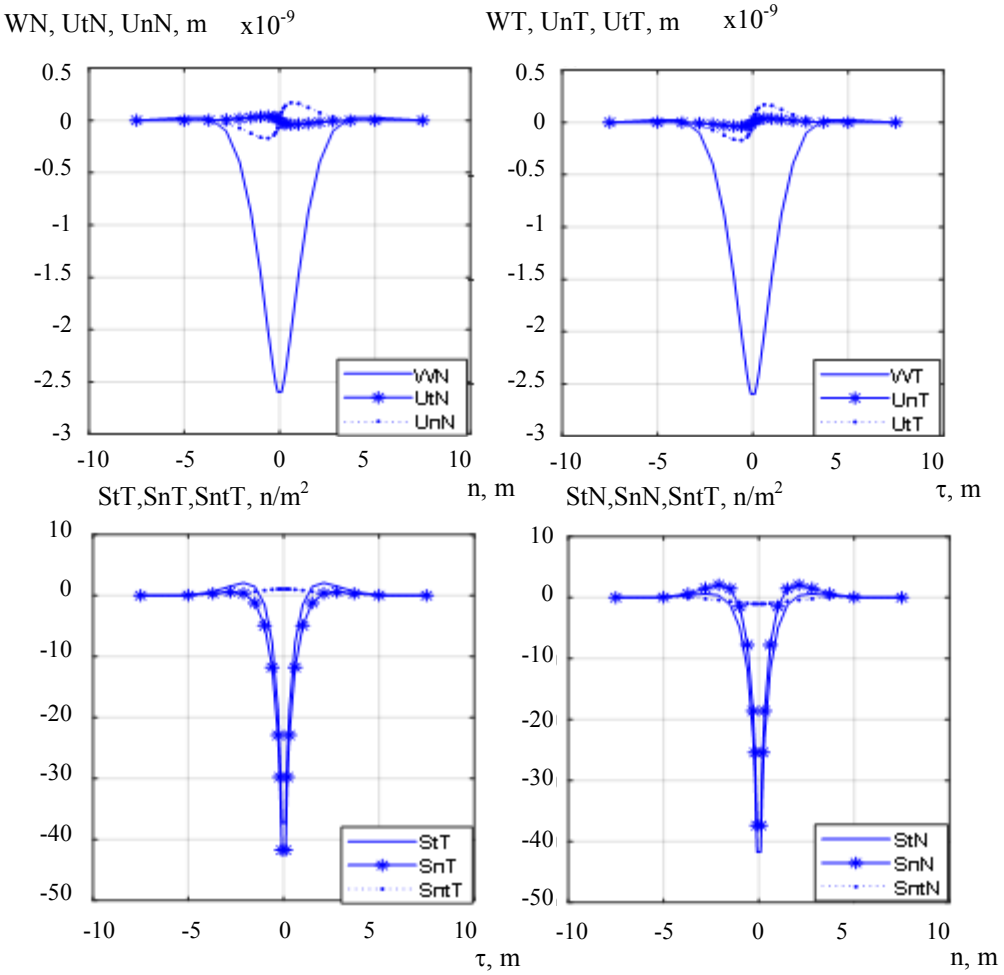

Fig. 12. Variation of displacements and stresses (w_t = 155.0314 m/s^2)

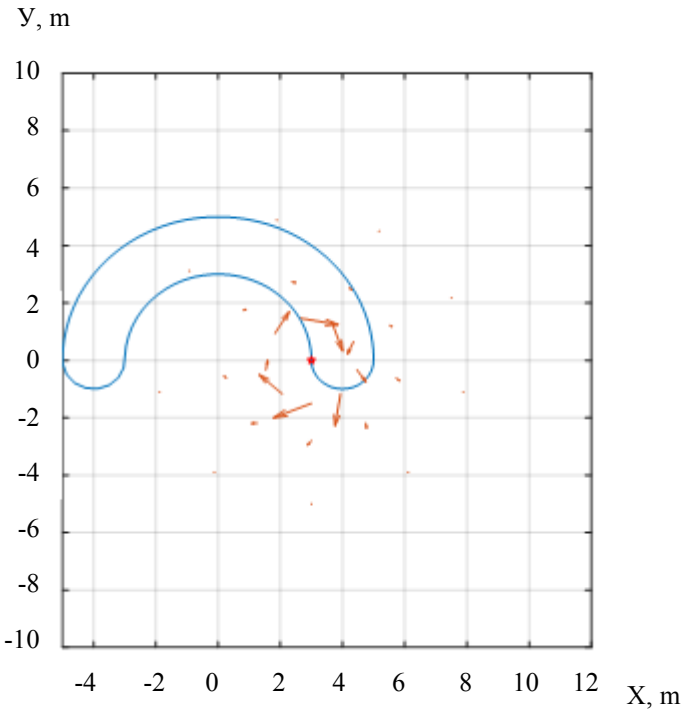

Fig. 13. Energy flux vector (w_t = 155.0314 m/s^2)

Fig. 14 and 15 show peak value graphs of displacements and stresses depending on the tangential acceleration of the concentrated force.

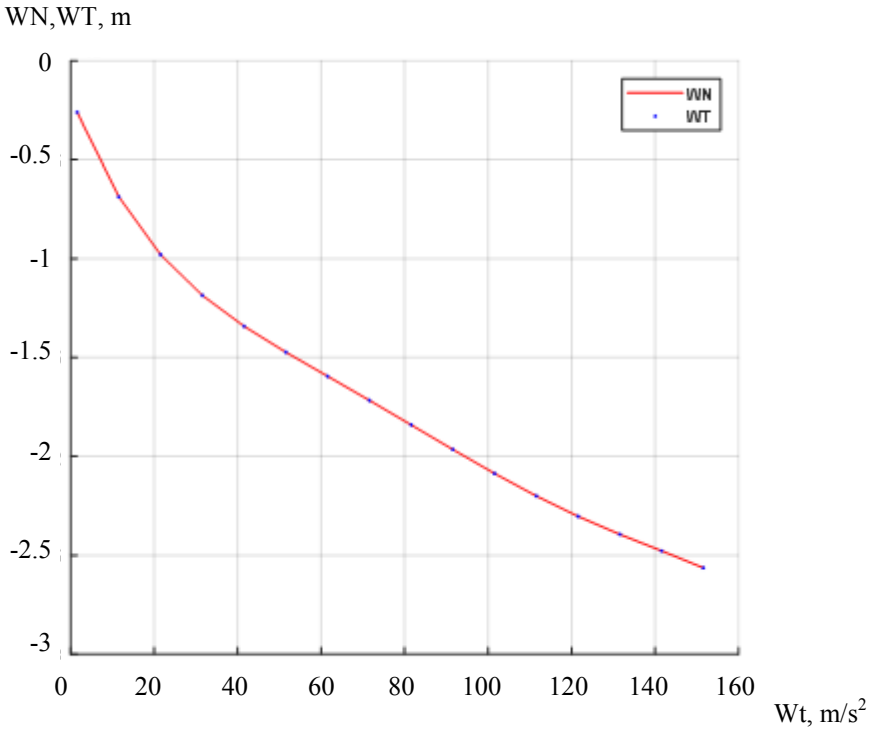

Fig. 14. Peak value graph of displacements depending on tangential acceleration

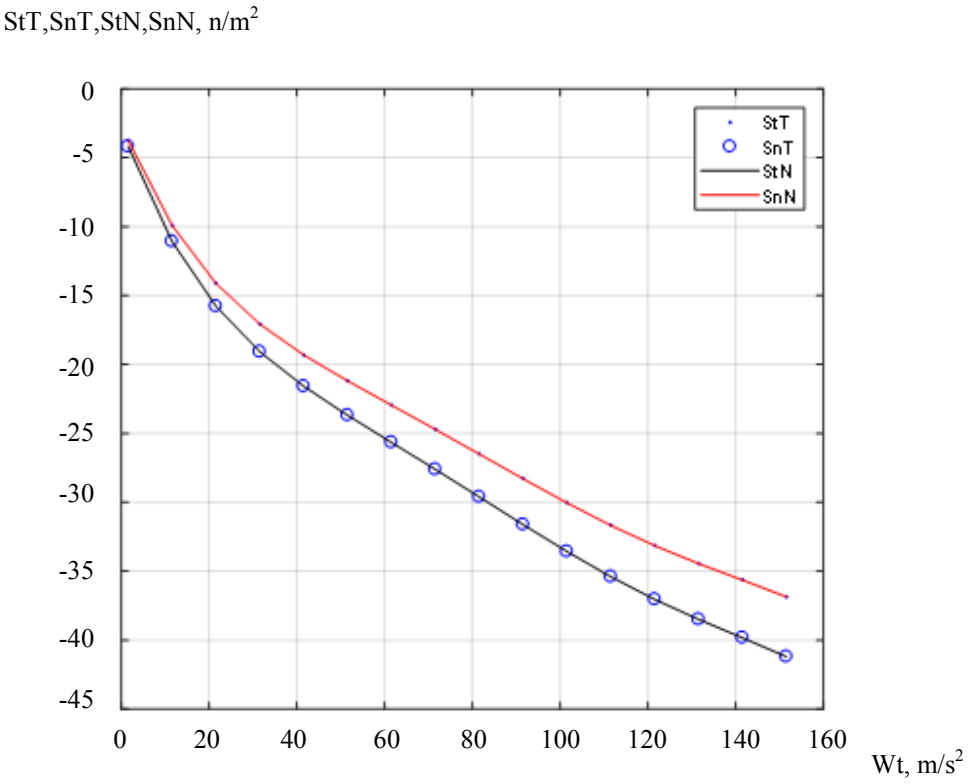

Fig. 15. Peak value graph of stress values depending on tangential acceleration

Discussion and Conclusions. There is a pronounced dependence of the fields of displacements and stresses on the speed and acceleration of the force movement at the parameter variation limits considered above. The nature of elastic wave energy propagation also depends significantly on the speed and acceleration.

Sufficiently large values of the speed and acceleration of the force motion were specially considered to test the proposed method under such conditions. The results obtained allow us to conclude that the method is quite stable over a wide range of variable parameters.

The use of the proposed method is quite acceptable for solving more complex problems. For that, it is required that the differential equations describing them provide the analytical construction of the fundamental solution. This method is economical and simple since it uses already known problem decisions to build a solution.

References

1. Aleksandrov VM, Mark AV. Dvizhenie s postoyannoi skorost'yu zhestkogo shtampa po granitse vyazkouprugoi poluploskosti [Motion of rigid punch over boundary of viscoelastic half-plane at constant velocity]. Journal of Friction and Wear. 2006;27(1):5–11. (In Russ.)

2. Sahin O, Ege N, Erbas B. Response of a 3D elastic half-space to a distributed moving load. Hacettepe Journal of Mathematics and Statistics. 2017;46(5):817–828. DOI: 10.15672 /HJMS.2017.434

3. Kaplunov J, Prikazchikov D, Erbas B, et al. On a 3D moving load problem for an elastic half space. Wave Motion. 2013;50(8):1229-1238. DOI:10.1016/j.wavemoti.2012.12.008

4. Kalinchuk VV, Belyankova TI, Shmid G, et al. Dinamika sloistogo poluprostranstva pod deistviem dvizhushcheisya i ostsilliruyushchei nagruzki [Dynamic of layered half-space under the action of moving and oscillating load]. Vestnik SSC RAS. 2005;1(1):3–11. (In Russ.)

5. Prikazchikov DA. Okolorezonansnye rezhimy v statsionarnoi zadache o podvizhnoi nagruzke v sluchae transversal'no izotropnoi uprugoi poluploskosti [Near-resonant regimes of a steady-state moving load on a transversely isotropic elastic half-plane]. Izvestiya of Saratov University. 2015;15(2).:215–221. (In Russ.)

6. Chen Y, Beskou ND, Qian J. Dynamic response of an elastic plate on a cross-anisotropic poroelastic halfplane to a load moving on its surface. Soil Dynamics and Earthquake Engineering. 2018;107:292–302.

7. Beskou ND, Chen Y, Qian J. Dynamic response of an elastic plate on a cross-anisotropic elastic half-plane to a load moving on its surface. Transportation Geotechnics. 2018;14:98–106.

8. Oblakova TV, Prikazchikov DA. O rezonansnom rezhime v nestatsionarnoi zadache o podvizhnoi nagruzke dlya uprugogo poluprostranstva [On the resonant regime of a transient moving load problem for an elastic half-space]. Engineering Journal: Science and Innovation. 2013;9:1–8. (In Russ.)

9. Kaplunov J, Prikazchikov D, Rogerson GA. The edge wave on an elastically supported Kirchhoff plate. The Journal of the Acoustical Society of America. 2014;136(4):1487–1490. DOI: 10.1121/1.4894795

10. Glukhov YuP. Dinamicheskaya zadacha dlya dvukhsloinoi polosy na zhestkom osnovanii [Dynamic problem for two-layered stripe on the rigid basis]. Proceedings of Odessa Polytechnic University. 2014;2:9–14. (In Russ.)

11. Egorychev OO. Vozdeistvie podvizhnoi nagruzki na mnogosloinuyu vyazkoupruguyu plastinu, lezhashchuyu na vyazkouprugom osnovanii [Effect of a moving load on a multi-layer viscoelastic plate lying on a viscoelastic base]. Vestnik MGSU. 2007;1:39–42. (In Russ.)

12. Doszhanov MZh, Iskak EN, Saktaganov BZh, et al. Dinamicheskoe povedenie bezgranichnoi uprugoi plastinki pri vozdeistvii podvizhnoi (begushchei) nagruzki [Dynamic behavior of infinite elastic plate affected by mobile load]. The Way of Science. 2016;1(11-33):26–28. (In Russ.)

13. Shishmarev KA. Postanovka zadachi o vyazkouprugikh kolebaniyakh ledovoi plastiny v kanale v rezul'tate dvizheniya nagruzki [Problem formulation of ice plate viscoelastic oscillations in a channel caused by a moving load]. Izvestia of Altai State University. 2015;1/2(85):189–194. DOI: 10.14258/izvasu(2015) 1.2–35. (In Russ.)

14. Dyniewicz B, Pisarski D, Bajer CI. Vibrations of a Mindlin plate subjected to a pair of inertial loads moving in opposite directions. Journal of Sound and Vibration. 2017;386:265–282.

15. Esen I. A new finite element for transverse vibration of rectangular thin plates under a moving mass. Finite Elements in Analysis and Design. 2013;66:26–35.

16. Song Q, Shi J, Liu Z. Vibration analysis of functionally graded plate with a moving mass. Applied Mathematical Modelling. 2017;46:141–160.

17. Song Q, Liu Z, Shi J, et al. Parametric study of dynamic response of sandwich plate under moving loads. Thin-Walled Structures. 2018;123:82–99.

18. Qu, Y, Zhang W, Peng Z, et al. Time-domain structural-acoustic analysis of composite plates subjected to moving dynamic loads. Composite Structures. 2019;208:574–584.

19. Foyouzat MA, Estekanchi HE, Mofid M. An analytical-numerical solution to assess the dynamic response of viscoelastic plates to a moving mass. Applied Mathematical Modelling. 2018;54: 670–696.

20. Galaburdin AV. Primenenie metoda granichnykh integral'nykh uravnenii k resheniyu svyaznykh zadach termouprugosti s podvizhnoi nagruzkoi [Applying of boundary integral equation method to the decision of flat problems

of thermoelasticity with mobile load]. Izvestiya vuzov. Severo-Kavkazskiy region. Natural Sciences. 2012;4:29–31. (In Russ.)

21. Galaburdin AV. Primenenie metoda granichnykh integral'nykh uravnenii k resheniyu zadach o dvizhushcheisya nagruzke [Application of a method of the boundary integrated equations to the decision of problems on moving loading]. Izvestiya vuzov. Severo-Kavkazskiy region. Natural Sciences. 2015;1:9–11. (In Russ.)

22. Galaburdin AV. Zadacha o beskonechnoi plastine, nagruzhennoi normal'noi siloi, dvizhushcheisya po slozhnoi traektorii [The problem of infinite plate loaded with normal force following a complex trajectory]. Vestnik of DSTU. 2019;19(3):208–213. (In Russ.)

23. Rekach VG. Rukovodstvo k resheniyu zadach prikladnoi teorii uprugosti [Guide to solving problems in the applied theory of elasticity]. Moscow: Vysshaya shkola; 1973. 384 p. (In Russ.)

24. Zav'yalov YuS, Kvasov BI, Miroshnichenko AL. Metody splain-funktsii [Methods of spline-functions]. Moscow: Nauka; 1980. 352 p. (In Russ.)

Submitted 27.07.2020
Scheduled in the issue 05.10.2020

About the Author:

Galaburdin, Alexander V., associate professor of the Mathematics and Computer Sciences Department, Don State Technical University (1, Gagarin sq., Rostov-on-Don, 344003, RF), Cand.Sci. (Phys.-Math.), associate professor, ORCID: http://orcid.org/0000-0003-0411-6724, Galaburdin@mail.ru

The author has read and approved the final manuscript

MACHINE BUILDING AND MACHINE SCIENCE

UDC 621.9.015 https://doi.org/10.23947/2687-1653-2020-20-4-382-389

Rationale for granulometric medium characteristics under vibration processing of parts with small grooves and holes

M. A. Tamarkin[1], E. N. Kolganova[1], M. A. Yagmurov[2]
[1] Don State Technical University (Rostov-on-Don, Russian Federation)
[2] North Caucasus Federal University (Stavropol, Russian Federation)

Introduction. The design technique for a highly efficient technological process of vibration finishing of parts with small grooves and holes is presented. The decision is based on the selection of the granulometric characteristics of the processing environments. The cross-sectional shape and geometrical dimensions of burrs on typical parts of radio electronic equipment (REE) are analyzed. A generalized burr model has been developed. Methodological principles for the selection of particle size characteristics of operating environments are determined.

Materials and Methods. The new classification and coding according to the constructive and technological principles of REE components will provide reasonable selection of the equipment, environments and modes when designing their finishing process.

Results. A technique has been developed for selecting the granulometric characteristics of operating environments with the account of the major technological problems. Based on the design and technological features of the REE components, the dependences are proposed for determining the size and shape of the processing granules. The acceptance criteria for evaluating the results of vibration processing are determined. It is noted that one of the major tasks in the vibration processing of parts with small grooves and holes is to provide such in-process time at which burrs are removed, and the roughness and other surface parameters meet the technical requirements. In this case, the accuracy of the linear dimensions of the processed surfaces should be considered an indicator of quality. Quantitatively, this criterion is assessed on a specific index whose calculation considers the largest actual size before vibration processing, the burr height, the smallest allowable size after processing, and the tolerance established by the technical requirements. The process efficiency criterion is defined as the ratio of the machinability index to the processing time of a batch of parts or the cycle time per part. The proposed criterion enables to compare treatment processes under validating the solution to technological problems.

Discussion and Conclusions. The study results enable to confirm that vibration processing in the organic environment contributes to the effective removal of burrs and edge smoothing of small-sized parts of electronic equipment with small grooves and holes.

Keywords: vibration treatment, roughness, surface pattern, burrs, edge smoothing.

For citation: M. A. Tamarkin, E. N. Kolganova, M. A. Yagmurov. Rationale for granulometric medium characteristics under vibration processing of parts with small grooves and holes. Advanced Engineering Research, 2020, vol. 20, no. 4, pp. 382–389. https://doi.org/10.23947/2687-1653-2020-20-4-382-389

Introduction. The recently increased demand for precision machining of parts is particularly topical in the machine and instrument industry, since in these industries, the annual volume of manufactured parts exceeds hundreds of thousands of pieces. It should be emphasized that the details of radio-electronic equipment (REE) have a rather complex configuration of the outer contour. Most of them are characterized by such non-technological elements as grooves and

small holes, deep holes, blind threaded holes, etc. Finishing of such parts in granular media has proved its effectiveness [1, 2]. Currently, there are no methods for designing finishing and clearing operations for such parts, which limits the widespread introduction and further improvement of vibration processing.

Materials and Methods. Based on the design-engineering analysis of REE parts manufactured at the instrument-making plant, classification was developed and their coding was performed according to the design-engineering principles. The new classifier will provide selecting equipment, environments and operation modes at the design stage of the part finishing process with account for their design-engineering features.

Finishing and clearing processing plays a special role in providing the quality of REE parts, which is difficult to perform under modern production conditions due to the complex structural shape of products.

One of the major methods of forming blanks in mechanical engineering and instrument making is edge cutting machining. However, any mechanical processing based on cutting results in defects such as burrs, sharp edges, etc. They occur due to the laws of continuum mechanics, so these disadvantages cannot be excluded even when using modern processing centers and optimum processing modes. As a result, functional, aesthetic, and ergonomic problems may occur during the manufacture and operation of parts [3, 4]. This proves urgency of the problem of deburring under finishing and clearing operations of REE parts.

The research work objective is to improve the methodology for designing highly efficient vibration treatment of parts with small grooves and holes based on the selection of granulometric characteristics of flexible working environments.

To achieve this goal, it is necessary to solve the following tasks:

— to analyze cross-section shapes and geometric characteristics of burrs on typical parts of devices,

— to develop a generalized burr model,

— to justify methodological approaches when choosing granulometric characteristics of processing environments.

To study the geometry and parameters of the cross-section profile of burrs, micro-sections were examined using a metallographic inverted microscope equipped with the Thixomet Pro system. As the study has shown, the main shape of the burr cross section is a triangle. At the same time, the height of the burr is on average 2-3 times greater than the thickness of its base, and the linear thickness sizes do not exceed 0.4 mm (Fig. 1).

a)

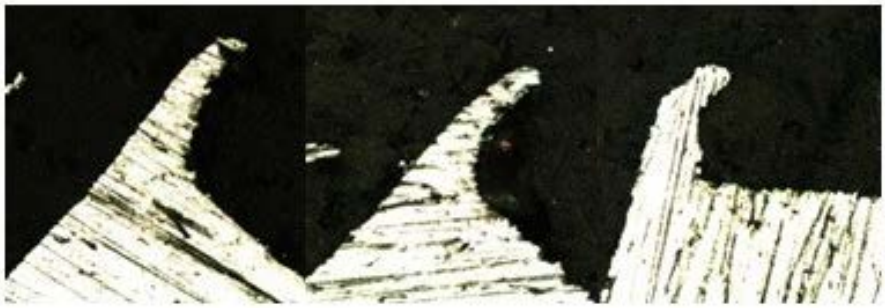

b)

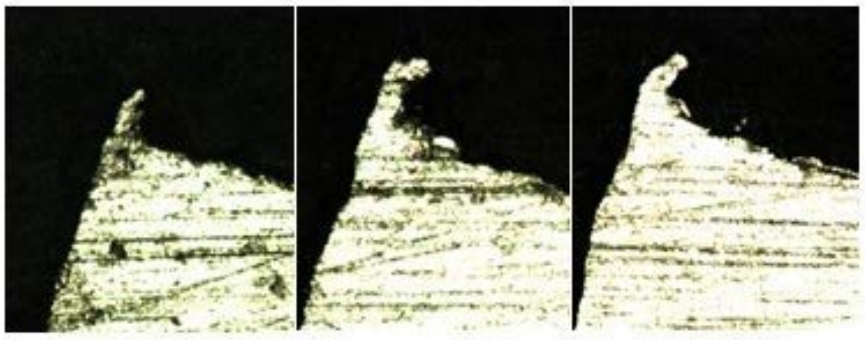

c)

Fig. 1. Cross section of burrs in the studied samples. Sample material: *a*) BrOC4-3; *b*) LS-59-1; *c*) AMg6

In this case, the choice of characteristics of the processing environment has a decisive influence on the surface quality of parts and process performance [5–7]. At enterprises, they use working media whose granules can be classified according to their geometric shape and size, material, and size of cutting grains, as well as material of a bundle of grains, structure and the production method.

For ease of designing finishing and clearing vibration treatment, a system classification and coding of granules of working media is proposed.

Finishing and clearing of REE parts provides for deburring and surface preparation for coatings. In instrument engineering, various coatings are used: galvanizing, cadmium-plating, nickelizing, chrome-plating, brassing, palladizing, silvering, gold plating, passivation, etc. To the surface patches of the electrocontact parts of devices, electrolytic coatings (silver, gold) are applied. They are characterized by high electrical and thermal conductivity and chemical resistance under the increased humidity conditions [8, 9]. Electroplating requires a certain quality of the workpiece. No burrs or sharp edges are allowed.

As the analysis of structures under finishing and clearing REE parts has shown, environments that meet the following requirements should be used:

— high density (at least 1.2 g/cm^2) with a low weight of the granule;

— suitable for processing non-rigid workpieces;

— suitable for processing workpieces with angled surfaces and areas with limited access to the granule of the processing environment;

— high wear resistance and ability to keep its shape during processing;

— uniform structure of the granules.

Taking into account these requirements and the data of the works [10, 11], it should be recognized that the use of stone granular media are most appropriate. When crushing the fruit pips and walnut shells, freeform granules with V-shaped edges are formed. Thanks to this, the granule becomes an analog of a cutting tool. In this case, different areas of the part are available for microcutting.

Research Results. So, environments made of natural materials are optimal for finishing and clearing REE parts with small grooves and holes. The widespread use of this approach is hindered by insufficient knowledge of such environments and the unavailability of methods for designing finishing and clearing operations using them.

As a rule, under finishing and clearing vibration processing of REE parts, three technological tasks arise.

First. If it is sufficient to remove the burrs and smooth the edges on the workpieces, there is no need to process the internal surfaces of the grooves and holes. This is the most typical task that is solved under processing parts. In general, it can be solved through applying granules with size R_{rp}, greater than the size of the largest hole or groove L, i.e., $R_{rp} > L$. This will eliminate jamming in them.

The processing environment contact will be considered as the contact of a single granule until the burr is completely removed and the required amount of edge smoothing is obtained (Fig. 2).

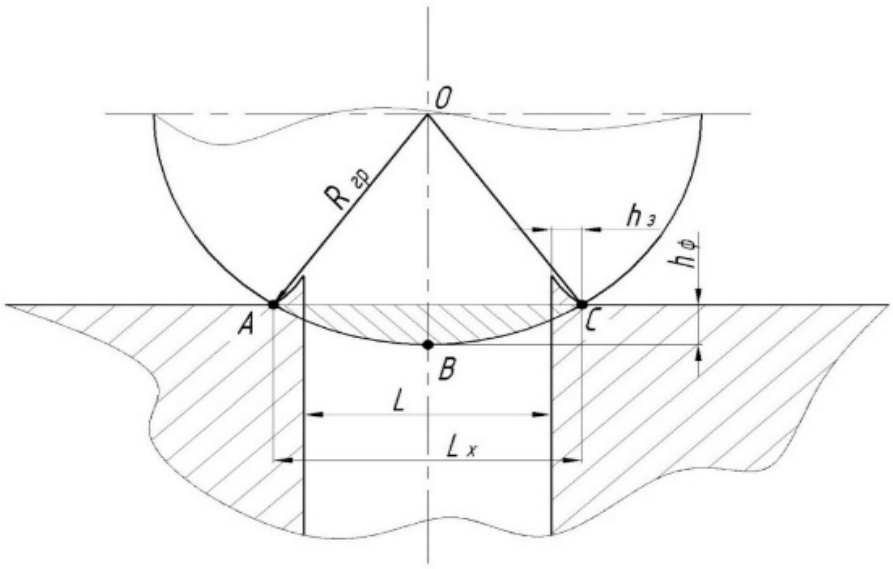

Fig. 2. Geometric layout of granule contact with hole edges

We take into account the wear coefficient of the granule K_u, which largely determines the consumption of the processing environment, as well as the process performance and the quality of the surfaces. The optimal radius of the working medium granule is determined by the expression:

$$R_{\text{гр}} = K_{\text{и}} \frac{(L+2h_{\text{з}})^2+h_{\text{ф}}^2}{8h_{\text{ф}}},$$

where $h_{\text{з}}$ — thickness of the base of the formed burr, mm; $h_{\text{ф}}$ — chamfer size that meets the technical requirements, mm; L — linear or diametric value of the processed element, mm.

Compliance with this condition guarantees the burr removal on the outer surfaces and providing the radius of smoothing edges required by the drawing.

Second. This problem occurs when it is necessary to process and prepare for coating the internal surfaces of grooves or holes. In this case, the criterion for selecting the particle size should be the size of the smallest hole or groove L_{min} of the part.

To avoid jamming of the working environment particles in the holes and grooves, it is recommended to select their size from the ratio:

$$D_{\text{гр}} = 0.6 \div 0.7 L_{min},$$

where $D_{\text{гр}}$ — effective diameter of the processing environment granules, mm.

However, when selecting the size of the working environment particles using this ratio, it is critically important to analyze its applicability for processing other holes and grooves of the part that are larger than L_{min}. If their size is equal to $2D_{\text{гр}}$ or $3D_{\text{гр}}$, it is possible to jam the particles of the working environment, which will interrupt processing the surface of the hole or groove. To prevent this phenomenon, the dimensions of the holes and grooves to be processed L should be within the range $L_{min} < L < 1.7D_{\text{гр}}$, $2.2D_{\text{гр}} < L < 2.7D_{\text{гр}}$, $L > 3.2D_{\text{гр}}$ (Fig. 3).

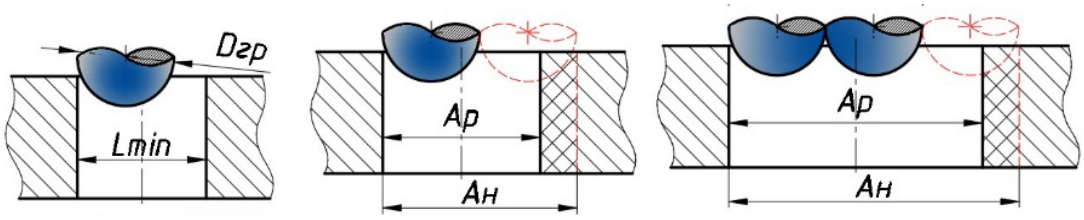

Fig. 3. Dimensions of holes that prevent jamming of the working environment bodies:
Ar — recommended size, An — unacceptable size

Third. The primary process task is treatment of the interface points of surfaces. Its solution causes the greatest difficulties, since it is hard for granules to reach surfaces that are at an angle to each other. One example is thread. If the technical requirements of the part specify the radius of the interface of the surfaces, the size of the granule of the working environment must be equal to it or less:

$$R_{\text{гр}} \leq r.$$

As shown in [12–14], due to violation of this condition, three conditional zones can be formed during vibration treatment of angled surfaces:

— a dead zone (no processing occurs in it)

—- an open zone,

— an unstable roughness zone (Fig. 4).

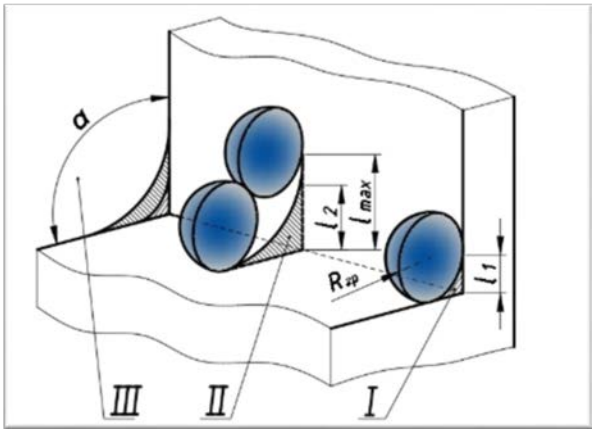

Fig. 4. Untreated areas that occur with the wrong selection of granule sizes

The dimensions of the dead zone and the zone with unstable roughness can be calculated from the formulas:

$$CD \le R_{\text{гр}}\left[\frac{1}{\cos\frac{180^0-\alpha}{2}}-1\right];$$

$$CB = R_{\text{гр}}\tan\frac{180^0-\alpha}{2}.$$

For processing hard-to-reach surfaces with organic V-shaped particles, we can introduce the concept of the granule permeability coefficient, which is determined from the ratio of the mating angle of the surfaces to the angle of the V-shaped edge forming the cutting edge:

$$K_{\text{пр}} > \frac{\alpha}{\beta}.$$

Considering the permeability coefficient when selecting the shape of granules will solve a complicated process task associated with finishing treatment of surface interfaces.

To control the finishing and clearing result, it is required to formulate criteria for the validity of parts or their batches. For REE parts, these criteria will be the surface roughness parameters and the stability of the quality characteristics of the treated surface (Fig. 5).

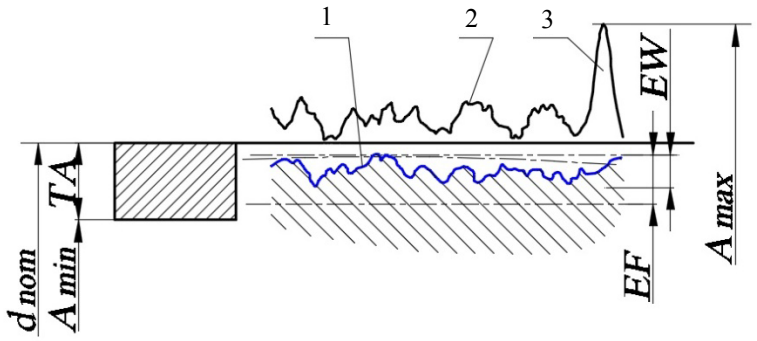

Fig. 5. Scheme for determining the processibillity index: 1 — surface roughness after processing; 2 — actual surface roughness; 3 — burr; *EW* — waviness deviation; *EF* — shape deviation; A_{max} — the largest size before processing with account for the burr height; A_{min} — minimum size after processing; TA — tolerance for the processed size

The main condition for solving this process problem:

$$\overline{R}_t - \delta > [R_{imin}],$$

where $\overline{R}_t$ — the average statistical reading of the data values taken by the indicators, which correspond to the arithmetic mean deviation of the reference surface contour; δ — the scattering field of the values of qualitative indicators, which cor-

respond to the values of metal removal rates under processing; $[R_{imin}]$ — the value of the quality indicators within tolerance.

Quality indicators within a batch of parts will be random variables distributed according to probabilistic laws. Therefore, the criteria for batch validity (i.e., the optimality of the proposed technology) can be set by the inequality proposed above. At the same time, you need to take into account the defective ratio that does not exceed the probability *Pi* [15]:

$$P_i\left(\left|R_{ij} - \bar{R}_i\right| \geq \delta\right) < \frac{D_i}{\delta^2},$$

where P_i — the probability of *i*-th quality indicator falling outside the boundaries of the scattering field; D_i — the calculated value of variance R_i.

One of the main tasks under the vibration treatment of parts with small grooves and holes is to provide such process duration at which burrs are removed, and the roughness and other surface parameters meet the technical requirements. The quality indicator is the accuracy of the linear dimensions of the processed surfaces. This criterion is quantified by the processibillity index (Fig. 5):

$$C_{\text{o}} = \frac{A_{max} - A_{min}}{\text{TA}},$$

where A_{max} — the largest valid size before vibration processing with account for the burr height; A_{min} — minimum permissible dimension after treatment; TA — work dimensional tolerance set by technical requirements (Fig. 5).

The criterion of process efficiency is defined as the ratio of the processibillity index to the duration of the processing of batch of parts, or cycle time reduced to one part:

$$K_{\text{э}} = \frac{C_o}{t_{\text{ц}}}.$$

The proposed criterion provides comparing treatment processes when justifying the solution to the problems.

Discussion and Conclusions. The paper analyzes the cross-section shape and geometric dimensions of burrs of typical parts of REE devices. A generalized burr model has been created, and methodological principles for selecting the characteristics of granules of working environments have been proposed.

Methods for selecting granulometric characteristics of processing media depending on the main process tasks are described. Dependences are obtained for determining the size and shape of processing granules based on the design and technological features of REE parts. The validity criteria for evaluating the vibration treatment results are proposed.

The study results suggest that finishing and clearing vibration treatment in an environment of crushed pips contributes to the effective removal of liquids, including burrs, as well as the edge smoothing in the radio-electronic equipment parts of complex configuration.

References

1. Kolganova EN, Goncharov VM, Fedorov AV. Investigation of deburring process at vibro-abrasive treatment of parts having small grooves and holes. Materials today. 2019;19(5):2368–2373.

2. Tamarkin MA, Smolentsev EV, Kolganova EN. Analiz sovremennogo sostoyaniya finishnykh metodov obrabotki v srede svobodnykh abrazivov detalei, imeyushchikh malye pazy i otverstiya [Analysis of the modern condition of deburring details having small grooves]. Bulletin of Voronezh State Technical University. 2019;15(1):122–129. (In Russ.)

3. Antonova NM, Shorkin VS, Romashin SN, et al. Adhesion of a vibration mechanochemical solid-lubricant MoS(2) coating. Journal of Surface Investigation: X-ray, Synchrotron and Neutron Techniques. 2019;13(5):848–854. DOI: 10.1134/S1027451019040025

4. Ivanov VV, Babichev AP, Pogorelov NP. The research of technological characteristic of the vibrowave mechanical and chemical oxide coating formation. In: 13th International scientific-technical conference on dynamic of technical systems (DTS): MATEC Web of Conferences. 2017;132:01004. DOI: 10.1051/matecconf/201713201004

5. Ivanov VV, Popov SI, Kirichek AV. Qualitative Characteristics of MoS2 Solid-Lubricant Coating Formed by Vibro-Wave Impact of Free-Moving Indenters. Key Engineering Materials. 2017;736:18–22.

6. Lebedev VA, Serga GV, Khandozhko AV. Increase of efficiency of finishing-cleaning and hardening processing of details based on rotor-screw technological systems. In: IOP Conference Series. Materials Science and Engineering. 2018;327:042062. DOI: 10.1088/1757-899X/327/4/042062

7. Babichev AP, Ivanov VV, Motrenko PD. Issledovaniya osnovnykh tekhnologicheskikh parametrov formirovaniya vibratsionnogo mekhanokhimicheskogo pokrytiya i kachestva oksidnoi plenki [Research of the main technological parameters of the formation of a vibrational mechanochemical coating and quality of the oxide film]. Strengthening Technologies and Coatings. 2011;5:33–38. (In Russ.)

8. Antonova NM. Evaluation of adhesion strength of protective coatings with Al powder by adhesion work of initial suspension towards metal surface. In: International Conference on Modern Trends in Manufacturing Technologies and Equipment (ICMTMTE 2018): MATEC Web of Conferences. 2018;224(1):03011. URL: https://www.matec-conferences.org/articles/matecconf/pdf/2018/83/matecconf_icmtmte2018_03011.pdf (accessed: 12.11.2020).

9. Antonova NM, Zinovjev IA, Khaustova EU, et al. Opredelenie adgezii putem tsifrovoi obrabotki izobrazhenii poverkhnosti pokrytii [Determination of adhesion by digital image processing of surface coatings]. Engineering Journal of Don, 2019, no. 1. URL: ivdon.ru/ru/magazine/archive/n1y2019/5549 (accessed: 20.10.2020). (In Russ.)

10. Lebedev VA, Krupenya EYu, Shishkina AP. Povyshenie ehffektivnosti vibratsionnoi otdelochnoi obrabotki detalei na osnove primeneniya sred organicheskogo proiskhozhdeniya [Improving the efficiency of vibration finishing of parts based using organic media]. In: Advanced engineering technologies, equipment and tools. A.N. Kirichek, ed. Moscow: Spektr. 2015;6:268–326. (In Russ.)

11. Lebedev VA, Serga GV, Khandozhko AV. Increase of efficiency of finishing-cleaning and hardening processing of details based on rotor-screw techno-logical systems. In: IOP Conference Series. Materials Science and Engineering. 2018;327(4):042062. DOI: 10.1088/1757-899X/327/4/042062

12. Zverovshchikov AE. Rasshirenie tekhnologicheskikh vozmozhnostei ob"emnoi tsentrobezhno-planetarnoi obrabotki [Enhancement of solid centrifugal-planetary machining]. Science Intensive Technologies in Mechanical Engineering. 2013;7:17–23. (In Russ.)

13. Martynov AN, Zverovshchikov VZ, Zverovshchikov AE. Opredelenie skorosti rezaniya pri ob"emnoi tsentrobezhno-planetarnoi obrabotke [Determination of the cutting speed under high volume centrifugal planetary processing]. Vestnik Mashinostroeniya. 1996;9:25–27. (In Russ.)

14. Zverovshchikov VZ, Ponukalin AV, Zverovshchikov AE. O formirovanii sherokhovatosti poverkhnosti na trudnodostupnykh uchastkakh profilya detali pri ob"emnoi tsentrobezhnoi obrabotke granulirovannymi sredami [On the surface roughness formation on the detail profile hard-to-reach areas under large centrifugal processing with granulated media]. University Proceedings. Volga region. Technical Sciences. 2010;3(15):114–122. (In Russ.)

15. Shtyn SU, Lebedev VA, Gorlenko AO. Thermodynamic aspects of the coating formation through mechanochemical synthesis in vibration technology systems. In: IOP Conference Series. Materials Science and Engineering. 2016;177:012127. DOI: 10.1088/1757-899X/177/1/012127

Submitted 01.07.2020
Scheduled in the issue 05.09.2020

About the Authors:

Tamarkin, Mikhail A., Head of the Engineering Technology Department, Don State Technical University (1, Gagarin sq., Rostov-on-Don, 344003, RF), Dr.Sci. (Eng.), professor, ORCID: http://orcid.org/0000-0001-9558-8625, tehn_rostov@mail.ru

Kolganova, Elena N., postgraduate student of the Engineering Technology Department, Don State Technical University (1, Gagarin sq., Rostov-on-Don, 344003, RF), ResearcherID: AAL-5802-2020, ORCID: https://orcid.org/0000-0002-9466-9658, elenkolg@list.ru

Yagmurov, Mikhail A., senior lecturer of the Engineering Technology and Process Equipment Department, Institute of Engineering, North-Caucasus Federal University (1, Pushkin St., Stavropol, 355017, RF) Researcher-ID: AAL-6938-2020, ORCID: https://orcid.org/0000-0003-4554-0257, myagmurov@gmail.com

Claimed contributorship

M. A. Tamarkin: academic advising; analysis of the research results; correction of the conclusions. E. N. Kolganova: basic concept formulation; research objectives and tasks setting; text preparation; formulation of conclusions. M. A. Yagmurov: computational analysis; the text revision.

All authors have read and approved the final manuscript.

MACHINE BUILDING AND MACHINE SCIENCE

UDC 621 https://doi.org/10.23947/2687-1653-2020-20-4-390-396

Technological features of crankshaft hardening by vibration shock method

V. A. Lebedev[1], F. A. Pastukhov[1], M. M. Chaava[1], G. V. Serga[2]
[1]Don State Technical University (Rostov-on-Don, Russian Federation)
[2]Kuban State Agrarian University (Krasnodar, Russian Federation)

Introduction. The technological features of the processing crankshafts by the vibration shock method of surface plastic deformation (SPD), which is widely used in the technology of manufacturing machine parts, are considered. The research objective is to justify the efficiency of the influence of vibration shock hardening treatment on improving the quality and performance of crankshafts (CS).
Materials and Methods. The methodological studies included the validation of the vibration shock processing flowchart and the development of an analytic model for assessing the effect of processing on the change in the macrogeometry (warpage) of the CS.
Results. Flowcharts have been developed for volumetric vibration shock finishing and hardening treatment of CS using a vibratory machine with a U-shaped work chamber. Its overall dimensions measure alike or exceed the overall dimensions of the CS being processed, and ensure the location of the shaft in such a way that its main axis, coinciding with the axis of the main bearing journals, is in the zone of the conditional axis of working mass rotation. The surface quality parameters were investigated during their processing on the UVG 4X10 vibratory unit according to the proven techniques using the dedicated tooling. It has been established that the vibration shock hardening treatment (ViHT) enables, due to plastic deformation of microroughness, to obtain a qualitatively new surface microrelief and to reduce its initial roughness, to drastically increase the surface microhardness of the CS main and rod journals; at that, it changes the stressed state of their surface layer. A calculated dependence is proposed to assess the total warpage of the CS strengthened under the ViHT, and its adequacy is confirmed. It is shown that the warpage of the shaft after the ViHT is due to the different tension of the rod and main journals of the CS at the level of $K_н \approx 0.6$.
Discussion and Conclusions. Vibration shock treatment of CS provides an improvement in the geometric and physicomechanical parameters of surfaces of the rod and main journals. As a result of processing all surfaces of the shaft, warpage does not exceed the permissible values established by the technical requirements. So, we can conclude on the efficiency of the considered method of hardening CS with the aim of increasing their operational properties.

Keywords: crankshaft, surface plastic deformation, vibration shock method, hardening, surface quality, warpage.

For citation: V. A. Lebedev, F. A. Pastukhov, M. M. Chaava, et al. Technological features of crankshaft hardening by vibration shock method. Advanced Engineering Research, 2020, vol. 20, no. 4, pp. 390–396. https://doi.org/10.23947/2687-1653-2020-20-4-390-396

Introduction. A set of measures to preserve the accuracy of the CS achieved through forming includes improving the methods for obtaining blanks, mechanical processing, as well as the introduction of strengthening treatment operations into the general process designed to enhance the service properties of these products. One of the most common SPD methods that strengthen chamfers and increase the fatigue resistance of CS is running-in and caulking [1–7]. However, the CS strengthening through methods of running-in and caulking chamfers is accompanied by their warpage, which causes an increase in the main journal runout, the violation of the initial geometric shape that requires additional adjustment. In this regard, the development of new processing techniques of finishing and strengthening by SPD methods, which increase the reliability and durability of CS under difficult operating conditions, is urgent. Of particular interest in this area is vibration shock treatment, which has received wide practical application in the technology of manufacturing machine parts [8–15]. In this regard, the research objective is to validate the effectiveness of the vibration-shock hardening impact on the quality and performance of CS.

Materials and Methods. To achieve this goal, the following tasks are set:

— to develop flowcharts for vibration shock hardening of all components of CS;

— to study the impact of vibration shock treatment on the geometric and physicomechanical parameters of the surface of rod and main journals;

— to propose a computational model for assessing changes in the macrogeometry (warpage) of CS under vibration shock treatment and validate it.

The research was carried out on the UVG 4X10 vibratory unit according to the proven techniques. A special device simulating a crankshaft was used to determine the quality parameters of the hardened surface. The measurement results were processed using mathematical statistics. The warpage of the studied shafts was determined through measuring the radial runout of the journals before and after hardening by an indicator reading in 0.01 mm. At the same time, the CS was installed with its main journals on prismatic supports and rotated by hand.

Research Results. Fig. 1 shows flowcharts for volumetric vibration shock finishing and hardening treatment of CS using a vibratory machine with a U-shaped work chamber, whose overall dimensions measure alike or exceed the overall dimensions of the CS being processed. During processing, the shaft is installed in such a way that its main axis coinciding with the axis of the main bearing journals, is in the zone of the conditional axis of working mass rotation. As a result of this arrangement of the shaft, the central zone of low activity is excluded, and the cylindrical surfaces of the main and rod journals displaced relative to the main axis of the shaft are processed in the zones of medium and maximum pressure. CS is installed in the bed along the guiding groves and is held on the supports attached to it. The bed with the shaft is immersed in the chamber with the working medium and fixed on racks attached to the frame. Supports allow the shaft to scroll around its axis and evenly strengthen under the dynamic impact of the working environment (Fig. 1. *a, b*) or through imparting an oncoming or passing rotation to it using an independent drive (Fig. 1 *c*).

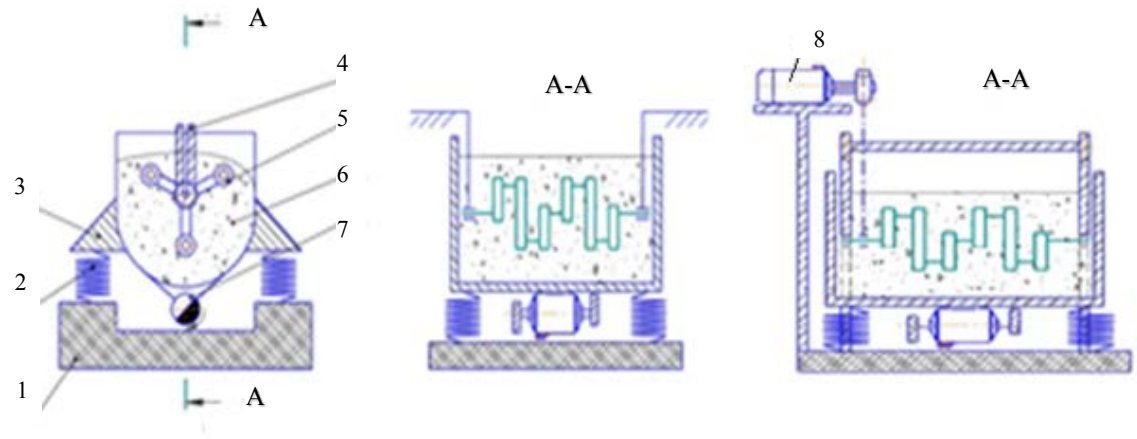

a) *b*) *c*)

Fig. 1. Flowcharts for processing CS with rotation under the action of the working medium (*a, b*) and using an additional drive (*c*):
1 — frame; 2 — springs; 3 — working chamber; 4 — bed; 5 — crankshaft; 6 — working medium;
7 — vibrator, 8 — auxiliary drive

To determine the preferred modes of processing CS, geometric and physicomechanical parameters of the surface of rod and main journals were studied using cylindrical and annular samples made of 45 and 40X steels with initial roughness R_a=0.16-0.42 μm. Processing was carried out by a working medium consisting of steel balls with a diameter of 3–6 mm, according to the basic technological scheme shown in Fig. 1. *a, b*, using a special mandrel (Fig. 2) with different amplitude-frequency characteristics and the process time.

a) *b*)

Fig. 2. Experimental mandrel simulating the crankshaft: *a)* general view;
b) installation in the working chamber of the vibration unit

It is established that under ViHT, a qualitatively new microrelief is formed on the surface of the samples, whose arithmetic mean deviation of the profile is less than on the initial surface. The change in the arithmetic mean deviation of the profile is critically affected by the amplitude of the working chamber vibrations and the processing time. So, for the same processing time period t = 20 min, at frequency f = 25 Hz, under increasing the amplitude from 2 to 3 mm, mean arithmetic deviation of surface profile is decreased by 1.7 times, and a change in the oscillation frequency from 20 to 30 Hz at the amplitude A = 3 mm has reduced arithmetic mean deviation of the surface profile by 1.1 times.

Taking into account the capabilities of vibratory machines, the established regularities made it possible to validate the amplitude-frequency parameters that provide the most effective power impact on the part under the ViHT process at the level of A = 3 mm and f = 25 Hz. Processing samples in these modes for 20 min, as shown in Fig. 3, reduces the arithmetic mean deviation of the initial surface profile by 2.6 times or 60 %. Increasing the processing time to 40 minutes does not cause a significant change in the parameter under consideration.

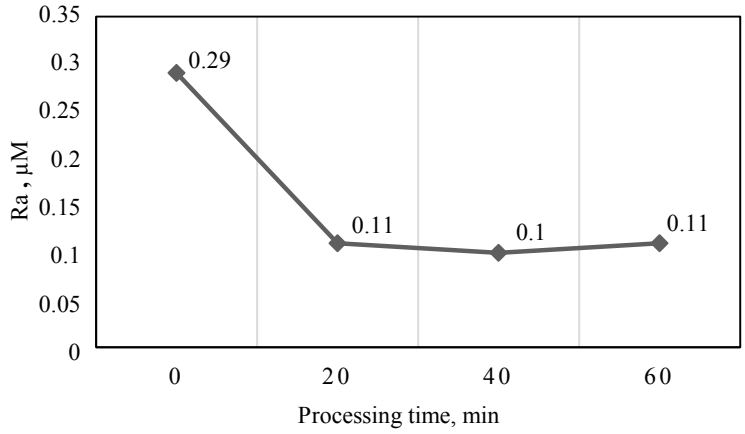

Fig. 3. Dependence of arithmetic mean deviation of the surface profile on duration of vibration shock treatment

The efficiency of the selected modes is validated by the study results of physicomechanical characteristics of the surface layer after processing with steel balls in the mode: A = 3 mm, f = 25 Hz (Fig. 4, 5). Microhardness was evaluated on hardness tester PMT3, the stress state was estimated by the value of residual compressive stresses determined by the Davidenkov method through cutting ring samples.

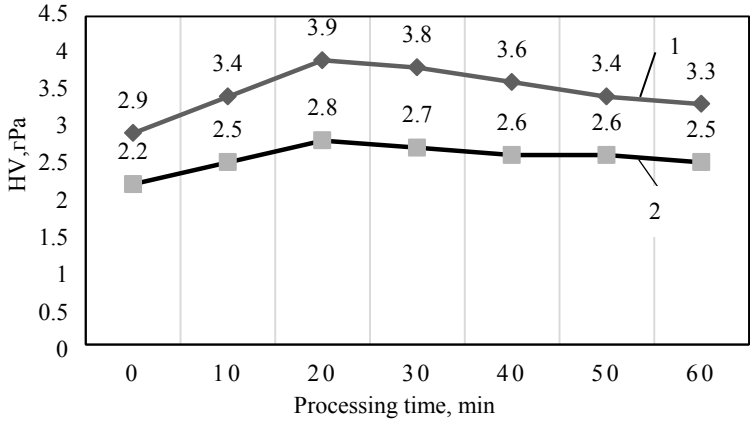

Fig. 4. Effect of processing time on microhardness of the surface layer for the ball material: 1 — steel 40X; 2 — steel 45

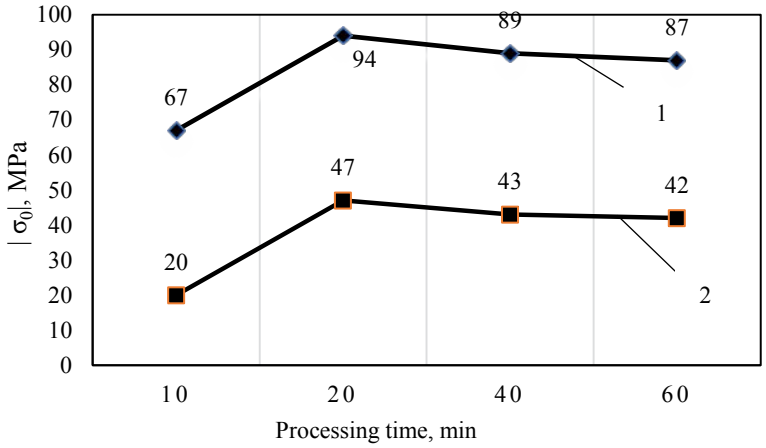

Fig. 5. Dependence of residual compressive stresses σ_o on ViHT duration of samples installed on the bushings (1) and on the shaft (2)

Analysis of the stress state of samples hardened under ViHT (Fig. 5) has shown that the residual compressive stresses of samples fixed on bushings and simulating CS rod journals are 35% higher than those of samples fixed on the shaft and simulating main journals. This is due to the difference in the intensity of exposure to the processing medium in various areas of the working chamber.

The next stage of research provided for the development of a computational model for estimating the macrogeometry (warpage) variation of CS under vibration shock treatment, and its experimental validation. V. N. Emelyanov [1] proposed a graphoanalytical method for analyzing the macro deformation of CS after hardening treatment by the SPD method (Fig. 6).

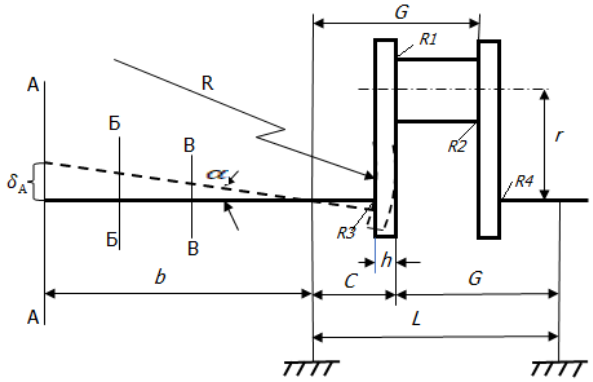

Fig. 6. Scheme of CS warpage after SPD of chamfers of main and rod journals

The method consists in determining the displacement of the shaft end δ_A in section A–A depending on its geometric dimensions: r — the distance from the axis of the main journal (MJ) to the axis of the rod journal (RJ); h — the thickness of the crank web; b — the distance from the MJ axis to the end of the CS; L — the distance between the MJ axes of one crank; C — the distance from the crank web from the RJ to the MJ axis.

The offset δ_A corresponds to the angle of deviation of the shaft axis from the horizontal whose value depends on the angular position of the crank web α, which is rigidly connected to the main and rod journals. The interrelated parameters δ_A and α depend on the average value of the residual compression stresses σ_o in the surface layer after the SPD and the depth of their occurrence δ_σ. In addition, it is shown in [1] that the value of warpage of a multicrank CS is mainly determined by the degree of hardening of the MJ and RJ chamfers attached to the end web of the end crank.

Using the considered method, an expression is obtained for calculating the total warpage of CS reinforced through ViHT:

$$\delta_A = \frac{6(1-\nu)}{E} \cdot \frac{r}{h^2} \cdot \frac{b}{L} \cdot K_y \cdot \sigma_{дт} \cdot K_{ко2}[-K_н(L + h - C) + (L - C)], \quad (1)$$

where E — elasticity modulus of the first kind; ν — Poisson's ratio; $\sigma_{дт}$ — dynamic yield strength; $K_{ко2}$ — coefficient of adjustment of the value of the RJ residual compressive stresses depending on their diametrical dimensions and deformation parameters of the power impact of a part of the working medium; K_y = 1.1–1.5 — coefficient of correction of the depth of residual compressive stresses; $K_н$ — coefficient that takes into account the difference between the stress

state of the MJ and the stress state of the RJ. According to the results of these studies, this coefficient depends on the distance from the walls of the working chamber and is $K_н \approx 0.6$.

To validate the model (1), experimental studies were carried out on 5 full-scale CS that underwent complete mechanical processing. The crankshaft material was as follows: steel 45, hardness after annealing 180 – 228 HB, rod journals of 25 mm diameter subjected to the HFC hardening to a depth of 2–4 mm to hardness of 52–65 HRC, while the chamfers of 2–3.2 mm radius with roughness $R_a = 1.6$ μm remain without heat treatment. Mechanical characteristics of the CS material are: $\nu = 0.25$; $E = 2 \cdot 10^5$MPa; $\sigma_т = 360$ MPa. The CS dimensions are: $r = 37.5$ mm, $h = 27$ mm, $L = 254$ mm, $C = 60$ mm.

CS hardening was carried out according to the basic technological scheme (Fig. 1, *a, b*) on 2×50 UVG vibratory unit with a working chamber volume of 50 dm^3. The working environment was a mix of hardened polished balls of 3 – 6 mm diameter from steel ShKh15 of 60–62 HRC hardness. The processing parameters were: vibration amplitude — 3 mm; vibration frequency — 25 Hz; processing time — 20 min.

Warpage of the shafts was determined through measuring the radial runout of the main journals before and after hardening by an indicator reading in 0.01 mm. The CS was installed by its main journals on prismatic supports and rotated by hand. Fig. 7 shows the experimental and calculated values of the CS radial runout after ViHT in sections of the shaft end removed from the end crank web of the end crank at the distances: A–A = 123 mm, B–B = 77 mm, C–C = 17 mm. From these data, it follows that the deviation of the actual values of CS warpage from the calculated values is on average no more than 15–20 %, which allows us to recommend the dependence (1) for calculating CS warpage under vibration shock treatment.

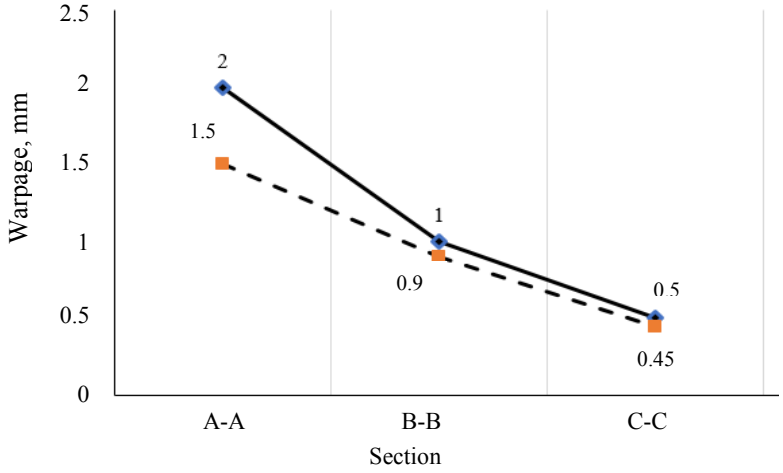

Fig. 7. Dependence of CS radial runout on the location of the controlled section:
solid line — experimental values, dotted line — calculated values

Discussion and Conclusions. Vibration shock treatment improves the geometric and physicomechanical parameters of the surfaces of rod and main journals of CS. As a result of processing all surfaces of the crankshaft by this method, the amount of warpage does not exceed the permissible values established by the technical requirements. This allows us to draw a conclusion about the efficiency of the considered method of strengthening CS to increase their operational properties.

References

1. Zaides SA, Emelyanov VN. Vliyanie poverkhnostnogo plasticheskogo deformirovaniya na kachestvo valov [The effect of surface plastic deformation on the quality of the shafts]. Irkutsk: INITU Publ. House; 2017. 380 p. (In Russ.)

2. Sidyakin YuI, Bocharov DA. Povyshenie tsiklicheskoi prochnosti galtelei stupenchatykh valov obkatkoi rolikami ili sharikami [Increasing the cyclic strength of step shafts by running in rollers or balls]. Izvestia VSTU. 2009;8(56):37–40. (In Russ.)

3. Chajnov ND, Suslikov VV. Matematicheskoe modelirovanie tekhnologicheskogo protsessa obkatki galtelei kolenchatogo vala [Mathematical Simulation of Bearing Fillet Rolling Process]. Vestnik MSTU. 2012;10(10):101–110. DOI: 10.18698/2308-6033-2012-10-395 (In Russ.)

4. Emelyanov V. Research on Hogging process of Crankshaft with Five Rod Journals because of Stamping. Journal of Engineering and Technology Research. 2014;2(2):65–69.

5. Butakov BI, Marchenko DD. Povyshenie kontaktnoi prochnosti stal'nykh detalei obkatyvaniem rolikami [Promoting contact strength of steel by rolling]. Journal of Friction and Wear. 2013,34(4):404–414. (In Russ.)

6. Lebedev VA. Tekhnologiya dinamicheskikh metodov poverkhnostnogo plasticheskogo deformirovaniya [Technology of dynamic methods of surface plastic deformation]. Rostov-on-Don: DSTU Publ. Centre; 2006. 183 p. (In Russ.)

7. Babunelson V. Stress analysis and optimization of crankshafts subject to static loading. International Journal of Engineering and Computer Science. 2014;3:5579–5587.

8. Babichev AP, Motrenko PD, Gillespie LK. Primenenie vibratsionnykh tekhnologii na operatsiyakh otdelochno-zachistnoi obrabotki detalei [Application of vibration technologies for finishing and clearing operations of parts]. Rostov-on-Don: DSTU Publ. Centre; 2010. 289 p. (In Russ.)

9. Kopylov, YuR. Vibroudarnoe uprochnenie [Vibration shock hardening]. Voronezh: Izd-vo Voronezh. gos. un-ta; 1999. 386 p. (In Russ.)

10. Lebedev VA, Kirichek AV, Sokolov VD. Energy State of a Plastically Deformed Surface Layer. In: International Conference on Industrial Engineering, ICIE 2016. Procedia Engineering. 2016;150:775–781. DOI: 10.1016/j.proeng.2016.07.106

11. Lebedev VA, Kochubey AA, Kirichek AV. The use of the rotating electromagnetic field for hardening treatment of details. IOP Conf. Series: Materials Science and Engineering. 2017;177:012126. DOI:10.1088/1757-899X/177/1/012126

12. Jalal Fathi Sola, Farhad Alinejad. Fatigue life analysis of an upgraded diesel engine crankshaft. In: 11th World Congress on Computational Mechanics (WCCM XI), 5th European Conference on Computational Mechanics (ECCM V), 6th European Conference on Computational Fluid Dynamics (ECFD VI). Barcelona, Spain; July 20–25, 2014.

13. Ali Keskin, Kadir Aydin. Crack analysis of a gasoline engine crankshaft. University Journal of Science. 2010;23(4):487–492.

14. Metkar RM, Sunnapwar VK, Hiwase SD. A fatigue analysis and life estimation of crankshaft – a review. International Journal of Mechanical and Materials Engineering. 2011;6(3):425–430.

15. Mar'ina NL. Kontsentratsiya napryazhenii v kolenchatom vale v usloviyakh poverkhnostnogo plasticheskogo deformirovaniya [Stress concentration in the crankshaft under conditions of surface plastic deformation]. Sovremennye materialy, tekhnika i tekhnologii. 2016;1(4):142–145. (In Russ.)

Submitted 08.06.2020
Scheduled in the issue 20.08.2020

About the Authors:

Lebedev, Valerii A., professor of the Engineering Technology Department, Don State Technical University (1, Gagarin sq., Rostov-on-Don, 344003, RF), Cand.Sci. (Eng.), professor, ORCID: https://orcid.org/0000-0003-1838-245X, va.lebidev@yandex.ru

Pastukhov, Filipp A., lead engineer, Research Institute for Vibrotechnology, senior lecturer of the Engineering Technology Department, Don State Technical University (1, Gagarin sq., Rostov-on-Don, 344003, RF), ORCID: https://orcid.org/0000-0002-0668-5739, vibrotech@mail.ru

Chaava, Mikhail M., associate professor of the Engineering Technology Department, Don State Technical University (1, Gagarin sq., Rostov-on-Don, 344003, RF), Cand.Sci. (Eng.), associate professor, Researcher ID: AAO-7848-2020, ORCID: https://orcid.org/0000-0003-3726-4950, miho_ch@list.ru

Serga, Georgii V., Head of the Descriptive Geometry and Engineering Graphics Department, Kuban State Agrarian University (13, Kalinina St., Krasnodar, 350044, RF), Dr.Sci. (Eng.), professor, ORCID: https://orcid.org/0000-0002-8931-0464, serga-georgy@mail.ru

Claimed contributorship

V. A. Lebedev: basic concept formulation; research objectives and tasks setting; academic advising. F. A. Pastukhov: analysis of the research results; text preparation; formulation of conclusions. M. M. Chaava: computational analysis; text preparation; formulation of conclusions. G. V. Serga: correction of the conclusions.

All authors have read and approved the final manuscript.

MACHINE BUILDING AND MACHINE SCIENCE

UDC 621.9.048 https://doi.org/10.23947/2687-1653-2020-20-4-397-404

Investigation of technological parameters effect on metal removal during centrifugal rotary machining

Nguyen Van Tho [1,2], Eh. Eh. Tischenko[1], I. A. Panfilov[1], A. A. Mordovtsev[1]
[1] Don State Technical University (Rostov-on-Don, Russian Federation)
[2] Hai Phong University (Hai Phong City, Vietnam)

Introduction. The study results on the single interaction under the centrifugal rotary part machining in the abrasive discrete medium are presented. Simultaneously with the numerical simulation, experiments were carried out on a centrifugal-rotary unit, and the maximum depth of penetration into the surface of the part, the single-track sizes, metal removal in one blow of an abrasive granule, were investigated. The removal of metal from workpieces was investigated depending on the processing modes, characteristics of the abrasive particle and the processed material.
Materials and Methods. The dependences for determining the metal removal from workpieces (steels 45, copper Cu-OF, and aluminum alloy D16T) are taken into account depending on the grain size (N_3) of abrasive particles. The process of a single interaction of an abrasive particle and the workpiece surface is considered within the framework of the dynamic contact problem of the elasticity theory. The authors have carried out finite element modeling of the considered structures in CAE ANSYS package.
Results. The results of theoretical and experimental studies on the metal removal from workpieces depending on the grain size of abrasive particles are presented. The technique of their implementation, the tool and equipment used are described. The results of theoretical and experimental studies are compared. Their fine precision is established. Abrasive tools and processing modes are selected.
Discussion and Conclusions. The dependences constructed in the work provide determining the rational values of the technological parameters of the centrifugal rotary machining (CRM) process. They can be used under designing the CRM processes. Therefore, time and financial resources can be saved to achieve the desired surface quality.

Keywords: metal removal from the workpiece surface, penetration depth, single interaction, metal removal analysis, centrifugal rotary machining.

For citation: Nguyen Van Tho, Eh. Eh. Tischenko, I. A. Panfilov, et al. Investigation of technological parameters effect on metal removal during centrifugal rotary machining. Advanced Engineering Research, 2020, vol. 20, no. 4, pp. 397–404. https://doi.org/10.23947/2687-1653-2020-20-4-397-404

Introduction. In mechanical engineering, grinding technology always provides high surface accuracy, which is the last step in surface treatment of parts. Materials with high temperature resistance, hardness, and high strength can be processed using grinding technology [1]. To increase the efficiency of the centrifugal rotary machining (CRM) process, it is required to optimize the model of friction interaction between abrasive particles and the workpiece surface.

Machining in a free abrasive environment enables to process parts of various shapes, sizes and materials using simple and reliable equipment. Temperature in the processing zone is much lower than under grinding, and the machining is accompanied by the supply of process fluid. In [2, 3], the thermal texture analysis and workpiece wear forecast were performed using the finite element method and the Gaussian process. The studies presented in [4, 5] have shown that when a particle of aluminum oxide is sliding, the workpiece surface is destroyed, and the metal is removed from the part. This paper deals with the process of a single interaction of a workpiece and an abrasive medium under CRM. Simultaneously with numerical modeling, experiments were conducted to study the depth of penetration of the

abrasive granule into the surface of the part. The effect of the grit size on the metal removal from the processed parts is studied.

The research to determine the impact of technological parameters of CRM processing on quality and productivity is not deep. This hinders a widespread introduction of CRM technology into production. To solve this problem, it is required to obtain a theoretical model of the CRM process that provides predicting the results of processing at the design stage.

Installation Description. The CRM operation principle (Fig. 1) is as follows: the workpiece (4) and abrasive particles are loaded into the working chamber (1); abrasive particles and the workpiece move in a spiral orbit; the rotating bottom (rotor) (2) is connected to the engine; the inner surface of the bottom is covered with a wear-resistant material to reduce friction.

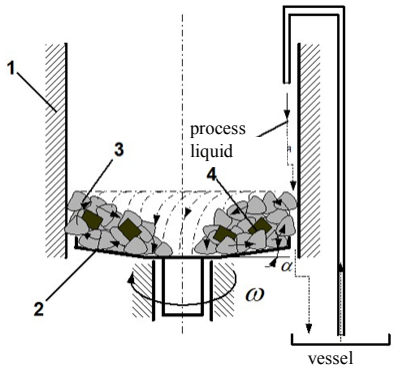

Fig. 1. Centrifugal rotary machining flowchart: 1—cylindrical shell; 2 — rotor;
3 — abrasive media; 4 — workpieces

Fig. 2 shows a three-dimensional model of the interaction of an abrasive particle and a workpiece.

In [6], the process of a single interaction of an abrasive granule and a part was studied. The features of this process are presented in [7–10]. It is known from [11] that the temperature in the processing zone is low and does not change the structure of the surface layer of the workpiece. This paper studies the contact interaction of an abrasive particle and the workpiece surface; the abrasive moves at a speed of v_0, the angle of contact with the processed workpiece surface is $\alpha = 15° – 25°$ (Fig. 2).

Investigation of single interaction process. Solving the problem of theoretical modeling of a single interaction will allow us to study the effect of technological parameters on the CRM. To create a mathematical model of metal removal from the surface of a part, it is required to describe impact of the factors on the shape and size of traces of interaction between the granule and the surface.

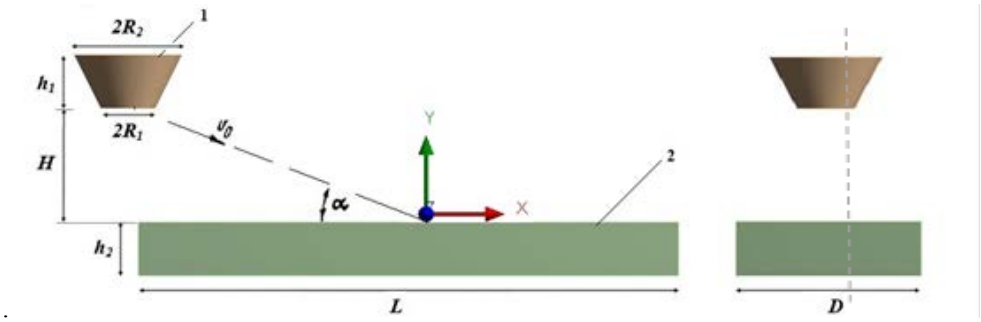

Fig. 2. Model of the abrasive particles and the workpiece:
1 — abrasive particle; 2 — workpiece

Many papers were devoted to the process of single interaction [12, 14, 15]. Analysis of the works [12–14] shows that the interaction of an abrasive particle and the workpiece surface occurs as follows: when a moving particle collides with the surface of the workpiece at a certain angle α, the abrasive particle is affected by resistance force P, which consists of tangent P_τ and normal P_N.

The problem is reduced to the movement of a circular cone at a constant speed $v > 0$. In [5, 6], the maximum depth of penetration under a single interaction is determined.

$$h_{\max} = 2V_{эф} R \sin\alpha \sqrt{\frac{\rho_{ш}}{3\kappa_s c \sigma_s}} \quad (1)$$

where $\rho_{ш}$ — material density; k_s — coefficient considering the effect of the workpiece surface roughness on the true contact area; c — coefficient of bearing capacity of the contact surface; σ_s — yield strength of the part material; R — radius of the abrasive particle; α — angle of contact of the abrasive particle with the workpiece surface; $V_{эф}$ — effective velocity of the moving abrasive particle determined from the formula:

$$V_{эф} = \kappa_{эф}\omega R_{эф}, \tag{2}$$

where $R_{эф}$ — effective rotor radius; ω — rotor rotational rate; $\kappa_{эф}$ — generalized coefficient of effective velocity.

Based on the work [4], when an abrasive particle collides with a workpiece with the formation of an elliptical processing trace, the values of the semi-axes *a, b* are found from the formula:

$$b = \sqrt{R^2 - (R - h_{\max})^2}.$$

$$a = \frac{\pi}{2}(ctg\alpha - f)h_{\max} + b, \tag{3}$$

where f — particle workpiece surface friction coefficient.

The destruction of the surface layer occurs due to microcutting. Therefore, when calculating the removal of metal, it is sufficient to take into account the number of interactions N_P, that lead to microcutting [16]:

$$Q=N_p q,$$

where Q — metal removal from the workpiece surface.

Substituting value N_p from the dependencies above, we get:

$$Q = P_1 P_2 \omega t q \frac{S_{дет}}{4R^2} \text{ при } S_{дет} \succ 4R^2 \tag{4}$$

$$Q' = P_1' P_2 \omega t q \text{ при } S_{дет} \prec 4R^2 \tag{5}$$

Finite element models of abrasive particles and parts were built in the ANSYS program to explore the maximum penetration depth under a single interaction based on the parameters of the CRM technology.

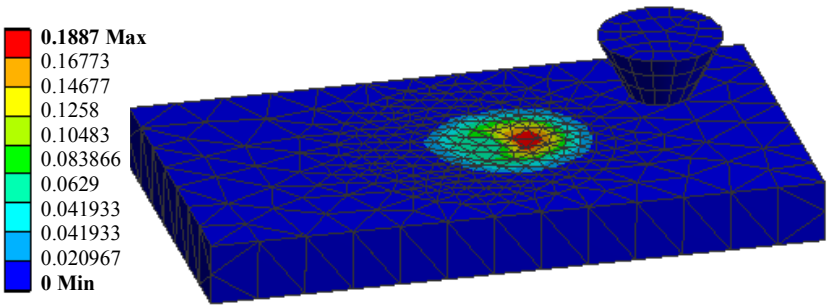

Fig. 3. Maximum penetration depth under a single interaction

Fig. 3 shows the distribution of vertical displacement during impact and sliding of an abrasive particle fragment on the workpiece surface calculated in ANSYS with account for the plasticity of the part material (bilinear model).

Experimental Research Methods. The study of the process of removing metal from the workpiece surface was carried out on cylindrical samples made of various materials: steel 45, aluminum alloy D16T, copper Cu-OF, 12 pieces per sample (Fig. 4). The hardness (HB) was measured on the Brinell hardness tester. The hardness (HB) and yield strength of the sample materials are shown in Table 1.

The following were selected as abrasive media: white prisms PT 15×15 conditionally equated to 25 grit (Fig. 5 a); porcelain balls 10 mm in diameter conditionally equated to M60 grit (Fig. 5 b); PT 25×25 conditionally equated to 12 grit (Fig. 5 d); abrasive white-green cone with 8 grit, d=30 mm, h=30 mm (Fig. 5 d).

Abrasive granules and blanks are loaded into the working chamber of the CRM. Processing is performed at the rotation speed of ω=12 rev/s. Every 30 minutes, the treatment is stopped, the samples are removed from the chamber, thoroughly washed and dried. Ad 200 scales were used to determine the removal. To avoid corrosion, a 0.2% solution of soda ash was used.

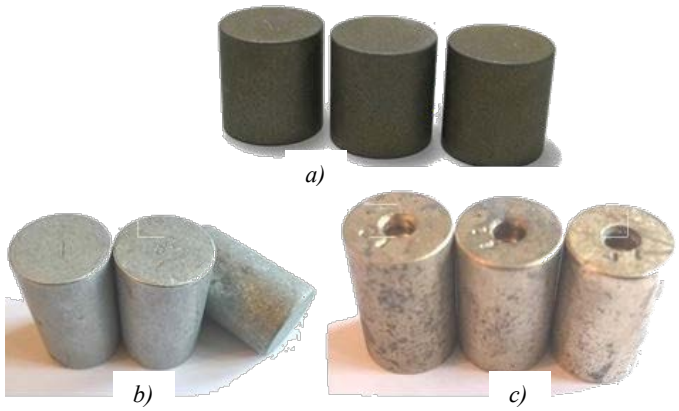

Fig. 4. Samples for determining metal removal from the workpiece surface:
a) steel 45; *b*) copper Cu-OF, *c*) aluminum alloy D16T

Table 1

Dimensions and mechanical properties of sample materials

Sample materials	Sample dimensions, mm	Hardness, HB	Yield stress σ_T, MPa
Steel 45	∅ 20x20	190–200	340
Aluminum alloy D16T	∅ 30x50	80–82	240
Copper Cu-OF	∅ 15x20	56–59	180

Fig. 5. Abrasive particles used in CRM: *a*) white prisms PT; *b*) porcelain balls;
c) PT 25×25; *d*) white-green abrasive cone

Experimental Results. The dependence of the metal removal process on the abrasive grit size (N_3) is studied. For a comprehensive test of the theoretical model, the comparison based on the results of processing 12 samples of each grade was made. The theoretical calculation results using dependencies (4) and (5) were compared to the experimental results. Based on the results of experimental and theoretical studies, graphs are constructed.

Fig. 6–8 show the dependences of metal removal from the surface of the part on the grain size of abrasive particles M60; 8; 12; 25; part materials are steel 45; aluminum alloy D16T, copper Cu-OF; the processing mode — the rotor speed is ω=12 rev/s.

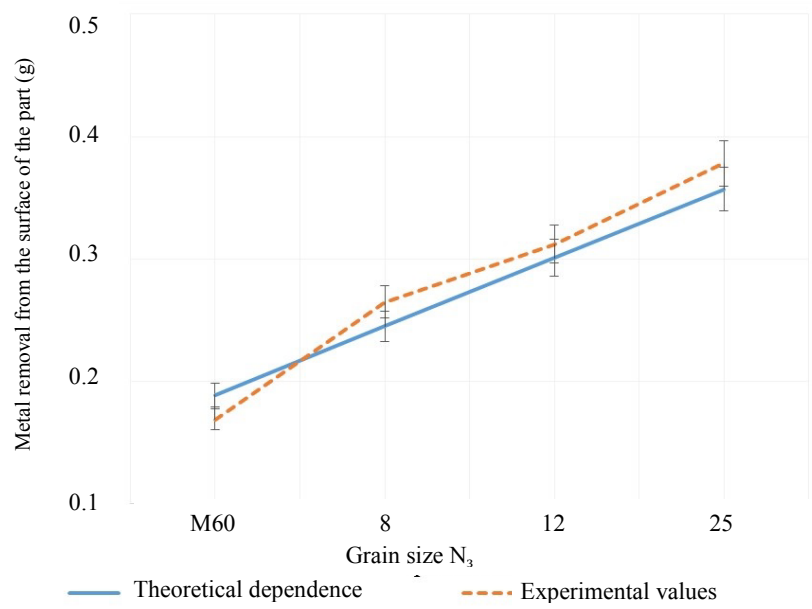

Fig. 6. The dependence of metal removal on N_3, the workpiece materials steel 45

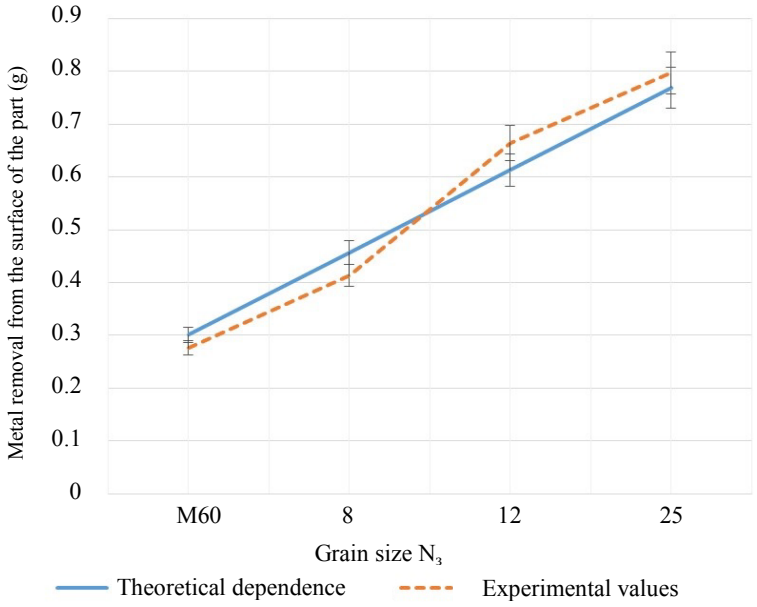

Fig. 7. The dependence of metal removal on N_3, the workpiece material is D16T

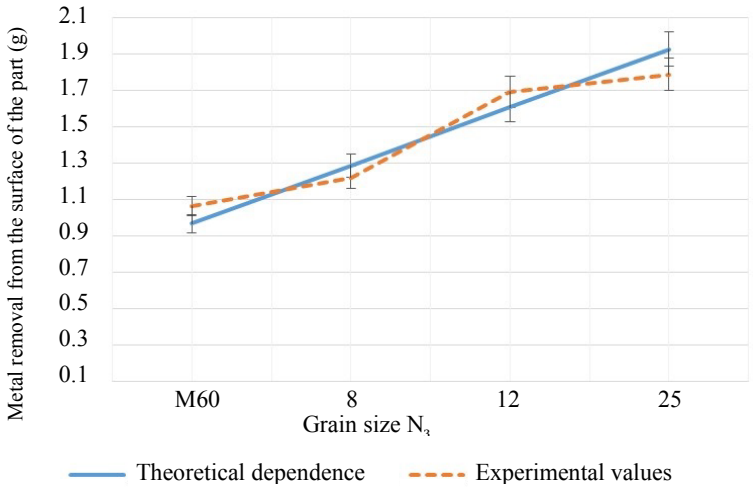

Fig. 8. The dependence of metal removal on N_3, the workpiece material is Cu-OF

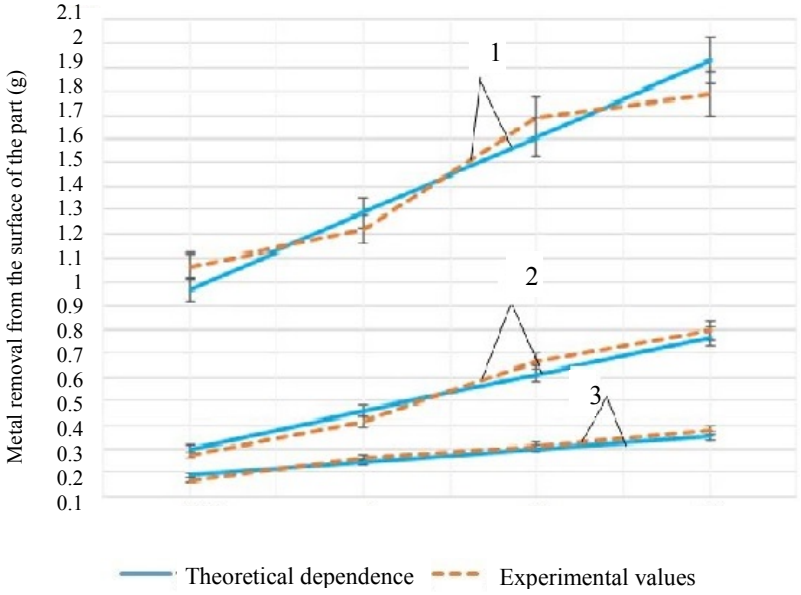

Fig. 9. Comparison of theoretical and experimental dependences of metal removal on N_3: 1 — copper Cu-OF; 2 — aluminum alloy D16T; 3 — steel 45

Discussion and Conclusions. Based on the results of theoretical and experimental studies, the dependences presented in Fig. 6–9 were found. After analyzing the research results, the following conclusions can be drawn:

1. The metal removal Q is proportional to the increase in the grit size of abrasive particles. When processing at ω=12 rev/s, for steel 45 at N_3=M60, Q=0.169g, at N_3=25 Q=0.37g; for aluminum alloy D16T at N_3=M60 Q=0.267g, at N_3=25 Q=0.797g; for copper Cu-OF at N_3=M60 Q=1.065g, at N_3=25 Q=1.789g.

2. The effect of the abrasive medium grain size, the mechanical properties of the material and the processing mode, reflects correctly the theoretical model of a single interaction.

3. When comparing the results of experimental studies and theoretical data, the difference is less than 20 % (with account for the metal removal on the grain size of abrasive particles N_3).

4. The introduction of research results into production enabled to increase the processing productivity by 1.5–2 times with the required quality of the treated surface and reduction of the working media wear.

The results obtained can be used to improve the efficiency of process design of the CRM and to expand technological capabilities.

References

1. Rowe WB. Principles of Modern Grinding Technology. William Andrew; 2014. 480 p.

2. Li Xin, Peng Gaoliang, Li Zhe. Prediction of seal wear with thermal-structural coupled finite element method. Finite Elements in Analysis and Design. 2014;83:10–21. DOI: 10.1016/j.finel.2014.01.001

3. Anh Tran, Furlan JM, Krishnan V, et al. A computationally efficient machine learning framework for local erosive wear predictions via nodal Gaussian processes. Wear. 2019;422-423:9–26. DOI: org/10.1016/j.wear.2018.12.081

4. Gee M, Nunn J. Real time measurement of wear and surface damage in the sliding wear of alumina. Wear. 2017;376—377:1866–1876.

5. Tamarkin MA, Tishchenko EE, Druppov VV. Issledovanie udaleniya metalla pri tsentrobezhno-rotornoi obrabotke v abrazivnoi srede [Investigation of metal removal during centrifugal rotary processing in abrasive medium]. Vestnik of P.A. Solovyov Rybinsk State Aviation Technical University. 2007;11(1):169–186. (In Russ.)

6. Tamarkin MA, Tishchenko EE, Korol'kov YuV, et al. Povyshenie ehffektivnosti tsentrobezhno-rotatsionnoi obrabotki v srede abraziva [Improving the efficiency of centrifugal rotary processing in abrasive medium]. STIN. 2009;2:26–30. (In Russ.)

7. Tamarkin MA, Rozhnenko OA, Tishchenko EE, et al. Teoreticheskie i ehksperimental'nye issledovaniya protsessov obrabotki fasonnykh poverkhnostei detalei svobodnym abrazivom [Theoretical and experimental study of

process of shaped parts surfaces by loose abrasive]. Strengthening Technologies and Coatings. 2011;11:27–31. (In Russ.)

8. Tamarkin MA, Glazman BS, Korol'kov YuV, et al. Reducing abrasive wear in centrifugal-rotary machining. Russian Engineering Research. 2014;34(1):60–64.

9. Soloviev AN, Tamarkin MA, Nguyen Van Tho, et al. Computer Modeling and Experimental Research of Component Processing Procedure in the Centrifugal-Rotary Equipment. Advanced Materials. 2020;6:513–528.

10. Nguyen Van Tho, Soloviev AN, Tamarkin MA, et al. Finite Element Modeling Method of Centrifugally Rotary Processing. Applied Mechanics and Materials. 2019;889:140–147.

11. Soloviev AN, Tamarkin MA, Nguyen Van Tho. Konechno-ehlementnoe modelirovanie termouprugogo kontaktnogo vzaimodeistviya v abrazivnoi obrabotke poverkhnosti detalei mashin [Finite element modeling of thermoelastic contact interaction in the abrasive surface treatment of machine components]. Ecological Bulletin of Research Centers of the Black Sea economic cooperation. 2019;16(1):51–58. DOI: 10.31429/vestnik-16-1-51-58 (In Russ.)

12. Nepomnyashchy EF. Trenie i iznos pod vozdeistviem strui tverdykh sfericheskikh chastits [Friction and wear caused by a jet of solid spherical particles]. In: Contact interaction of solids and calculation of friction and wear forces. Moscow: Nauka; 1971. P. 190–200. (In Russ.)

13. Mikhin NM. Vneshnee trenie tverdykh tel [External friction of solids]. Moscow: Nauka; 2002. 222 p. (In Russ.)

14. Babichev AP, Babichev IA. Osnovy vibratsionnoi tekhnologii [Fundamentals of vibration technology]. Rostov-on-Don: DSTU Publ. Centre; 1998. 624 p. (In Russ.)

15. Tamarkin MA, Tishchenko EE, Druppov VV. Formirovanie parametrov kachestva poverkhnosti dlya tsentrobezhno-rotornoi obrabotki v abrazivnoi srede [Formation of parameters of quality of surface at centrifugal-rotational processing in the environment of the abrasive]. Strengthening Technologies and Coatings. 2007;10:19–24. (In Russ.)

16. Yushchenko AV, Flek MB. Issledovanie protsessa s"ema metalla pri abrazivnoi galtovke [Study on metal removal process under abrasive rumbling]. Vestnik of DSTU. 2013;13(3–4):125–133. (In Russ.)

Submitted 27.08.2020
Scheduled in the issue 20.10.2020

About the Authors:

Nguyen Van Tho, postgraduate student of the Engineering Technology Department, Don State Technical University (1, Gagarin sq., Rostov-on-Don, 344003, RF), researcher of the Electrical and Mechanical Engineering Department, Haiphong University (117, Phan Dang Luu sq., Haiphong, Vietnam), ORCID: https://orcid.org/0000-0002-9105-7701, thonguyen239@gmail.com

Tishchenko, Elina E., associate professor of the Engineering Technology Department, Don State Technical University (1, Gagarin sq., Rostov-on-Don, 344003, RF), Cand.Sci. (Eng.), associate professor, ORCID:https://orcid.org/0000-0001-5156-5544, lina_tishenko@mail.ru

Panfilov, Ivan A., associate professor of the of Theoretical and Applied Mechanics Department, Don State Technical University (1, Gagarin sq., Rostov-on-Don, 344003, RF), Cand.Sci. (Phy-Mat.), associate professor, ORCID: http://orcid.org/0000-0002-0955-0282, panfilov_i@prof-cad.ru

Mordovtsev, Alexey A., postgraduate student of the Engineering Technology Department, Don State Technical University (1, Gagarin sq., Rostov-on-Don, 344003, RF), ORCID https://orcid.org/0000-0002-9333-2076, mordovtsev_aa@mail.ru

Acknowledgments

The authors are deeply grateful to Dr.Sci. (Eng.), Professor Mikhail A. Tamarkin and Dr.Sci. (Phys.-Math.), Professor Arkady N. Solovyev for their valuable advice in planning the research and recommendations on the design of the paper.

Claimed contributorship

Nguyen Van Tho: basic concept formulation; research objectives and tasks setting; conducting experiments; development of the program in ANSYS package and computational analysis; analysis of the research results; text preparation. E. E. Tishchenko: conducting experiments; analysis of the research results. I. A. Panfilov: development of the program the package. A. A. Mordovtsev: analysis of the research results and correction of the conclusions.

All authors have read and approved the final manuscript.

INFORMATION TECHNOLOGY, COMPUTER SCIENCE, AND MANAGEMENT

UDC 519.2, 51-74 https://doi.org/10.23947/2687-1653-2020-20-4-405-413

An approach to forecasting damage due to unfavorable circumstances associated with indistinguishability of source data

V. F. Zolotukhin[1], A. V. Matershev[2], L. A. Podkolzina[3]
[1, 2] SC "VNII 'Gradient'" (Rostov-on-Don, Russian Federation)
[3] Don State Technical University (Rostov-on-Don, Russian Federation)

Introduction. When administering complex multi-parameter systems, management decisions are often made under uncertainty. There is an acute problem of reduction of the likelihood of unwanted events and mitigation of possible damage. The efficiency of predicting damage to complex systems depends directly on the quality of processing methods, systematization, and the amount of input data. It is required to improve methods for assessing and predicting damage and to develop new approaches and criteria for statistical forecasting of damage and evaluating the system reliability. The solution to such problems is complicated by a large number of indicators, data uncertainty, short series of observations, incomplete initial information, insufficiently developed scientific methodological apparatus. Existing methods for predicting damage in the systems of potentially dangerous objects do not take into account the causes of accidents that happened due to unfavorable circumstances. As a consequence, management decisions are made upon unreliable forecasting results. In this regard, an urgent scientific task is the development of methods and techniques for the formation of viable management decisions, free from this shortcoming. The major study objective is to consider a particular problem for predicting damage due to unfavorable circumstances associated with the indistinguishability of the initial data. The tasks are to consider this kind of uncertainty which includes indistinguishability of the true system condition and the real value of its quantitative characteristics; to formulate a combinatorial problem for the case when a rather dangerous composite feature is determined by the joint manifestation of two or more simple features.
Materials and Methods. Under the conditions of multiple indistinguishability, the following was used as the source data: a set of indistinguishable outcomes with reliable information on the event instance and the uncertainty of assigning the event to a certain type; a family of sets having the same number of elements. The Cartesian product of the families of the corresponding sets and the actual value of the group of a compound potentially dangerous factor with a compound rather dangerous feature are taken into account. The resulting mono-element fuzzy group is presented, which is also a possible event resulting from the intersection of two necessary events.
Results. It is established that the problem of predicting damage due to unfavorable circumstances corresponds to a combinatorial-type problem, which consists in enumerating all sets of arguments. The resulting range, which is an elemental group of indistinguishability, characterizes the smaller and larger possible values of the size of the group of a potentially dangerous factor with a composite rather dangerous feature. It is shown that the formulated combinatorial problems without significant changes are applicable to problems in a generalized form, when composite rather dangerous features are determined using not only the operation of intersection, but also uniting and difference; thereby, the initial groups are not necessarily the objects with simple features.
Discussion and Conclusions. The results obtained are focused on the construction of analytical algorithms for establishing indistinguishability under the monitoring, modeling, forecasting state-related processes and complex dynamic multi-parameter objects.

Keywords: indistinguishability, probability, mathematical model, risk, random event, accident potential.

For citation: V. F. Zolotukhin, A. V. Matershev, L. A. Podkolzina. An approach to forecasting damage due to unfavorable circumstances associated with indistinguishability of source data. Advanced Engineering Research, 2020, vol. 20, no. 4, p. 405–413. https://doi.org/10.23947/2687-1653-2020-20-4-405-413

Funding information: the research is supported by RFFI grant no. 19-01-00357.

Introduction. Activities in the technogenic sphere involve risks and critical situations. This can be the destruction of systems (engineering), loss of control (military matters), bankruptcy (economy). The prediction problem is a challenge for many industries and is directly related to the need to improve, develop, and apply the mathematical apparatus of control tools for complex multiparametric systems.

Issues of simultaneous processing of dynamic arrays of varying degrees of granularity remain urgent. The prototypes of mathematical models containing such structures are also optimization problems of practical resource allocation under the conditions of possible hard-to-formalize impacts [1]. A high degree of process uncertainty reduces the feasibility of using resource-intensive distribution algorithms. At the same time, it is necessary to obtain many alternative solutions. This is particularly important in situations when information on existing threats is uncertain and inconsistent [2]. If an object or process changes unexpectedly, an adequate mathematical model may not be available at the time of decision-making. At the same time, the failure of complex production facilities often causes man-made emergencies with severe economic, environmental and social consequences, which makes it necessary to improve the mathematical foundations of risk analysis [3, 4].

Strategic decisions on managing complex multiparameter systems are made under conditions of uncertainty. The purpose of modern risk management is to avoid a critical situation. In the case of a negative scenario, it is required to minimize losses. To predict damage and make adequate decisions, constant monitoring is carried out, which identifies the major factors of the implementation of the critical situation [5].

It is necessary to rank and systematize risks according to the degree of impact on the protected object activity. Any system is characterized by many parameters, which are often random and changeable. The efficiency of predicting damage to complex systems depends directly on the quality of processing methods, systematization, and the amount of input data. Therefore, to estimate the time and condition of the occurrence of a critical situation, combined forecasting methods are used, which contain expert, analytical, and simulation parts and use the apparatus of probability theory [6, 7]. Critical values can be determined analytically based on the experimental data processing results. This is often performed under the conditions of lack of information, so errors are possible.

A quantitative characteristic of hazard (or security) of systems and situations is the risk. Hereinafter, the risk will be considered damage (consequences) from the implementation of a possible event in a complex system [8]. Due to the complexity and heterogeneity of the factors that affect the system and should be taken into account in the decision-making process, it is required to use a set of methods for analyzing and processing information to assess the damage caused by system failures.

Often, due to the complexity and high cost of monitoring, some of the parameters associated with the technical condition of the system (hereinafter — TCS) are indistinguishable. In general cases, indistinguishability is considered as the state uncertainty, which can manifest itself not only in the future, but also in the present (or near past) time [9–10]. Indistinguishability is described in terms of the theory of possibilities, in which methods for obtaining simple numerical characteristics — estimates of various TCS are developed. It also corresponds to the decision- making principle based on facts. According to this principle, the indistinguishability of the system states is caused by the uncertainty of knowledge on it and represents the concretization of the knowledge uncertainty on the operation, physical behavior. Uncertainties can be exogenous and endogenous, due to external and internal actions, respectively [11]. Each type of uncertainty can significantly impair the decision accuracy.

Current state of the problem. A significant number of papers are devoted to certain aspects of the problem of forecasting and risk assessment in case of data indistinguishability. However, these studies lack a general methodological basis. In the papers [12–27], particular solutions are proposed, but the general mathematical apparatus is not developed yet. Thus, in [14–15], it is assumed that the evaluation of each of the indistinguishable criteria is equal to the arithmetic mean of their numbers. The number of the entire group as a whole object in the ordering is taken for the rank of each of the indistinguishable criteria.

In the paper [16], it is offered to unify approaches to management of complex security of various systems; and also, the situation when the expert does not distinguish some criteria is shown.

In [17], the problem of constructing interval estimates for an unknown probability in the presence of multiple indistinguishable outcomes in the experimental results is considered. Two solution paths are proposed: to take into account all unobservable outcomes or to discard them. In both cases, roughening up the result, and errors are possible.

The paper [18] clarifies the uncertainty and indistinguishability that arise when diagnosing the state of power plants. Indistinguishability is understood as the uncertainty of the state of the managed object for the observer. At the same time, it is assumed that uncertainty decreases as we move down the hierarchical ranks of energy system management. In addition, it is proposed to introduce a certain threshold and consider the solutions indistinguishable if the square of the difference of the desired value does not exceed the set threshold.

The indistinguishability aspect is mentioned in light of the development of approximate set theory in [19]. The concepts of lower, upper approximation and border area are revealed. This provides creating decision rules "if ... then" and using facts only, without assumptions. Referring to [20], the author clarifies that one of the key decision-making methods in the field of multi-criterion optimization has been developed on the basis of the theory of approximate sets.

In the paper [21] devoted to the safe operation of lifting cranes, a method of expert assessment of the frequency of adverse events is proposed, which provides the development of recommendations for reducing the risk.

In [22], the problems on military operational research are considered in the following context: warships seek to contain and prevent sea robbery, and the model of pirate movement is based on forecasting the probability of piracy and on the Markov assumption. The author uses the solution to the flow problem with minimal costs. The number of search engines does not matter. It is assumed that they are identical and indistinguishable.

In the study [23], the T-indistinguishability operators stated geometrically are studied as a special case of generalized metric spaces for further application under researching fuzzy subgroups.

It is shown in [24] that the existing indistinguishability of data from a set of observations does not provide accurate estimates of the system state. Hence, an accurate prediction should be based on the probability density of indistinguishable states. This density can be calculated as follows: first, through calculating the maximum likelihood estimate of the state, and then – through an ensemble estimate of the density of states that are indistinguishable from the maximum likelihood state.

In [25], a characteristic of functions that provide combining partial T-indistinguishability (relations) operators into a new set, is presented. In [26], an aggregation of partial T-indistinguishability operators and partial pseudometric is considered. The aggregation of a set of partial T-distinguishability operators is analyzed, and the relationship between functions is shown. These relations:

— combine partial T-indistinguishability operators,

— preserve partial T-pseudometric under the aggregation process.

In [27], the connection of indistinguishability and fuzzy subsets is validated. It is proved that the basic relation for them is lattice isomorphism.

So, the known approaches to the problem of indistinguishability of influencing factors are functionally limited. They do not provide the required level of reliability when making management decisions. The weak points of their research and methodological procedure are obvious. This generally hinders the development of forecasting systems taking into account the factor of indistinguishability, and proves the demand for the development and improvement of the mathematical apparatus.

Thus, an important task of risk management is to predict the damage caused by adverse circumstances due to the indistinguishability of the initial data. Its solution is of considerable theoretical and practical interest for many complex parametric dynamical systems.

Existing methods of predicting damage in the systems of potentially hazardous objects do not take into account the causes of accidents that occurred due to adverse circumstances. As a result, management decisions are made on the basis of unreliable forecasting results. In this regard, it is an urgent scientific task to develop methods and techniques for the formulation of appropriate management decisions that are devoid of this disadvantage.

Research Problem Statement. Damage caused by the hazards and attacks is not always possible to predict in advance due to the difficulty of distinguishing between the usual states of multiparametric objects and systems whose

behavior is not determined. As a result, there is a need to study and evaluate two independent types of uncertainty: indistinguishability and nondeterminism. Consider a prediction model due to an unfavorable set of circumstances associated with the indistinguishability of the source data.

We show that in terms of set-theoretic modeling, a mathematical model of adverse circumstances represents a combinatorial problem with common source data. We formulate this problem for the case when a very dangerous compound feature is determined by the joint manifestation of two or more simple features.

Materials and Methods. Source data:

— a set of indistinguishable outcomes *U* with the number of elements *n* containing reliable information on the fact of the event implementation and the uncertainty of assigning the event to a certain type;

— family $\overline{A}_i$ of sets of the type A_i, having the same number n_i of elements.

Under the conditions of multiple indistinguishability, we are forced to consider all sets of type A_i, for each *i*, because any of them can represent a group of objects that have acquired the *i*-th simple feature.

Consider the Cartesian product of families $\overline{A}_1 \times \overline{A}_2 \times ... \times \overline{A}_k$. Its elements are all element sets ($A_1, A_2, ..., A_k$) of sets of type $A_1, A_2, ..., A_k$.

Let us consider the case when the set $U = \{1,2,3,4\}$, $k = 2$ of an element set of type A_1 contains $n_1 = 3$ elements, and of type A_2 — по $n_2 = 2$ elements.

Assume, $A_{1\phi} = \{1,2,3\}$, $A_{2\phi} = \{1,4\}$. Then

— the true value of the group of a compound potentially hazardous factor with a very dangerous compound feature. In this case, the families $\overline{A}_1$ and $\overline{A}_2$ have the form:

$$\overline{A}_1 = \{\{1,2,3\},\underline{\{1,2,4\}},\{1,3,4\},\{2,3,4\}\}, \quad (1)$$

$$\overline{A}_2 = \{\{1,2\},\{1,3\},\underline{\{1,4\}},\{2,3\},\{2,4\},\{3,4\}\}. \quad (2)$$

The composition of groups of a potentially hazardous factor with simple features has the form (3, 4), which represents mono multiple indistinguishability groups:

$$A_{1\phi}: \{\underline{1},\underline{2},\underline{3},\underline{4}\}, \quad (3)$$

$$A_{2\phi}: \{\underline{1},2,3,\underline{4}\}. \quad (4)$$

As can be seen, the obtained families (1) and (2) contain $C_4^3 = 4, C_4^3 = 6$ elements, represent multielement groups of indistinguishability, and are *necessary events.*

The Cartesian product of these families will represent a collection containing the following $n_{1,2} = C_4^3 \cdot C_4^3 = 24$ distinct pairs of elements $\overline{A}_1$ и $\overline{A}_2$:

$$\begin{gathered}(\{1,2,3\}\{1,2\}),(\{1,2,3\}\{1,3\}),...,(\{1,2,3\}\{3,4\}),\\ (\{1,2,4\}\{1,2\}),...,\underline{(\{1,2,4\}\{1,4\})},...,(\{1,3,4\}\{3,4\}),\\ .....\\ (\{2,3,4\}\{1,2\}),.....,(\{2,3,4\}\{3,4\}).\end{gathered} \quad (5)$$

You can see that $\overline{A}_1 \times \overline{A}_2$ is a family of distinct pairs of sets of A_1, A_2, type that have the same number of elements — 3 and 2, respectively. At $k > 2$ the Cartesian product $\overline{A}_1 \times \overline{A}_2 \times ... \times \overline{A}_k$ is a family of sets, each of which contains one set of type $A_1, A_2, ..., A_k$.

We will call the mentioned sets — elements $\overline{A}_1 \times \overline{A}_2 \times ... \times \overline{A}_k$ — *k*-sets. Each *k*-set will correspond to the intersection of the sets included in it, that is, we select common elements in such sets. For example, the intersections for the

sixth and ninth pairs in (5), which have the form $\left(\{1,2,3\}\{3,4\}\right)and\left(\{1,2,4\}\{1,4\}\right)$, will be the sets $\{1,2,3\}\cap\{3,4\}=\{3\}$ and $\{1,2,4\}\cap\{1,4\}=\{1,4\}$, respectively.

The general result (5) will be:

$$\left\{\begin{array}{cccccc} \{1,2\} & \{1,3\} & \{1\} & \{2,3\} & \{2\} & \{3\} \\ \{1,2\} & \{1\} & \underline{\{1,4\}} & \{2\} & \{2,4\} & \{4\} \\ \{1\} & \{1,3\} & \{4\} & \{3\} & \{1,4\} & \{3,4\} \\ \{2\} & \{3\} & \{4\} & \{2,3\} & \{2,4\} & \{3,4\} \end{array}\right\}. \tag{6}$$

The expression (6) is the resulting mono-element group of indistinguishability, as well as a *possible event* obtained as a result of the intersection of two necessary events (1) and (2).

Now consider function f with arguments that are the mentioned intersections of sets of type $A_1\cap A_2\cap\ldots\cap A_k$, and with values equal to the number of elements of these intersections:

$$f\left(A_1\cap A_2\cap\ldots\cap A_k\right)=\left|A_1\cap A_2\cap\ldots\cap A_k\right|=r, \tag{7}$$

where k — the number of elements of the corresponding set.

For the sixth and ninth pairs discussed above:

$$f\left(\{1,2,3\}\cap\{3,4\}\right)=f\left(\{3\}\right)=1,$$
$$f\left(\{1,2,4\}\cap\{1,4\}\right)=f\left(\{1,4\}\right)=2.$$

Now you can see that we are talking about a combinatorial type problem, which consists in enumerating all sets-arguments to obtain different values from them. Such an enumeration can be found after determining the smaller and larger values f, that coincide with the smaller and larger possible values of the population of a group of objects with a compound potentially dangerous factor.

Research Results. Consider the following definition: *C* — a possible event under the implementation of *E* event, if $\mathrm{E}\cap\mathrm{C}\neq\emptyset$.

We will proceed from the fact that the concept of the possibility of an event is usually associated with assumptions under uncertain circumstances. Therefore, the application of this concept is inappropriate if *E*, *C* are known, and the realized outcome $\mathrm{x}\in\mathrm{E}$. With the appearance of *E*, it is clear that *C* either takes place, if $\mathrm{x}\in\mathrm{C}$, or it does not — otherwise. At the same time, there is no uncertainty.

The most common, productive, and sufficient concept for our purposes is the concept of a possible event, due to the uncertainty in the form of indistinguishability of the outcome that has appeared among other outcomes *E*. In this regard, *C* is referred to as a possible event under the additional conditions listed below.

Condition 1. The events *E* and *C* are known, and, therefore, their intersection $\mathrm{E}\cap\mathrm{C}\neq\emptyset$ (by definition, this is not an empty set).

Condition 2. The outcome x'_i is not set, because of which *E* occurs if more than one element belongs to $E=\{x_1, x_2, \ldots, x_n\}$. It is only known that x'_i — one of the elements of *E*, but it is not established which one exactly, i.e., $\exists!\,\mathrm{x}'_i\in\mathrm{E}$.

With account for conditions 1 and 2, the generally accepted meaning of the statement that *C* is an important event is specified. So, *C* either *was realized*, if indistinguishable actual outcome $\mathrm{x}'_i\in\mathrm{E}\cap\mathrm{C}$ (and thus, $\mathrm{x}'_i\in\mathrm{C}$), or it *was not realized* — otherwise (if $\mathrm{x}'_i\notin\mathrm{E}\cap\mathrm{C}$). Consider an example that illustrates a possible event of this kind.

Let *E* and *C* consist, respectively, in the appearance of an even number and more than three points when throwing a dice, that is $E=\{2, 4, 6\}$, $C=\{4, 5, 6\}$. Here, $\mathrm{E}\cap\mathrm{C}=\{4,6\}\neq\emptyset$. It is known that *E* occurred, but it was not established which of its outcomes took place. As a result, the above conditions are met, according to which *C* is a possible event: it was realized if either the outcome $\mathrm{x}'_2=4$, or the outcome $\mathrm{x}'_3=6$, and it was not realized if the outcome $\mathrm{x}'_1=2$ was realized.

An important special case of the possible event is necessary event *C*. It takes place if E ∩ C ≠ ∅ (condition 1), condition 2 is met, and E ⊂ C, that is, in the case when all the outcomes of *E* belong to *C*. Whichever of them appears, it causes the implementation of *C*.

In this example, from $n = 4$, $n_1 = 3$, $n_2 = 2$, we find that f takes two values: 1 and 2. This indicates that there are only one- and two-element intersections $A_1 \cap A_2$ of sets of the type $A_1, A_2 \subset U$, $U = \{1,2,3,4\}$, i.e., in a group of potentially dangerous objects with a compound very dangerous feature, there can be either 1 or 2 objects, and the indistinguishability group (8) is a numerical mono-element indistinguishability group:

$$\{1,2\}. \quad (8)$$

The next specific task that follows from the considered model of adverse circumstances, consists in the fact that each obtained above value f should be divided by *n*, i.e., finding its normalized values — a set of alternative frequencies for an arbitrary object to acquire a compound very dangerous feature under the conditions of multiple indistinguishability and nondeterminism. The latter consists in the fact that quotients $n_i \backslash n$ represent the frequencies of occurrence on an arbitrary object of the *i*-th simple feature for all $i = 1, ..., k$.

We formulate the purpose of solving the following combinatorial problem corresponding to the frequency problem: to determine number *s* of elements $\overline{A}_1 \times \overline{A}_2 \times ... \times \overline{A}_k$, to find $s(r)/s$ for all *r*.

Quotients $s(r)/s$ for all *r* represent the probabilities that the number of objects with a compound very dangerous feature will be equal to a certain value *r*. To calculate such probabilities in this regard, we use the dependence:

$$s = C_n^{n_1} \cdot C_n^{n_2} \cdot ... \cdot C_n^{n_k}. \quad (9)$$

Similarly, by expanding the scope of a specific problem, it is possible to determine a set of alternative frequencies of particular interest (absence of a compound very dangerous feature on an arbitrary object). It can be found through replacing sets of type A_1, A_2 with their complements of type $U \backslash A_1$, $U \backslash A_2$ with the number of elements $n - n_1 = 1$ and $n - n_2 = 2$, respectively, in the source data. In this case, at the preliminary stage, families, the Cartesian product of families whose elements are assigned intersections of sets of the type ($U \backslash A_1 \cap U \backslash A_2$), and the function whose values are the numbers of elements of such intersections, are defined in the same way. Having determined these numbers, we solve a combinatorial problem corresponding to one specific problem, and after normalization — to another one. In terms of modeling the first problem in relation to the new source data, the second one will represent:

— set *U* with the number of elements *n*,

— various sets $U \backslash A_1$ with the same number of elements $n - n_1$,

— various sets $U \backslash A_2$ with the number of elements $n - n_2$ each.

The combinatorial problem corresponding to the problem with new source data is of great importance for practice. To solve it, it is advisable to use the result of the following arguments. Let along with a set of ascending-sorted values *f*, we obtain a set of similarly ordered values — the same as *f* of function *g*, whose arguments correspond to the new data. It can be shown that the first and second sets have the same number of elements. Let f_h and g_h be elements of these sets with number *h*. We can make sure that element g_h of the second set corresponds to the same number of arguments of function *g*, as element f_h of the first set, and the number of all arguments (variants) *f* and *g* are the same, that is, equal to *s*.

Therefore, the quotients of $s(r)/s$ type, where $r = f_h$ correspond to arbitrary value g_h of function *g* in terms of the model. These quotients represent the corresponding probabilities of the presence of groups of objects without a compound very dangerous feature of different numbers, if the probabilities of the appearance of different groups of objects of the same number with a simple feature *i* for all $i = 1...k$ are the same.

It can be shown that the formulated combinatorial problems are applicable without significant changes to problems in a generalized form, when compound very dangerous features are determined using not only the intersection operation, but also the population $A_1 \cup A_2 \cup ... \cup A_k$, differences $A_1 \setminus A_2$, $A_2 \setminus A_1$, etc., and the source groups are not necessarily only those of objects with simple features.

Discussion and Conclusions. Thus, it is established that the problem of predicting damage due to unfavorable circumstances corresponds to a combinatorial type problem. It consists in:

— enumeration of all sets-arguments,

— derivation of different values *f*,

— determination of smaller and larger values *f*,

— obtaining the range of possible values of function *f*, in which its true value is found.

This range is an element group of indistinguishability, it characterizes the smaller and larger possible value of the group size of a potentially hazardous factor with a compound very dangerous feature, and includes several operations.

The results obtained are focused on the construction of analytical algorithms for establishing indistinguishability under the monitoring, modeling and forecasting processes related to the state, and complex dynamic multiparameter objects.

References

1. Ventsov NN, Chernyshev YuO. Formirovanie startovoi populyatsii v usloviyakh neopredelennostei [Formation of the starting population under conditions of uncertainty]. In: Proc. Int. Sci.-Tech. Conf. on Intelligent Systems and Information Technologies — 2019. Rostov-on-Don: DSTU Publ. Centre; 2019. P. 25–30. (In Russ.)

2. Podinovsky VV. Potentsial'naya nedominiruemost' v zadachakh vybora neskol'kikh luchshikh variantov [Potential nondomination in problems of choice of several best options]. Moscow Witte University Bulletin. Educational Resources and Technologies. 2013;2:57–63. (In Russ.)

3. Chernyshev YuO, Ventsov NN, Pshenichnii IS. Ehvolyutsionnyi algoritm poiska mnozhestva al'ternativnykh marshrutov v usloviyakh vozmozhnykh vozdeistvii [Evolutionary algorithm of search of a set of alternative routes in the conditions of possible influences] Engineering Journal of Don. 2018;4(51):42–56. (In Russ.)

4. Kravtsova MV. Otsenka tekhnogennogo riska tekhnicheski slozhnykh proizvodstvennykh ob"ektov mashinostroeniya [Risk assessment of technogenic technically complex production facilities engineering]. Proceedings of the Samara Scientific Center of RAS. 2012;14(1–3):877–884. (In Russ.)

5. Bunkovsky DV. Instrumenty upravleniya predprinimatel'skimi riskami [Entrepreneurial risks management tools]. Management Issues. 2019;1(37):65–76. DOI: 10.22394/2304-3369-2019-1-65-76 (In Russ.)

6. Belykh AA. Osnovy metodologii prognozirovaniya i otsenki ehffektivnosti informatsionnykh sistem [The foundations for prognoses methodology and for information system efficiency estimation]. Scientific Journal of KubSAU. 2011;71:11–133. (In Russ.)

7. Orlov AI. Menedzhment [Management]. Moscow: Izumrud; 2003. 298 p. (In Russ.)

8. Ostreikovsky VA, et al. Matematicheskoe modelirovanie tekhnogennogo riska [Mathematical modeling of technogenic risk]. Surgut: SurSU Publ. Center; 2010. 96 p. (In Russ.)

9. Germeier YuB. Vvedenie v teoriyu issledovaniya operatsii [Introduction to the theory of operations research]. Moscow: Nauka; 1971. 384 p. (In Russ.)

10. Zolotukhin VF, Zakharov AA, Reva VYu. Kharakteristiki tekhnogennoi bezopasnosti v usloviyakh nerazlichimosti [Characteristics of the technogenic safety under the conditions of indistinguishability]. Izvestiya SFedU. Engineering Sciences. 2009;91(2):54–58. (In Russ.)

11. Tseligorov NA, Tseligorova EN, Mafura GM. Matematicheskie modeli neopredelennostei sistem upravleniya i metody, ispol'zuemye dlya ikh issledovaniya [Mathematical model uncertainties management systems and methods used for their research]. Engineering Journal of Don. 2012;23(4–2):48. (In Russ.)

12. Zolotukhin VF. Fundamental'nye chislovye kharakteristiki, vozmozhnosti, vozmozhnye raspredeleniya i mery [Fundamental numerical characteristics of contingency, contingent distributions and measures]. Automation and Remote Control. 2003;12:152–159. (In Russ.)

13. Gusev LA, Khutorskaya OYe. Ob odnoi otsenke ehffektivnosti mashinnoi diagnostiki dvigatel'nykh narushenii [On an estimation of the effectiveness of computer diagnosis of movement disorders]. Automation and Remote Control 2003;12:112–121. (In Russ.)

14. Litvak BG. Ehkspertnaya informatsiya: metody polucheniya i analiza [Expert information: methods of obtaining and analysis]. Moscow: Radio i svyaz'; 1982. 184 p. (In Russ.)

15. Azhmukhamedov IM. Modelirovanie na osnove ehkspertnykh suzhdenii protsessa otsenki informatsionnoi bezopasnosti [Modeling based on the expert judgments in the process of informational safety evaluation]. Vestnik of Astrakhan State Technical University. Series: Management, Computer Sciences and Informatics. 2009;2:101–109. (In Russ.)

16. Azhmukhamedov IM. Analiz i upravlenie kompleksnoi bezopasnost'yu na osnove kognitivnogo modelirovaniya [Cognitive-modeling-based integrated security analysis and management]. Large-scale Systems Control. 2010;29:5–15. (In Russ.)

17. Gusev LA. Interval'nye otsenki veroyatnosti pri nalichii nerazlichimosti [Interval estimates of probability in the presence of indistinguishability]. Control Sciences. 2013;4:16–22. (In Russ.)

18. Krokhin GD. Istochniki informatsii i prichiny ee neopredelennosti, vyyavlennye pri diagnostike sostoyaniya ehnergoustanovok [Information sources and causes of its uncertainty revealed under diagnosis of powerplant status]. Vestnik NSUEM. 2014;1:292–311. (In Russ.)

19. Fatuev VA, Safronova MA. Upravlenie dinamicheskimi sistemami s ispol'zovaniem situatsionnykh i regressionnykh modelei [Management of dynamic systems using situational and regression models]. Izvestiya Tula State University. 2012;2:118–127. (In Russ.)

20. Greco S, Matarazzo B, Slowinski R. Rough sets theory for multicriteria decision analysis. European Journal of Operational Research. 2001;129(1):1–47.

21. Korotkiy AA, Yegelskaya EV, Sherstyuk AP. Obosnovaniya bezopasnosti gruzopod"emnykh kranov [Safety case: cargo cranes]. Vestnik of DSTU. 2017;91(4):136–143. (In Russ.)

22. Bourque F-A. Solving the moving target search problem using indistinguishable searchers. European Journal of Operational Research. 2019;275(1):45–52. DOI:10.1016/j.ejor.2018.11.006

23. Jacas J, Recasens J. The group of isometries of an indistinguishability operator. Fuzzy Sets and Systems. 2004;146(1):27–41. DOI:10.1016/j.fss.2003.11.004

24. Judd K, Smith L. Indistinguishable states: I. Perfect model scenario. Physica D: Nonlinear Phenomena. 2001;151(2–4):125–141. DOI:10.1016/s0167-2789(01)00225-1

25. Calvo T, Fuster P, Valero O. On the problem of aggregation of partial T-indistinguishability operators. Atlantis Studies in Uncertainty Modelling. 2019;1:52–59. DOI: 10.2991/eusflat-19.2019.8

26. Sánchez TC, Fuster-Parra P. Aggregation of partial *T*-indistinguishability operators and partial pseudometrics. Fuzzy Sets and Systems. 2021;403:119–138. DOI: 10.1016/j.fss.2019.10.009

27. Mattioli G, Recasens J. Structural analysis of indistinguishability operators and related concepts. Information Sciences. 2013;241:85–100.

Submitted 29.07.2020
Scheduled in the issue 12.10.2020

About the Authors:

Zolotukhin, Vladimir Ph., employee, SC "VNII "Gradient" (96, Sokolov Pr., Rostov-on-Don, 344010, RF), Dr.Sci. (Tech.), professor, ORCID: http://orcid.org/0000-0002-8449-5826, ScopusID: 7006603308, chita1983@rambler.ru

Matershev, Alexander V., postgraduate student of the Radiophysics Department, Southern Federal University (105/42, Bolshaya Sadovaya St., Rostov-on-Don, 344006, RF), Cand.Sci. (Eng.) applicant, ORCID: http://orcid.org/0000-0002-9533-3785, matershev.aleksandr@mail.ru

Podkolzina, Lubov A., postgraduate student of the Information Technologies Department, Don State Technical University (1, Gagarin sq., Rostov-on-Don, 344003, RF), ORCID: http://orcid.org/0000-0001-9476-5802, ScopusID: 57200151503, Researcher ID: M-5035-2019, podkolzinalu@gmail.com

Claimed contributorship

V. F. Zolotukhin: basic concept formulation; academic advising; analysis of the research results; the text revision; correction of the conclusions. A. V. Matershev: research objectives and tasks setting; computational analysis; formulation of conclusions. L. A. Podkolzina: literature review; analysis of calculations; text preparation; formulation of conclusions.

All authors have read and approved the final manuscript.

INFORMATION TECHNOLOGY, COMPUTER SCIENCE, AND MANAGEMENT

UDC 004.93 https://doi.org/10.23947/2687-1653-2020-20-4-414-421

Criteria of evaluating augmented reality applications

M. R. Ablyaev, A. N. Abliakimova, Z. S. Seidametova
Crimean Engineering-Pedagogical University (Republic of Crimea, Russian Federation)

Introduction. The field of augmented reality (AR) is growing rapidly and has great advances in interaction, navigation and tracking. Nowadays there are a lot of trends for AR applications in different areas (education, entertainment, business, medicine, etc.). However, there is a lack of research to provide the evaluating AR apps framework to support developers when creating suitable AR applications for specific needs. We provide a practical approach to quantify some of the AR applications features. We focus on the development of criteria for evaluating augmented reality applications. We discuss the criteria of choosing dimensions for that space such as standards for AR, tools for AR development, navigation and tracking, content management, usability. We provide analysis and evaluation of AR apps through each characteristic using guidelines which we have developed.
Materials and Methods. An AR application is a software application that integrates digital visual, audio and other types of content into a real-world environment. The software quality and performance are the main characteristics of the application, which are key factors for AR applications. The analysis of scientific papers, documents and standards made it possible to determine characteristics that are the most significant quality indicators based on well-grounded users' needs and demands.
Results. The criteria we have developed for evaluating applications with augmented reality enable developers to create their own software products in stages, based on step-by-step requirements for them, evaluating the development process by characteristics. This approach will allow you to create high-quality software products using standardized, modern development tools.
Discussion and Conclusions. In addition, developers will have a detailed understanding of each stage of creating the application and the necessary development tools and technologies to obtain the highest quality result. That will give an opportunity to decide on specific development tools, methods, models and technologies before starting work on a project. As a result, it will provide the final high-quality software product with good extensibility and compliance with the modern requirements of the digital industry market.

Keywords: augmented reality, software development kit, navigation and tracking, content management, usability.

For citation: M. R. Ablyaev, A. N. Abliakimova, Z. S. Seidametova. Criteria of evaluating augmented reality applications. Advanced Engineering Research, 2020, vol. 20, no. 4, pp. 414–421. https://doi.org/10.23947/2687-1653-2020-20-4-414-421

Introduction. The development of the modern market of augmented reality (AR) technology contributes to the emergence of a larger number of AR-applications widely used in industries including healthcare, public safety, gas and oil, tourism and marketing, entertainment and academia. In connection with the increased interest in this technology, the development of functional capabilities of AR projects is also carried out, which stimulates an increase in the needs of AR-technology using in the most diverse sectors of modern society.

Unfortunately, some significant aspects of the AR applications development and implementation and AR services, often ignored for the design simplicity and implementing speed, are the compliance with such systems to real conditions and the evaluating under real operating conditions. To develop successful and highly efficient AR systems that can be adopted in everyday scenarios, user assessment and feedback are very important [1].

Augmented reality is a very young industry, and there are still no generally accepted standards for developing

AR applications. Although the main platforms for creating augmented reality applications have been defined: ARKit[1], ARCore[2] and Unity[3] (mostly used) – even now AR applications developed using these tools are available for launch only on a limited type of digital and mobile devices.

The situation is exactly the same with wearable devices, HoloLens and Magic Leap glasses – each manufacturer offers its own unique software for creating augmented reality programs. Experts give several years before the industry consolidates and common standards allow making the development of augmented reality applications accessible and universal for all AR developers.

Rapid progression of the AR field requires effective and validated methods of design evaluation to be developed. Failure to consider the usability of AR applications during the design process will result in an increase in user errors and accidents, limiting user trust of the technology and undermining user perceptions of the technology, for both AR and Virtual Reality (VR) technologies [2].

The authors of the papers [1–3] provided an overview of the important designing and implementing features of AR applications and proposed theoretical evaluation of AR systems and frameworks through the standardization aspects. Endsley and others [4] described principles of design heuristics for AR for multi-dimensional augmented environments. Some examples of user experience evaluations were presented in the papers [5–10].

J. L. Gabbard and J. E. Swan [11] proposed a Usability Engineering (UE) for Augmented Reality approach that inserts iteratively a series of user-based studies into a traditional usability-engineering life cycle. Several usability testing methods of the AR application (subjective measurement using human perception, objective measure from observation, evaluation by expert through cognitive walkthrough, heuristic evaluation, lab observation, questionnaire) were described by Pranoto and others [12]. Martins and others [13] presented practical use of the usability methods for evaluating an AR children's book with multiple methods. Other aspects of AR technology tools and AR applications evaluating were presented in the papers [14] and [15].

Akgul and others [16] adapted an existing deep learning architecture to solve the detection problem in AR application using camera-based tracking. Other methods that help to improve AR application and to increment the productivity in manufacture were described in [17–19].

There are several survey papers on AR development, but none is dedicated to Mobile Augmented Reality. Huang and others [20] present the results of the latest technologies and methods survey that improves run-time performance and energy efficiency for the practical implementation of mobile AR applications.

We have presented AR application "Tilsimli arifler" ("Magic letters") and special features of design and developing mobile AR application for enhancing early literacy skills in our papers [21–22].

Software quality and performance. An AR application is a software application that integrates digital visual, audio and other types of content into a real-world environment. The software quality and performance are the main characteristics of the application, which are key factors for AR applications. Software development is a complex and multi-faceted process, in which a large number of specialists of various areas of expertise and various skill levels participate. In addition, many technical, technological, and managerial issues intertwine in the application development process. The success of the project and the quality of the developed product depend on their adequate involvement.

The analysis of papers, documents (e.g., [2, 3, 10, 16, 22]) and standards (e.g., ISO-IEC JTC 1 SC 24, 18521-1[4], ISO 9000[5]) shows that the following characteristics are the key quality indicators based on well-grounded users' needs and demands:

— inadequate functioning of the software product;

— insufficient interaction of the product with other software, hardware, telecommunications;

— failures of the software application during the intended use;

— the slowed down time of the software product and the delay in the presentation of intermediate and output information;

— incomplete display of information;

— inconsistency of stored data and information entered by the operator;

— loss of relevance of the information;

— violation of the confidentiality of information.

In addition to such "primary" quality data coming directly from the consumer, developers use "internal" indicators to evaluate the parameters of the current project:

[1] Augmented Reality – Apple Developer. https://developer.apple.com/augmented-reality/
[2] ARCore – Google Developers. https://developers.google.com/ar
[3] Unity for all. https://unity.com/
[4] Kim G. Augmented Reality Continuum Concepts and Reference Model – Part 1: ARC Reference Model (Work Item Proposal), ISO-IEC JTC 1 SC 24, 18521-1. 2012.
[5] ISO 9000 Family Quality Management. https://www.iso.org/iso-9001-quality-management.html

— the lines of code in the standard mode;
— the number of detected errors per 1000 lines of code;
— program complexity parameters;
— the probability of occurrence of specific errors;
— the project complexity and cost of a code unit;
— price of a “man-month”;
— statistical characteristics of processes (expectation, variance, correlation function, etc.) and other estimated parameters.

Augmented Reality Application Evaluation Criteria. Ten experts with more than 3 years’ experience in AR application development help us to create criteria for evaluating AR apps. We divided the main criteria for assessing the quality of augmented reality applications into 5 groups (Fig 1):

— AR app design and Art design;
— Graphic programming;
— AR applications programming;
— Application profiling and optimization;
— Publishing applications (build).

When developing an *AR application design*, we recommend the following characteristics that should be considered:

1. The surface. How the application can adapt to various surfaces. If you use frameworks, you can use the built-in surface detection function. For example, the application can recognize the floor, walls and objects.
2. Shine. Evaluation of illumination is very important for the realism of objects. It is advisable to use dynamic lighting with shadows in real time.
3. Space needed. Users can experience AR in three different sizes: table scale, room scale, and open environment. The user should always have enough space to simply enjoy the experience. Thus, it is necessary to think over this before the user starts using the application. For example, if an application requires an open environment, you need to inform the audience in advance before they start using the product.
4. Single-user or multi-user product. If you are developing a multi-user interface, you should design the product when everyone is involved in the process. It is important to create a sense of audience connection with the product. For example, if you are developing an AR game, you can provide a map that shows the location of users and provides real-time status notifications.

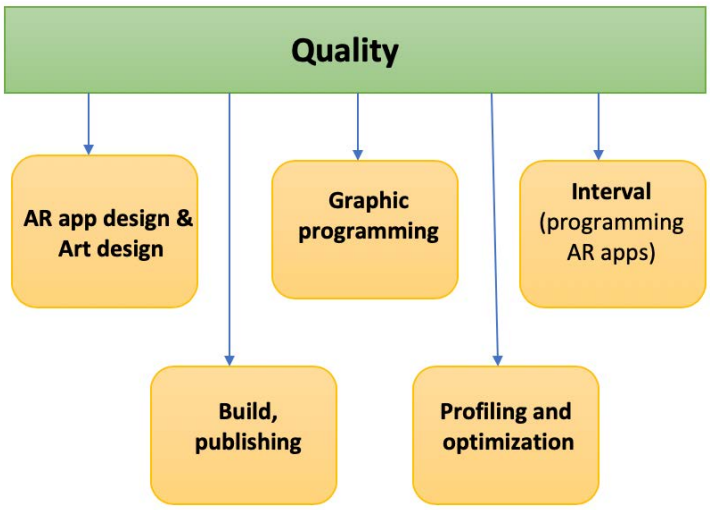

Fig. 1. Evaluation criteria for AR applications

The main criteria are highlighted as follows (Table 1).

Table 1

AR App Design and Art Design evaluation points

AR App Design and Art Design	25
Actual requirements (of the market) in terms of application design	2
Interface design requirements	2
UX features for AR applications	1
Target platform specifications	2
3D modeling principles	1
Principles of work with particle systems	1
Types and features of the creation and use of textures	1
Principles of working with shaders and materials, rendering features	2
Features for customizing models and textures, as well as materials for export to the game engine	1
Create high-quality 3D models in modern editors	2
Create UV-scan in modern editors	2
Texturize models in modern editors	2
Rigging and animating models in modern editors	2
Customize animation in game engines	2
Create and customize shaders, materials in simulation programs and game engines	2

The initial version of Table 1 was proposed by the authors, then it was discussed with ten experts in AR development using brainstorming techniques.

To solve the problems of displaying complex graphic objects, it is necessary to develop effective methods and algorithms for processing graphic information at the stages of input, encoding, transformation and image formation. All of this makes up a set of basic computer graphics tasks, so we have identified the main components needed to create a high-quality graphic component (Table 2).

Graphic programming enables to create visual effects through the development of shaders using the functions of graphic libraries, customizing the rendering of the development environment, using effective postprocessing libraries, customizing shadows, and more. All these components make it possible to obtain high-quality images by applying various effects, as well as improve the optimization of application performance.

Table 2

Graphic programming evaluation points

Graphic programming	25
Rendering features on the target platform	2
Using textures and materials in the game engine	2
Features of the work of graphic libraries	2
Principles of rendering geometric objects and images	2
Principles of proper postprocessing	3
Features of implementing lighting and shadows on the used game engine and target platform	3
Configure static and dynamic lighting in the used game engine	2
Optimize rendering processes	3
Customize postprocessing and final image appearance	2
Create procedural geometry using game engine tools	2
Programming the rendering of the frame	2

Evaluation points presented in Table 2 were proposed by the authors and later they were discussed with ten experts in AR development.

During the development of the software part of the mobile application with augmented reality, it is necessary to precisely determine the fundamental development tools, and, accordingly, the programming languages, programming environments, patterns, architecture, etc. This is necessary for a clearer and more coordinated team work, understanding the requirements and tasks, comprehension of the logic and sequence of application development, orientation in the

project, reducing risks, and interaction of each team member with each other. To achieve this, we have identified the following points for the programming phase, which should be followed in order to obtain a positive result of the development process (Table 3).

Table 3

AR Applications Programming evaluation points

AR Applications Programming	25
Modern programming languages used in AR development	2
OOP principles	2
Building an application architecture	2
Principles of building AR applications	2
Code design standards	2
Basic math for AR applications	2
Work with a network in the context of AR	2
Work with modern AR application development environments	2
Write high-quality code in modern programming languages used in AR	2
Implement specific application mechanics as soon as possible	2
Use development environments for writing and debugging code	2
Work with necessary SDKs for AR	2
Use collaboration tools	1

The evaluation points presented in Table 3 were proposed by the authors and brainstormed with ten experts in AR development.

When developing applications with augmented reality, it is important to consider the features of application optimization for PC and mobile devices, as well as the architecture of mobile devices in the context of application optimization. In this regard, we have identified the points that we advise to adhere to during the development in order to achieve maximum optimization of AR applications (Table 4).

The profiler tool provides specific data on game performance and facilitates its optimization process. The profiler provides frame-by-frame metrics with which you can more easily identify problem areas.

Table 4

Application Profiling and Optimization evaluation points

Application Profiling and Optimization	16
Optimization of AR application performance	3
Optimization of 3D objects	2
Geometry optimization	2
Optimization of textures and materials for the target platforms	2
Optimization of the main application processes	2
Optimization of physics in the application	2
Using built-in game engine profilers, as well as external profilers	3

Table 4 was created by the authors and then it was discussed with ten experts in AR development.

After completion of all stages of the application development, it is important to publish the application. The publication represents the release of the application on any platform where the customer (end-user) can easily download the final version of product, get acquainted with it, get all the necessary documentations, technical support and feedback from the developer. Each of the platforms puts forward its specific requirements to the publishing application, which are necessary for correct displaying the application in the platform's market, obtaining all information about the application's operation, ensuring end-user security, promoting the application, and more. In this regard, the publication is one of the most important and crucial stage of the development. We have identified several main platforms, before using which it is necessary to familiarize yourself with all the documentation and assembly features for the appropriate platform (Table 5).

Table 5

Publishing applications (build) evaluation points

Publishing applications (build)	9
Features of building an application for Windows	3
Features of the build application for Android.	3
Features of the build application for OS X/ iOS.	3

Evaluation points presented in Table 5 were proposed by the experts in AR development.

Conclusions. Nowadays, the augmented reality is one of the most innovative and a new digital trend in the developing applications for all type of devices. The AR technology opens a new horizon and is going to get more popular in the foreseeable future.

The criteria we have developed for evaluating applications with augmented reality enable developers to create their own software products in stages, based on step-by-step requirements for them. This will allow you to create high-quality software products using the standardized, modern development tools.

In addition, developers will have a detailed understanding of each stage of creating the application and the necessary development tools and technologies to obtain the highest quality result. That will give an opportunity to decide on specific development tools, methods, models and technologies before starting work on a project; and, in the process of working on the basis of existing criteria, gradually create key application stages, with possible subsequent upgrades and improvements. As a result, it will provide the final high-quality software product with good extensibility and compliance with the modern requirements of the digital industry market.

In the follow-up study, we are going to apply this approach for evaluating several AR applications. To thoroughly verify the proposed criteria, additional testing will be required, where more software field experts should be involved. Engaging third-party experts will assess the suitability of the proposed criteria. We believe that this approach will become part of the AR application development process.

References

1. Ritsos PD, Ritsos DP, Gougoulis AS. Standards in augmented reality: a user experience perspective. In: 2nd International Workshop on AR Standards. 2011;17:9.

2. Lee J, Lee Y, Lee S, et al. Standardization for augmented reality: introduction of activities at ISO-IEC SC 24 WG 9. In: Proceedings of the 12th ACM SIGGRAPH International Conference on Virtual-Reality Continuum and Its Applications in Industry, 2013. P. 279−280. DOI: 1145/2534329.2534379

3. Perey C, Engelke T, Reed C. Current Status of Standards for Augmented Reality. Recent Trends of Mobile Collaborative Augmented Reality Systems. Springer, New York, NY, 2011. P. 21−38. DOI: 10.1007/978-1-4419-9845-3_2

4. Endsley TC, Sprehn KA, Brill RM, et al. Augmented Reality Design Heuristics: Designing for Dynamic Interactions. In: Proceedings of the Human Factors and Ergonomics Society Annual Meeting. 2017;61(1):2100–2104.

5. Dhir A, Al-kahtani M. A Case Study on User Experience (UX) Evaluation of Mobile Augmented Reality Prototypes. Journal of Universal Computer Science. 2013;19(8):1175−1196.

6. Caudell TP, Mizell DW. Augmented reality: an application of heads-up display technology to manual manufacturing processes. In: Proceedings of the Twenty-Fifth Hawaii International Conference on System Sciences. IEEE. 1992;2:659−669.

7. Olsson T, Lagerstam E, Kärkkäinen T, et al. Expected user experience of mobile augmented reality services: a user study in the context of shopping centres. Personal and ubiquitous computing. 2013;17(2):287−304.

8. Knoerlein B, Luca MD, Harders M. Influence of visual and haptic delays on stiffness perception in augmented reality. In: 8th IEEE International Symposium on Mixed and Augmented Reality, IEEE. 2009. P. 49−52.

9. Duenser A, Billinghurst M. Evaluating augmented reality systems. In: Handbook of augmented reality.

Springer, New York, NY, 2012. P. 289−307.

10. Arifin Y, Sastria TG, Barlian E. User experience metric for augmented reality application: a review. Procedia Computer Science. 2018;135:648−656.

11. Gabbard JL, Swan JE. Usability Engineering for Augmented Reality: Employing User-Based Studies to Inform Design. In: IEEE Transactions on Visualization and Computer Graphics 14, 2008. P. 513−525.

12. Pranoto H, Tho C, Warnars HL, et al. Usability testing method in augmented reality application. In: 2017 International Conference on Information Management and Technology (ICIMTech), 2017. P. 181−186.

13. Martins VF, Sanches GB, de Almeida NG, et al. Usability Evaluation of an Augmented Reality Children's Book. In: 2019 XIV Latin American Conference on Learning Technologies (LACLO), IEEE. 2019;1:381−386. DOI: 10.1109/LACLO49268.2019.00070

14. Da Silva MMO, Teixeira JMXN, Cavalcante PS, et al. Perspectives on How to Evaluate Augmented Reality Technology Tools for Education: A Systematic Review. Journal of the Brazilian Computer Socciety. 2019;25(1):1–18. DOI: 10.1186/s13173-019-0084-8

15. Guimaraes MDP, Martins VF. A Checklist to Evaluate Augmented Reality Applications. In: 2014 16th Symposium on Virtual and Augmented Reality, IEEE, 2014. P. 45−52. DOI: 10.1109/SVR.2014.17

16. Akgul O, Penekli HI, Genc Y. Applying deep learning in augmented reality tracking. In: 12th International Conference on Signal-Image Technology & Internet-Based Systems (SITIS), IEEE. 2016;1:47−54.

17. Harders M, Bianchi G, Knoerlein B, et al. Calibration, Registration, and Synchronization for High Precision Augmented Reality Haptics. In: IEEE Transactions on Visualization and Computer Graphics. 2009;15(1):138-149.

18. Ramírez H, Mendoza E, Mendoza M, et al. Application of augmented reality in statistical process control, to increment the productivity in manufacture. Procedia Computer Science. 2015;75:213–220. http://www.sciencedirect.com/science/article/pii/S1877050915037011

19. Chen H, Dai Y, Meng H, et al. Understanding the Characteristics of Mobile Augmented Reality Applications. In: 2018 IEEE International Symposium on Performance Analysis of Systems and Software (ISPASS), Belfast, 2018. P. 128−138.

20. Huang Z, Hui P, Peylo C, et al. Mobile augmented reality survey: a bottom-up approach. 2013. P. 112−126. arXiv preprint arXiv:1309.4413

21. Ablyaev M, Abliakimova A, Seidametova Z. Design of mobile augmented reality system for early literacy. Ermolayev V, Mallet F, Yakovyna V, et al. (eds.) In: Proceedings of the 15th International Conference, ICTERI 2019, Vol. I: Main Conference, CEUR Workshop Proceedings (CEUR-WS.org) on ICT in Education, Research, and Industrial Applications. Ukraine, Kherson, 12–15 June 2019. 2019;2387:274–285. CEUR-WS.org http://ceur-ws.org/Vol-2387/20190274.pdf (accessed: 22 March 2020).

22. Ablyaev M, Abliakimova A, Seidametova Z. Developing a mobile augmented reality application for enhancing early literacy skills. Ermolayev V, Mallet F, Yakovyna V, et al. (eds.) In: Information and Communication Technologies in Education, Research, and Industrial Applications. ICTERI 2019. Communications in Computer and Information Science Springer, Cham. 2020;1175:163–185. DOI: 10.1007/978-3-030-39459-2

Submitted 29.07.2020
Scheduled in the issue 12.10.2020

About the Authors:

Ablyaev, Marlen R., lecturer of the Applied Informatics Department, Crimean Engineering-Pedagogical University (8, per. Uchebny, Simferopol, Republic of Crimea, 295015, RF), ORCID: http://orcid.org/0000-0003-0571-2333, ablyaev.marlen@gmail.com

Abliakimova, Afife N., lecturer of the Applied Informatics Department, Crimean Engineering-Pedagogical University (8, per. Uchebny, Simferopol, Republic of Crimea, 295015, RF), ORCID: http://orcid.org/0000-0003-3867-5401, ablyakimova.afife@gmail.com

Seidametova, Zarema S., Head of the Applied Informatics Department, Crimean Engineering-Pedagogical University (8, per. Uchebny, Simferopol, Republic of Crimea, 295015, RF), Dr.Sci. (Pedagogics), Cand.Sci. (Phys.-Math.), professor, Scopus ID: 57189935002, ResearcherID: AAF-9106-2019, ORCID: http://orcid.org/0000-0001-7643-6386, z.seidametova@kipu-rc.ru

Claimed contributorship

M. R. Ablyaev: critical revision of the assessment criteria; writing the first version of the paper. A. N. Abliakimova: collection and processing of material; concept and design of the research; writing the first version of the paper. Z. S. Seidametova: collection and processing of material; concept and design of the research; writing the final version of the paper.

All authors have read and approved the final manuscript.

INFORMATION TECHNOLOGY, COMPUTER SCIENCE, AND MANAGEMENT

UDC 681.3.06 https://doi.org/10.23947/2687-1653-2020-20-4-422-429

Polynomially computable Σ–specifications of hierarchical models of reacting systems

V. N. Glushkova, K. S. Korovina
Don State Technical University (Rostov-on-Don, Russian Federation)

Introduction. Verification packages design and analyze the correctness of parallel and distributed systems within the framework of various classes of temporal logics of linear and branching time. The paper discusses a polynomially realizable class of $\Delta_0 T$ -formulas interpreted on multi-sorted models with hierarchical suspensions. The suspension structure is described by an arbitrary context-free (CF) grammar. The predicates and functions of the model signature are interpreted on the original CF-list, which is completed during the interpretation process.
Materials and Methods. A constant model is constructed for theories from $\Delta_0 T$-quasiidentities with Noetherian and confluence properties. We consider formulas of the multi-sorted first-order predicate calculus (PC) language with variables of the "list" sort interpreted on models with a hierarchized suspension. The theory is interpreted in terms of grammar inference trees describing the behavior of the specified system. The CF-grammar rules hierarchize the action space of the modeled system. It is noted that the expressive capabilities of $\Delta_0 T$-formulas are insufficient for modeling real-time systems. Therefore, expressions with unbounded universal quantifier ∀, known as PT formulas, are used for the specification.
Results. The logical specification of an automated complex which consists of a workpiece manipulator is given as an example. The location of the positions is fixed by sensors. The operating cycle of the manipulator is described. The specification of its operation consists in the hierarchization of actions by the rules of the CF-grammar and their description by the first-order PT-formulas taking into account the time values.
Discussion and Conclusions. The paper shows that the class of the considered formulas can be used to model real-time systems. An example of the logical specification of a manipulator behavior control device is given.

***Keywords**:* logical specification, theory model, reactive system, CF-grammar, first-order PC-formula.

For citation: V. N. Glushkova, K. S. Korovina. Polynomially computable Σ–specifications of hierarchical models of reacting systems. Advanced Engineering Research, 2020, vol. 20, no. 4, p. 422–429. https://doi.org/10.23947/2687-1653-2020-20-4-422-429

Introduction. Mathematically sound, practically significant methods of verification of complex software and technical systems are based on the apparatus of mathematical logic [1–4]. The technique of applying this approach to various types of real-time reactive systems (communication protocols, control systems, integrated onboard systems of space technology, etc.) is known.

This technique provides verification of model checking systems [5–7]. Numerous verification packages support the design and analysis of the correctness of parallel and distributed systems within various classes of linear and branching time temporal logics: LTL, CTL, TCTL, etc. [8].

To simulate time in these systems, the standard model of the time automaton is used. This is a finite state machine equipped with a special type of variable — local clock. Quantitative analysis of the time characteristics of the system is complicated by complex exponential algorithms for constructing time zones as equivalence classes [9]. Therefore, it is required to develop a more expressive, practically significant specification language to simplify the analysis.

It is proposed to use the language of Σ- specifications for simulation, highlighted in the concept of semantic programming, which is based on the model-theoretic approach [10]. In this case, the 1st order predicate calculus language, extended by axioms for list structure operations can be used to build a formal model of the analyzed system[1,2,3,4].

Materials and Methods. The paper uses terminology of the papers [11, 12]. Let $\mathcal{M}$ be a many-sorted signature model $\sigma = < I, C, F, R>$. Here, I is a set of sorts, including the "list" sort (*list*). C, F, R are sets of constants, functions, and predicates, respectively. All signature symbols have a type. If $f \in F$ is an n-local function, $n \geq 0$, then its type is $<i_1, \dots i_n, i>$, where $i_1, \dots i_n, i \in I$, and $i_1, \dots i_n$ are types of arguments, i is the type of the function value. Similarly, n- local predicate $r \in R$ is of type $< i_1, \dots i_n >$. The model carrier $\mathcal{M}$ is an indexed family of sets $U_j = C_j$, $j \in I$, where C_j is a set of constants of sort j; f: $U_{i_1} \times \dots \times U_{i_n} \to U_i$, $r \subseteq U_{i_1} \times \dots \times U_{i_n}$.

For the model $\mathcal{M}$, a list suspension $D_G(C)$ from the hierarchized CF-lists, whose structure is set by the CF-grammar, is formed over a set of constants C. Here, N, T are sets of nonterminal and terminal symbols. The set $D_G(C)$ is defined as the smallest set of all lists $<t_1, \dots, t_n>$, formed for each rule $A \to X_1 \dots X_n \in P$, $n \geq 1$ as follows: t_i is an arbitrary constant of C_{X_i}, if $X_i \in T$; otherwise, for $X_i \in N$, the element t_i is an arbitrary list of X_i.

Δ_0-formulas are defined in the traditional way as signature formulas σ using all logical connectives ($\neg$, $\wedge$, $\vee$, $\to$) and bounded quantifiers $\forall x \in t$, $\exists x \in t$, $\forall x \subseteq t$, $\exists x \subseteq t$. Here, x is a variable of an arbitrary sort; t is a term of the *list* sort that does not contain x; $\in$ is the list membership relation; $\subseteq$ the nesting relation for lists, defined as $< \alpha_1, \dots, \alpha_n > \subseteq < \alpha_1, \dots, \alpha_n >$, $m \geq n$.

Below, we will use only bounded quantifiers of the form $\forall x \in y$, $\forall x \ \dot{\in} \ y$, where переменная y is a variable of *list* sort, the relation $\dot{\in}$ is transitive closure of the relationship $\in$. Denote the indexed sequence of variables x_i by $\bar{x}$, and the membership relation or its transitive closure — by $\overset{\circ}{\in}$.

Rules of the CF-grammar hierarchize the action space of the simulated system. For reasons of computational efficiency, a class of $\Delta_0 T$-formulas with a "tree" prefix is distinguished. We introduce the relation $\prec$ — to the "left" for the list elements, namely, for the list $< \dots \propto, \beta \dots >$, we consider $\propto \prec \beta$.

Definition. Δ_0-formula of the form

$$(\forall v_1 \overset{\circ}{\in} r_1) \dots (\forall v_m \overset{\circ}{\in} r_m)\, (n_1 \prec l_1) \dots (n_p \prec l_p)\ \Phi(\bar{v}, \bar{r}),\ m \geq 1,\ p \geq 0$$

is called $\Delta_0 T$-formula if $n_j, l_j \in (\bar{v}, \bar{r})$, $1 \leq j \leq p$; for all prefix variables, the following condition is true: $r_{i+1} = r_i$, $1 \leq i < m$ or $r_{i+1} = v_k$, $k \leq i$. If $r_{i+1} = v_k$, then $v_{i+k} \neq v_k$ and $v_{i+k} \neq r_k$ for all $k \leq i$.

It is easy to show that the prefix of $\Delta_0 T$-formula, due to restrictions on variables, can be presented as a tree with root r_1, vertices v_i, r_i and arcs going from vertex r_i to vertex v_i, $1 \leq i \leq m$.

The expressive capabilities of $\Delta_0 T$-formulas are not sufficient for modeling real-time systems that function cyclically for an indefinite period of time. We will use for the specification of the PT-formula with a universal quantifier $\forall$.

Definition. The formula obtained from $\Delta_0 T$-formula through Φ unbounded universal quantification $\forall v\, \Phi(v)$, is called the PT-formula.

The model $\mathcal{M}$ is defined by a theory of quasi-identities of the form:

$$(\forall v_1 \dot{\in} r_1) \dots (\forall v_m \dot{\in} r_m)\ (n_1 \prec l_1) \dots (n_p \prec l_p)(\varphi(\bar{v}, \bar{r}) \to \psi(\bar{v}, \bar{r})).$$

[1] Glushkova VN. Verification of real-time robotic hierarchical systems. In: Proc. X All-Russian School-Seminar on Mathematical Modeling and Biomechanics in Modern University. Rostov-on-Don; Taganrog: SFU; 2015. P. 32. (In Russ.)
[2] Glushkova VN. Σ-specification of real-time robotic systems. In: Proc. Int. Conf. on Algebra and Logic, Theory and Applications. Krasnoyarsk: SFU; 2016. P. 22–23. (In Russ.)
[3] Glushkova VN. Logical means of diagnosing errors in a hierarchical S-models. In: Proc. Int. Conf. on Algebra and Mathematical Logic. Kazan: KFU; 2011. P. 58–59. (In Russ.)
[4] Glushkova VN. Logical modeling of robotic technological systems. In: Proc. VIII All-Russian School-Seminar. Rostov-on-Don: SFU; 2013. P. 44. (In Russ.)

Here, the formula φ (ψ) is a conjunction of atomic formulas (or their negations) of the form r, $\tau_1=\tau_2$, ($f=\tau$), $f \in F, r \in R$, τ_1, τ are terms of signature σ.

The *Int* model construction algorithm implements the modus ponens output rule (if φ and φ→ψ, then ψ). The input data for the interpreter is a set of initial values of functions and predicates of the form:
$S_0 = \{p(\bar{c}), f(\bar{c}) = c_{n+1} | p \in P, f \in F\}$, where $\bar{c}$ is a set of constants of n elements, $n \geq 1$.

Axioms (ax) are processed in a certain order, first, with positive occurrences of predicates in the left and right parts of ax, then, with negative occurrence until fixed points of calculations are obtained. The scope of functions and predicates included in the right-hand side of ax, expands when the left-hand side is true. This is because the interpreter sets new values for functions and predicates so that the right-hand side of ax is also true. Let the state S_n of the analyzed system at the n-th step of the calculation contain the values of all predicates and functions of the model signature, and function $\tau\ P(S) \to P(S)$ in (terminology [3] — predicate converter) reflects the state change when *Int* interpreter moves from the n-th step of the calculation to n+1. *Int* interpreter constructs the smallest fixed point μZ for the monotone converter τ on $P(S)$. $\tau(Z) = \cup_i \tau^i(S_0)$, где $\tau^0(Z) = Z$, $\tau^{i+1}(Z) = \tau(\tau^i(Z))$

Formally, functions $f \in F$ and predicate s$p \in R$ are interpreted on the CF-list $tl(n)$, which represents the derivation tree $tr(n)$ in grammar G, where n is the step of *Int* work. Due to the difficulty of presenting a compact form of the interpretation algorithm on the elements of the CF-list, we first give a verbal explanation of the algorithm, focusing on $tr(n)$ tree. The input data for the model construction algorithm (*Int*) are as follows: the derivation source tree $tr(0)$ in grammar G, which is expanded under the construction of model $\mathcal{M}$ and $Fact=S_0$. The CF-grammar is used in the process of building the model as follows. First, the rules P hierarchize the space of actions and states of the analyzed system. We assume that the action names represented in the model signature by predicates and the names of the corresponding nonterminal grammar symbols are the same. Secondly, the symbols from alphabet V of the grammar uniquely define the sorts of all elements of the model universe, including lists, which are assigned to the sort defined by the root mark of the corresponding tree. Sorts will be designated mnemonically with initial lowercase characters for the names of nonterminal and terminal grammar symbols with the addition of *s* (*sort*) symbol at the end. The main advantage of CF-grammars is the possibility of using effective syntactically oriented (SO) methods for analyzing the correctness (verification) of the model developed in the theory of syntactic analysis of programming languages.

The interpreter starts by viewing tree $tr(0)$ from the root top to bottom, from left to right. The prefix of all axioms satisfies the constraints $\Delta_0 T$-formulas. Prefix sorts are defined by the symbols of the CF-grammar G. The interpreter selects as constants the truth domains of the predicates included in axiom $ax \in Th$, the constants associated with the vertices of the tree bush, viewing it from top to bottom, from left to right. Moreover, the bush root is marked with the name of the corresponding predicate. To reflect the dependence of the simulated technical system on the sequence of input signals, it is required to complete the source tree $tr(0)$. To this end, the sequence of rules $pr^+(ax) \in P^+$ is attributed to the tree output obtained in the previous step of the algorithm. Moreover, constants from the truth domain of predicate r are used as terminal symbols subordinate to the tree vertex marked with nonterminal symbol r.

We describe the interpretation algorithm Int more formally, without detailing the procedure $Con(Q, Th)$ — obtaining all logical consequences from the set of formulas Q based on the axioms of the theory Th. $Th_0 = S_0$. Theory $Th_{pos} \subseteq Th$ includes only positive occurrences of predicates. $Th_{neg} \subseteq Th$ includes the negative occurrence of predicates on the right side of the axioms. We denote tr_{pos}, tr_{neg} — the derivation trees generated during the interpretation process.

Q:=∅;
Q':=Th_0;
while $Q \neq Q'$do
$Q_{pos} \coloneqq Q$;
$Q'_{pos} \coloneqq Q'$;
while $Q_{pos} \neq Q'_{pos}$ do

$Q_{pos} \coloneqq Q'_{pos}$;

$$Q'_{pos} \coloneqq Con(Q'_{pos}, Th_{pos})$$

end while

return (Q_{pos}, tr_{pos}) ;

$Q_{neg} \coloneqq \emptyset$;

$Q'_{neg} \coloneqq Q_{pos}$;

while $Q_{neg} \neq Q'_{neg}$ do

$Q_{neg} \coloneqq Q'_{neg}$;

$$Q'_{neg} \coloneqq Con(Q'_{neg}, Th_{neg})$$

end while

return (Q_{neg}, tr_{neg});

$$Q \coloneqq Q_{pos};$$
$$Q' \coloneqq Q_{neg}$$

end while

return (Q_{neg}, tr_{neg})

The verification of model $\mathcal{M}$ consists in checking the properties that the analyzed system should satisfy. We express these properties by arbitrary $\Delta_0 T$-formulas. Using SO-methods of checking formulas, a proof can be constructed in the same way as in [13].

Theorem. Arbitrary $\Delta_0 T$- formula with *m*-bounded generality quantifiers is tested on the CF-list of power *n* in time $O(n^{m+1})$.

The list power tl is equal to the cardinality of the set$\{s \mid s \dot{\in} tl\}$.

The estimate is upper, and it can be lowered to linear if you check the formulas using specific SO-methods of language processing

Research Results. We present a logical specification of an automated complex consisting of a manipulator maintaining a processing line (*tl*) with two positions: loading and unloading of parts (*ld* and *uld* , respectively) [14]. Sensors record the location of positions. The manipulator functions cyclically starting from the loading position.

We present a logical specification of an automated complex consisting of a manipulator maintaining a process line (tl) (ld and uld, respectively) [14].

CYCLE

1. In the initial position *ld* to load the part, the manipulator lifts the electric drive in 4 seconds. It compresses the automated claws and takes the workpiece (2 sec), lowers the electric drive (4 sec) and moves to the right to the machine until the position sensor is triggered *tl*.

2. To install the workpiece on the machine at position *tl*, the manipulator raises the electric drive, unclenches the automated claws (2 sec), lowers the electric drive. Next, the manipulator waits for 4 min, after which it repeats the same procedures as in position *ld*. Then, the manipulator moves to the left to the unloading position until the limit switch is triggered *uld*.

3. In 8 seconds, the part is unloaded on the conveyor. The manipulator moves to the left until the sensor is locked to the loading position *ld*. Further, the process of complex operation is cyclically repeated.

The system specification consists of several levels. The manipulator behavior is determined by the signals of sensors that record its position: *ld*, *uld*, *tl* (¬*ld*, ¬*uld*, ¬*tl*, negation indicates the absence of the corresponding sign). This sequence of signals is represented by the tuple *mc*=<*x*, *y*, *z*...>, where *x* = *ld* (¬*ld*), *y* = *uld* (¬ *uld*), *z*=*tl* (¬ *tl*). It is generated by a finite-state machine with an initial state *x*. This automaton is constructed according to a right-linear grammar with the rules:

$St \rightarrow ld\ St_1 \mid \neg\ ldSt_1 \mid \varepsilon$

$St_1 \rightarrow tl\ St_2 \mid \neg\ tl\ St_2$

$St_2 \rightarrow uld\ St \mid \neg\ uld\ St.$

Denote a set of lists, made up of symbol strings generated by this grammar, by *Dsig*.

The external discrete time (variable *n* in the logical specification) is determined by the number of transitions in the automaton. To describe the second level of the manipulator operation, the CF-grammar is used, which indicates the sequence of actions (*Oper*) of the manipulator:

— *L*, *La* — loading the workpiece by the manipulator in position *ld* and *tl,* respectively;

— *Unl*, *Unla* — unloading of the part in position *uld* and *tl*;

— *Mover*, *Movel* — movement of the manipulator to the right and to the left;

— *Lstop*, *Astop*, *Ulstop* — stop of the manipulator in the corresponding position;

— *Exp* — waiting;

— *Cr* — failure of the manipulator control device.

The states of the manipulator (symbol *Pos*) are affected by its actions. In this example, the state is characterized by continuous time *Timec* and discrete *Timed*, given by a natural number. The value of sort *Timec* is segments of the form $< t_1,\ t_2 >,\ t_1,\ t_2$ — constants, and < is replaced by (or [depending on whether the left border is included in the time segment or not, similarly for >.

When specifying the manipulator behavior, you disregard the value of the time of manipulator movement from one position to another (determined by signals from position sensors — input to the manipulator control device). The signals that are sent to the manipulator actuators for the movement and operation of the automated claws are output signals.

Below are the grammar rules *G*.

1. *Start*→ {*Oper*}*.
2. *Oper*→ *L* | *La* | *Unl* | *Unla* | *Mover* | *Movel* | *Lstop* | *Astop* | *Ulstop* | *Exp* | *Cr*.
3. *L*→ *St.*
4. *La*→ *St*.
5. *Unl* → *State*.
6. *Unla* → *State*.
7. *Mover* → *State.*
8. *Movel* → *State.*
9. *Lstop* → *State.*
10. *Astop* → *State.*
11. *Ulstop*→ *State.*
12. *Exp* → *State.*
13. *Cr* → *State*.
14. *State*→ *Timec Timed* | *Timed Timed*.
15. *Timec*→ *Timed* | (*Timed*, *Timed*) | [*Timed*, *Timed*) | (*Timed*, *Timed*] | [*Timed*, *Timed*].

Timed — a class of tokens whose values are natural numbers calculated under the interpretation of theory *Th.*

In theory *Th,* variables in formulas are designated mnemonically according to their sort: ρ (*state*) = ρ (*State*), ρ (*oper*) = ρ (*Oper*), ρ (*n*) = ρ (*t*) = ρ (*Timed*), ρ (*ct*) = ρ (*Timec*). Predicates *Ld*, *Tl*, *Unld* are defined on the set *Timed*. *Ld* (*n*) is true if the manipulator is in the loading position. Similarly, for *Tl* (*n*) — at the position of the processing machine, *Uld* (*n*) — at the position of unloading. Let us list the areas of definition of the remaining predicates: *Lstop*, *Astop*, *Ulstop*, *Mover*, *Movel*, *Cr* ⊆ *Timed*×*Timed*; *L*, *La*, *Unl*, *Unla*, *Exp*⊆*Timec* × *Timed*. The formulas use the standard functions *head* $(< x_1,...x_n >) = x_1$, *tail*$(< x_1,...x_n >) = < x_2,...x_n >$ and function *Mc*: *Timed*→ *Dc*. Here, *Dc* is a set of lists of sensor signals.

At the initial time $t = 0$, $n = 1$ and at the 1st step of the calculation, predicate *Lstop*(0,1) is executed; *Mc* (1) = *mc*, where *mc*∈*Dc*. In axioms 1–11, variables *t*, *n* and *ct* are bound by restricted quantifier ∀ *state* $\overset{*}{\in}$ *oper*, ∀ *t*,*n*, *ct*

$\in$ *state*. In axioms 12–17, variable *n* is bound by restricted quantifier $\forall$; s_0 = <<<<0,1>>>> — the initial value of the list on which the theory is interpreted. Its list constituents, in order of nesting depth, have the following sorts: ρ (*R*), ρ (*Oper*), ρ (*Lstop*), ρ (0) = ρ (1) = ρ (*Timed*). Tree T_0 corresponds to list s_0 (Fig. 1).

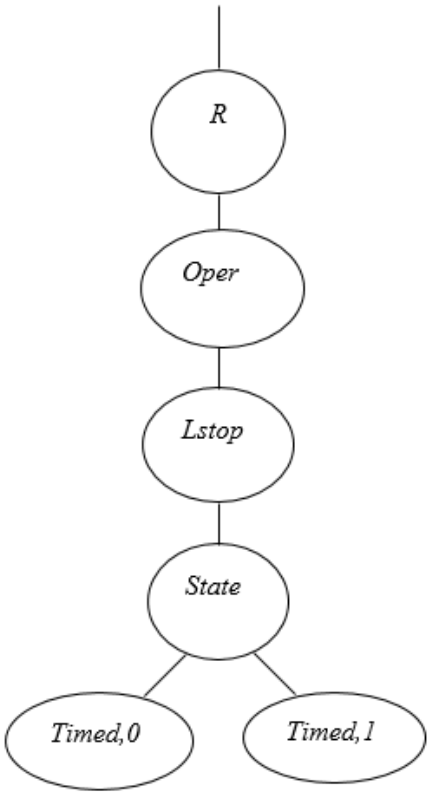

Fig. 1. Tree T_0 corresponding to list s_0

In axioms of the theory, the sequence of grammar rules *G*, that complete tree T_0 , is given in square brackets on the right.

Axioms of the theory

1. *Lstop*(*t*, *n*) ∧ *Ld* (*n*) → *L*([*t*, *t* + 7), *n*) ∧ *Mc* (*n* + 1) = *tail*(*Mc* (*n*)) [1; 2.1; 3; 14.1; 15.3].
2. *L*(*ct*, *n*) ∧ *Tl*(*n* + 1) → *Mover* (*ct* [2], *n* + 1) ∧ *Astop* (*ct* [2], *n* + 1) [1; 2.5; 7; 14.2;1; 2.8; 10; 14.2].
3. *Astop* (*t*, *n*)→ *Unla* ([*t*, *t* + 7], *n*) [1; 2.4; 6; 14.1; 15.2].
4. *Unla* (*ct*, *n*) → *Exp* ((*ct* [2], *ct* [2] + 180), *n*) [1; 2.10; 11; 14.1; 15.2]
5. *Exp* (*ct*, *n*) → *La* ([*ct* [2], *ct* [2] + 3), *n*) ∧ *Mc* (*n* + 1) = *tail*(*Mc* (*n*)) [1; 2.2; 4; 14.1; 15.2].
6. *La* (*ct*, *n*) ∧ *Uld* (*n* + 1) → *Movel* (*ct* [2], *n* + 1) ∧ *Ulstop* (*ct* [2], *n* + 1) [1; 2.6; 8; 14.2; 1; 2.9; 11; 14.2].
7. *Ulstop* (*t*, *n*) → *Unl* ([*t*, *t* + 7), *n*) ∧ *Mc* (*n* + 1) = *tail*(*Mc* (*n*)) [1; 2.3; 5; 14.1; 15.2].
8. *Unl* (*ct*, *n*) ∧ *Ld* (*n* + 1) → *Movel* (*ct* [2], *n* + 1) ∧ *Lstop* (*ct* [2], *n* + 1) [1; 2.6; 8; 14.2; 1; 2.7; 9; 14.2].
9. *Unl* (*ct*, *n*) ∧ ¬ *Ld* (*n* + 1) → *Cr* (*ct* [2], *n* + 1) [1; 2.11; 13; 14.2].
10. *La* (*ct*, *n*) ∧ ¬ *Unld* (*n* + 1)→ *Cr* (*ct* [2], *n* + 1) [1; 2.11; 13; 14.2].
11. *L* (*ct*, *n*) ∧ ¬ *Tl* (*n*+1) → *Cr* (*ct* [2], *n* + 1) [1; 2.11; 13; 14.2].
12. *head* (*Mc* (*n*)) = *ld* → *Ld* (*n*).
13. *head* (*Mc* (*n*)) = ¬ *ld* → ¬ *Ld* (*n*).
14. *head* (*Mc* (*n*)) = *tl* → *Tl* (*n*).
15. *head* (*Mc* (*n*)) = ¬*tl* → ¬ *Tl* (*n*).
16. *head* (*Mc* (*n*)) = *uld* → *Unld* (*n*)
17. *head* (*Mc* (*n*)) = ¬*uld* → ¬ *Uld* (*n*).

Theory *Th* has the Noetherian property, since the change of the variable under the quantifier $\forall$ is limited to *k* — the number of elements in the source list *mc*. In this case, *head* (*Mc* (*k*+1)) i9s undefined, because *Mc* (*k*+1)=< >. Note that the strings ¬*ld* and others, in the right part of axioms 12–17 have the sort *string*, and ¬ is considered not as a logical operation, but as a symbol.

For the initial value of function *Mc* (1) = <*ld*, *tl*, *uld*, *ld*, ¬ *tl*, *uld* > , we obtain a set of consequences: *Lstop*(0,1), *Ld* (1), *L* ([0,7), 1), *Mc* (2) = < *tl*, *uld*, *ld*, ¬ *tl*, *uld*>, *Mover* (7,2), *Astop* (7,2), *Unla* ([7, 14], 2), *Exp*([14, 194], 2), *La*([194, 197), 2), *Mc* (3) = <*uld*, *ld*, ¬ *tl*, *uld*>, *Movel* (197, 3), *Ulstop* (197, 3), *Unl* ([197, 204], 3), *Mc* (4) = <*ld*, ¬ *tl*, *uld* >, *Movel* (204, 4), *Lstop* (204, 4), *L* ([204, 211), 4), *Mc* (5) = < ¬ *tl*, *uld*>, *Cr* (211, 5).

The resulting set of consequences is hierarchized according to the inference in the grammar *G* obtained as a result of the rules assigned to the interpreted axioms. According to them, 12 more vertices, marked with the same symbol and connected by edges to the root, are added to tree T_0 to the right of the node marked with symbol *Oper*. Subtrees with roots marked with symbols *Ld*, *Mover*, *Astop, etc.,* with their states and constants of sort ρ (*Timed*) obtained as a result of interpretation, are added to the new vertices.

Discussions and Conclusions. On the constructed model, you can check the truth of arbitrary $\Delta_0 T$-formulas. For example, we formalize the statement: "If the manipulator was in the loading position at the instant of time *t* at step *n* of its operation cycle, then at step *n* + 2 after197 sec, it starts unloading for 7 sec". The formula below is tested on a given list *Oper* of sort ρ (*Oper*):

$$(\forall state \overset{*}{\in} oper)\ (\forall t \in State)\ (\forall n \in state)\ (Lstop(t, n) \rightarrow Unl\ ([t + 197, t + 204], n + 2).$$

References

1. Goguen JA, Meseguer J. Models and equality for logical programming. Lecture Notes in Computer Science. 1987;250:1–22.

2. Kowalski R. Logic for Problem Solving, Revisited. London: Imperial College; 2014. P. 321.

3. Clarke EM, Grumberg O, Peled D. Verifikatsiya modelei programm [Model checking]. Moscow: Moscow Center for Continuous mathematical Education Publ.; 2002. 416 p. (In Russ.)

4. Reps T, Thakur A. Automating Abstract Interpretation. In: 17th International Conference, VMCAI 2016, on Verification, Model Checking and Abstract Interpretation. St. Petersburg, FL, USA, January 17–19, 2016. Paris: Springer; 2016. P. 3–40.

5. Bloem R, Konighofer R, Seidl M. SAT-Based Synthesis Methods for Safety Specs. In: 15th International Conference, VMCAI 2014, on Verification, Model Checking and Abstract Interpretation. San Diego, CA, USA, January 2014. San Diego: Springer; 2014. P. 1–20.

6. Beyer D, Wendler Ph. Reuse of Verification Results. In: 20th International Symposium, SPIN 2013, on Model Checking Software. Stony Brook, July 8–9, 2013. Stony Brook: Springer; 2013. P. 1–15.

7. Alur R, Courcoubetis C, Dill DL. Model-checking for real-time system. Information and Computation. 1993;104(1):2–34.

8. Morbe G, Scholl Ch. Fully Symbolic TCTL Model Checking for Incomplete Timed Systems. In: Proceedings of the Automated Verification of Critical Systems (AVoCS 2013). 2013;66:1–9.

9. D´Silva V. Kroening D, Sousa M. Independence Abstractions and Models of Concurrency. In: 18th International Conference, VMCAI 2017, on Verification, Model Checking and Abstract Interpretation. Paris, France, January 15–17, 2017. Paris: Springer; 2017. P. 149–168.

10. Goncharov SS, Sviridenko DI. Theoretical aspects of Σ-programming. In: Proc. of the International Spring School, April 1985, on Mathematical Methods of Specification and Synthesis of Software Systems' 85. Berlin; Heidelberg: Springer-Verlag; 1985. P. 169–179.

11. Goncharov SS. Modeli dannykh i yazyki ikh opisanii [Data models and their description languages]. Vychislitel'nye sistemy. Logiko-matematicheskie osnovy problemy MOZ. 1985;107:52–70. (In Russ.)

12. Maltsev AI. Algebraicheskie sistemy [Algebraic systems]. Moscow: Nauka; 1976. P. 392. (In Russ.)

13. Glushkova VN. Otsenka slozhnosti realizatsii logicheskikh spetsifikatsii na osnove kontekstno-svobodnykh grammatik [Evaluating the complexity of implementing logical specifications based on context-free grammars]. Cybernetics and Systems Analysis. 1996;4:50–58. (In Russ.)

14. Gorbatov VA, Smirnov MI, Khlytchiev IS. Logicheskoe upravlenie raspredelennymi sistemami [Logical control of distributed systems]. Moscow: Ehnergoatomizdat; 1991. 288 p. (In Russ.)

Submitted 27.07.2020
Scheduled in the issue 05.10.2020

About the Authors:

Glushkova, Valentina N., associate professor of the Mathematics Department, Don State Technical University, (1, Gagarin sq., Rostov-on-Don, 344003, RF), Cand.Sci. (Phys.-Math.), senior researcher, ORCID: https://orcid.org/0000-0003-2719-8590, lar@aaanet.ru

Korovina, Ksenia S., senior lecturer of the Mathematics Department, Don State Technical University, (1, Gagarin sq., Rostov-on-Don, 344003, RF), ORCID: https://orcid.org/0000-0002-1196-3596, ksenichka_@inbox.ru

Claimed contributorship

V. N. Glushkova: formulation of the syntactically oriented hierarchical modeling concept; objectives and tasks of logical specification; academic advising; correction of the conclusions. K. S. Korovina: application of Σ-formulas for the technical system specification; analysis of system verification results and drawing conclusions; the text revision.

All authors have read and approved the final manuscript.

INFORMATION TECHNOLOGY, COMPUTER SCIENCE, AND MANAGEMENT

UDC 004.89, 004.032.26 https://doi.org/10.23947/2687-1653-2020-20-4-430-436

Automation of information distribution in adaptive electronic document management systems using machine learning

A. D. Obukhov
Tambov State Technical University (Tambov, Russian Federation)

Introduction. Electronic document management systems (EDMS) are used to store, process and transmit large amounts of information. Automation of these processes is a challenge that requires a comprehensive solution. Its solution will reduce the time and material costs for design and make the transition to a more advanced, adaptive EDMS. The paper is devoted to the development of new methods for automating the process of distributing information in the EDMS. The work objective is to improve the accuracy of the information distribution in the EDMS through moving from analytical or algorithmic solutions to the use of new methods based on machine learning technologies. The application of neural networks in the furtherance of this purpose will also improve the efficiency of software development through automating the analysis and processing of information.
Materials and Methods. A new method of the automated information distribution based on machine learning technologies including a mathematical description of the information distribution rules is proposed. The formulated list of conditions for the information distribution provides the implementation of software based on neural networks for solving the problem of automatic data distribution in the EDMS.
Results. The method of automated information distribution has been tested on the example of the EDMS subject area when solving the problem of analyzing the correctness of information entered by the user. In the course of experimental studies, it was found that the proposed method, based on machine learning technologies, provides better accuracy (8 % higher) and is more efficient (in accordance with the Jilb metrics and cyclomatic complexity).
Discussion and Conclusions. The results obtained confirm the efficiency and accuracy of the method proposed. The presented results can be used to automate the processes of distribution and verification of information in adaptive EDMS, as well as in other information systems. Based on the method developed, it is also possible to solve connected problems: search for duplicates and similar documents, classification and placement by file categories.

Keywords: electronic document management systems, information distribution, automation, adaptability, machine learning.

For citation: A. D. Obukhov. Automation of information distribution in adaptive electronic document management systems using machine learning. Advanced Engineering Research, 2020, vol. 20, no. 4, p. 430–436. https://doi.org/10.23947/2687-1653-2020-20-4-430-436

Funding information: the research is done under grant no. MK-74.2020.9 from President of the Russian Federation.

Introduction. Electronic document management systems (EDMS) are widely used for storing, processing and transmitting information of various types: documents, spreadsheets, graphic and audio information, engineering and accounting documentation, etc. The main functionality for working with documents over the years of the EDMS development has been formed. Further development is aimed at automating human activities, increasing flexibility and reliability, and implementing intelligent decision support modules [1–3].

However, such flexibility and adaptability of the EDMS causes additional time and material costs, increases the complexity of designing and upgrading the system. Therefore, the automation of system design is a challenge for the development of adaptive information systems, including EDMS. This implies many separate tasks for automating the processes of analysis, processing and transmission of documents, the solution of which in totality provides reducing the load on developers during the implementation of adaptive functions in EDMS.

Within the framework of study, the issue on classification of information and its subsequent automatic distribution into specified categories in the EDMS will be considered. This sub-task is one of the most common when organizing electronic repositories and archives, filing cabinets, and filling out document forms. Distribution refers to the placement of data and files in specified positions: by categories, media, directories, and so on [4]. Classical algorithms are not always able to detect an error in the placement of information without involvement of an expert or moderator.

Considering approaches to solving the problem of information distribution, we can distinguish approaches based on the use of machine learning[1]. The application of artificial intelligence technologies for solving classification problems has proved its efficiency in numerous studies and experiments [5-8]. When solving the problem and implementing the information distribution method, machine learning technologies will be used to automate the data classification process.

Based on the analysis of the information movement process, the following urgent tasks can be identified for the classification and distribution of data in adaptive EDMS:

— classification and determination of compliance of the entered data with the category in which the user placed them [9];

— data categorization[2] , and, in case of an error, moving them to the correct categories, or raising a warning to the user [10];

— definition of data duplication by features [11].

To solve these problems, it is proposed to develop a method for automated information distribution in adaptive EDMS, which generalizes existing approaches to information classification and is based on the use of machine learning methods for automating data processing.

Materials and Methods. We formalize the main stages of the method of automated data distribution in adaptive EDMS.

The method is based on the formation and training of a neural network for information classification. Therefore, at the first stage of the method implementation, it is required to prepare a set of information objects $X = \{x_1, ...x_N\}$ for training and testing the neural network. The object $x_i \in X$ can be represented by text or numerical information entered by the user in the form fields, or by files uploaded via the EDMS interface [12]. The data preparation process can include normalization, tokenization, lemmatization, and extraction of file properties and attributes. For the collected data, a set of categories $Y = \{y_1, ..., y_M\}$ is predetermined, that is, there is a continuous display $X \to Y$. We approximate this mapping by neural network NN:

$$NN(X) = Y.$$

With a sufficient amount of training data, it is possible to provide required accuracy of the classification. In accordance with the studies presented in [13], at least 50 copies of training data should be provided for each output feature. Then for $\forall x_i \in X$, we get $NN(x_i) = y_j$, where $j = 1..M$.

At the second stage of the method, information is distributed. Let the EDMS have a set of information objects $X = \{x_1, ..., x_N\}$ and a set of corresponding categories $Y = \{y_1, ..., y_M\}$. To distribute information, the following conditions should be checked:

— if $\forall x_i \in X$, $NN(x_i) = y_j$ and object x_i are placed by the user in category y_j, then the position x_i remains unchanged;

— if $\exists x_i \in X$, $NN(x_i) = y_m$ (where y_m — the category of malicious objects), then object x_i is removed from the EDMS, a warning is sent to the system administrator, the user who added object x_i, is blocked;

— if $\exists x_i \in X$, $NN(x_i) = y_j$, but object x_i is entered by the user in the category y_k

($y_k \neq y_j$), then it is required to redistribute the information in the EDMS.

Consider all possible options for redistribution:

1. Category y_j is free (empty), then object x_i is transferred from category y_k to y_j.

[1] Umadevi S, Marseline KSJ. A survey on data mining classification algorithms. In: 2017 International Conference on Signal Processing and Communication (ICSPC): IEEE, 2017. P. 264-268.

[2] Popova ES, Spitsyn VG, Ivanova YuA. Using artificial neural networks to solve the problem of text classification. In: Proc. 29th Int. Conf. on Computer Graphics and Vision "Graphicon". Bryansk, 2019. P. 270-273. (In Russ.)

2. Category y_j is occupied by some object x_q (such that $NN(x_q) = y_j$), then object x_i is transferred to the buffer, the user is given a warning about incorrect input x_i and duplication of information.

3. Category y_j is occupied by some object x_q (such that $NN(x_q) \neq y_j$), then object x_q is transferred to the buffer, and object x_i is transferred from the category y_k to y_j, the user is given a warning about incorrect input x_q.

The stages and conditions of information distribution considered in the framework of the method include the main scenarios for adding information to the EDMS. Through the use of machine learning technologies, it is possible to automate the distribution of information into specified categories.

Research Results. To implement and integrate the method into adaptive EDMS, we will use a microservice approach. The neural network is implemented using the Keras library (Python), then it is imported into a microservice, which can be implemented on the basis of any framework, for example, Flask. Data between the EDMS and the microservice is transmitted through the HTTP Protocol in JSON format, which provides compatibility with any EDMS implementation [14].

As an example of the data distribution task, we will use a document card form in the EDMS with 5 fields: document name; document author; contact information (address) of the author; date of creation; document description. In the course of the pilot study, the input of user data into the form and filling in the information in the specified 5 fields will be simulated. The neural network will classify the entered information and check it for compliance with the specified category.

To create a set of source data, we use the generator based on open database of Russian names, cities and countries, as well as sequences of Russian words and figures. This will enable to get constructions that correspond to real data, but do not store personal data of real people. Text data will be processed using a tokenizer to convert it to a numeric format. The maximum sentence length is limited to 20 words. We generate a training sample. We will generate 10,000 elements for each category. We will also add 50,000 items with incorrect and erroneous data. Thus, we get an array of 100 thousand elements.

The relationships between input attributes and categories are shown on the heatmap in Fig. 1. The map provides visualization of the correlation matrix and performing a visual analysis of the data to determine how the parameters affect each other and the output variables [15].

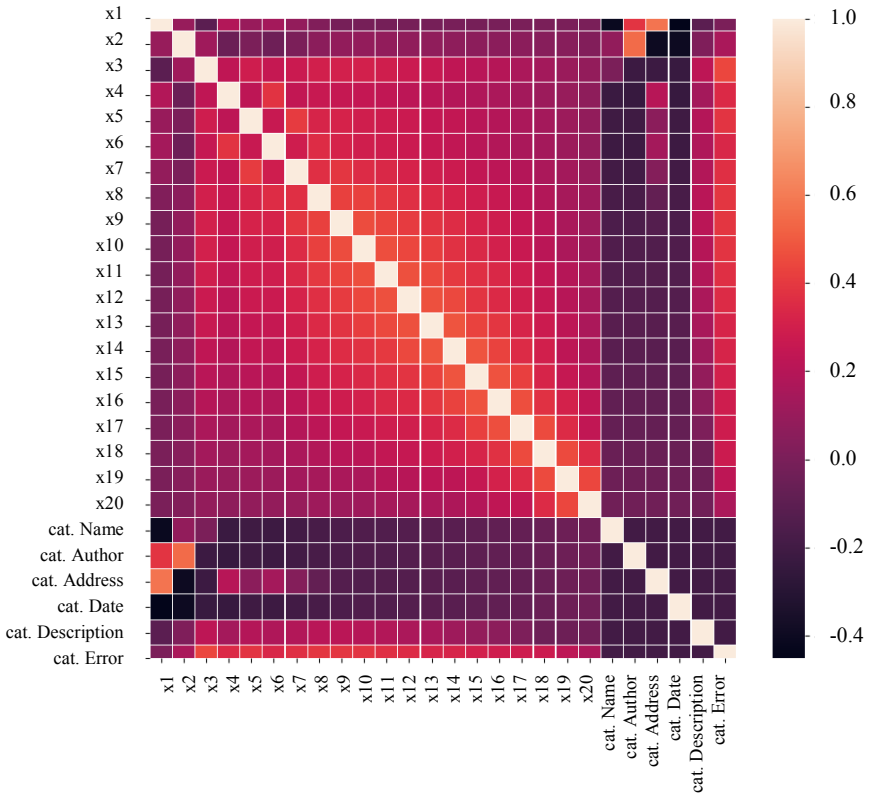

Fig. 1. Raw data heatmap

The network learning process is shown in Fig. 2. The final accuracy of the neural network on the test set after 5 epochs amounted to 97.8%.

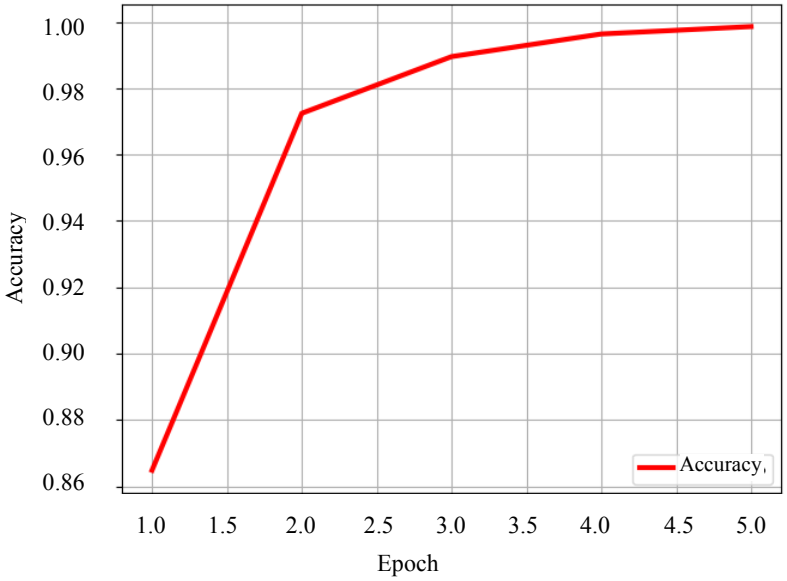

Fig. 2. Classification neural network learning process

The number of errors did not exceed 7 % for the "Author" category and 1 % for the "Description" category. In other categories, incorrect data was recognized in 100% of cases.

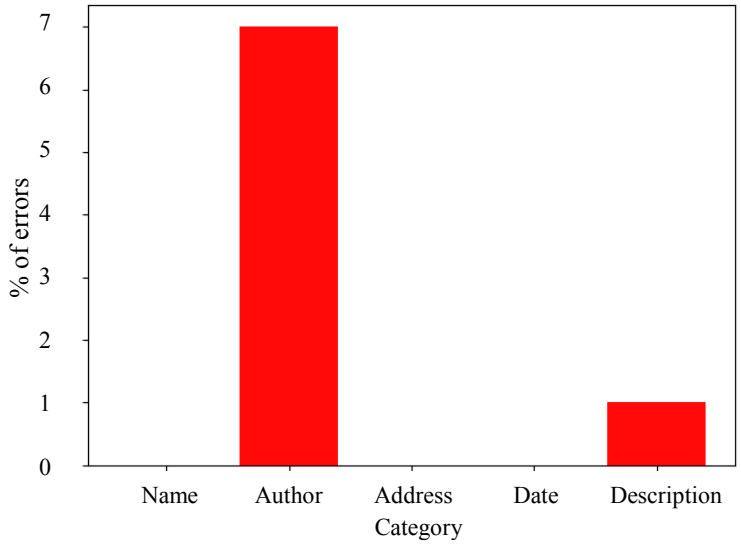

Fig. 3. Testing the neural network for incorrect data entry

The second experiment (Fig. 4) consists in entering data from j categories to i ($j \neq i$). A set of 100 elements for each category i consisting of elements of other categories (25 for each category) is formed. The graph shows the number of tests in which the neural network incorrectly recognized data from other categories as corresponding to the current category. In the second experiment, 1 % of errors was allowed in the "Name" category. The remaining categories were worked out without errors.

Next, we compare the accuracy of the proposed method (hereinafter referred to as the "neural network method") with the classical solution to the problem of classification and distribution of information (referred to as the "classical method"). For the classical method, the following results were obtained: 16 % of errors in the "Name" category, and 25 % — in the "Description" which is much worse than indicators of the neural network method (Fig. 5). On average, the use of neural network methods provides accuracy increase by 8 %.

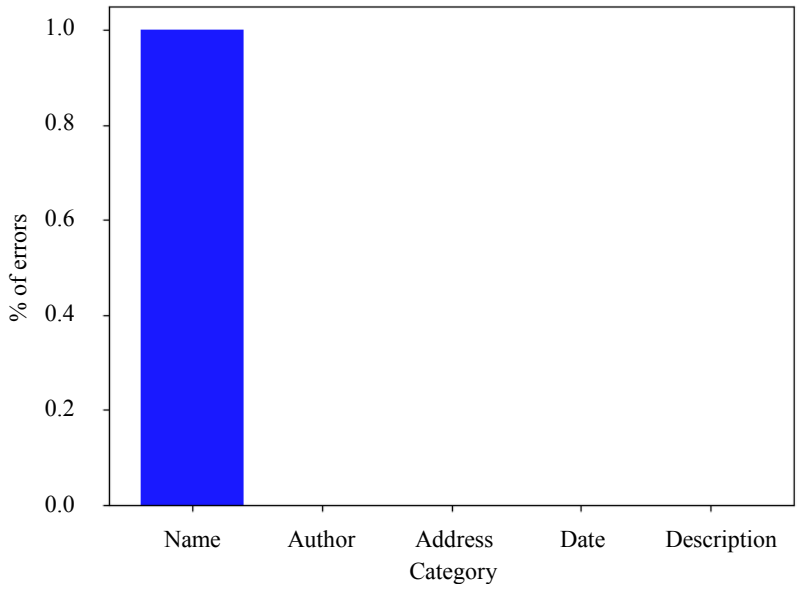

Fig. 4. Testing the neural network for incorrect data entry

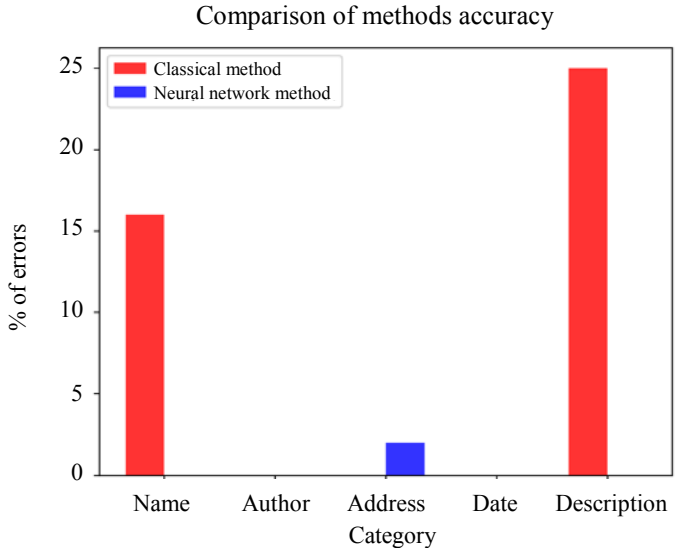

Fig. 5. Comparison of accuracy of neural network and classical methods

Next, we will compare the methods by metrics of software implementation complexity. The cyclomatic complexity expressed by McCabe number (total and averaged) [16], as well as the complexity according to the Jilb metrics [17], are used as metrics. The final results are presented in Table 1.

Table 1

Comparison of classical and neural network methods

Metrics	Classical method	Neural network method
Cyclomatic complexity (total)	26	22
Cyclomatic complexity (averaged)	A (3.71)	A (1.37)
Jilb metrics	0.8	0.15

Thus, the complexity of the neural network method in terms of cyclomatic complexity and Jilb metrics is lower. The accuracy of the developed method is almost 8% higher. It is worth noting that the complexity of implementing the classical and neural network methods of data classification and distribution is relatively small, so, they can be considered comparable. However, the obtained results on classification accuracy confirm the high efficiency of the neural network approach.

Discussion and Conclusions. The paper sets the task of automating the processes of data classification and distribution in adaptive EDMS. The proposed method of automated data distribution includes the formalization of the classification and distribution of data, the use of machine learning technologies to automate the solution to the problem. The formulated list of information distribution conditions provides implementing the software based on neural networks that solves the problem of automatic data distribution.

To test the developed method, experimental studies were conducted on the basis of generated data on documents in the EDMS. The accuracy of the trained neural network was about 98 %. Additional tests have shown that the neural network can detect incorrectly distributed data in almost 100 % of cases, and, under the worst conditions, the error did not exceed 7 %. Thus, the efficiency and accuracy of the proposed method is confirmed. The developed method, in comparison to the classical implementation based on algorithmic support, shows the following positive effect: an increase in average accuracy by 8 %, a decrease in the complexity of the implementation.

The presented results can be used to automate the processes of distribution and verification of information in adaptive EDMS, as well as in other information systems. In addition, on the basis of the proposed method, it is possible to solve related tasks: search for duplicates and similar documents, classification and placement by file categories.

References

1. Kuznetsova EV. Aktual'nye problemy ehlektronnogo dokumentooborota v organakh vlasti [Topical problems of electronic document management in the bodies of power]. Management Issues. 2013;4:73–77. (In Russ.)

2. Zhong RY et al. Intelligent manufacturing in the context of industry 4.0: a review. Engineering. 2017;3(5):616–630. DOI: 10.1016/J.ENG.2017.05.015

3. Xu D, et al. Enhancing e-learning effectiveness using an intelligent agent-supported personalized virtual learning environment: An empirical investigation. Information & Management. 2014;51(4):430–440. DOI:10.1016/j.im.2014.02.009

4. Kuznetsov SD, Poskonin AV. Raspredelennye gorizontal'no masshtabiruemye resheniya dlya upravleniya dannymi [Distributed, horizontally scalable data management solutions]. Proceedings of ISP RAS. 2013;24:327–358. (In Russ.)

5. Krasnyansky MN, Obukhov AL, Solomatina EM, et al Sravnitel'nyi analiz metodov mashinnogo obucheniya dlya resheniya zadachi klassifikatsii dokumentov nauchno-obrazovatel'nogo uchrezhdeniya [Comparative analysis of machine learning methods for solving the problem of classification of documents of a scientific and educational institution]. Proceedings of Voronezh State University. Series: Systems Analysis and Information Technologies. 2018;3:173–182. (In Russ.)

6. Karampidis K, Papadourakis G. File type identification-computational intelligence for digital forensics. Journal of Digital Forensics, Security and Law. 2017;12(2):6. DOI: 10.15394/jdfsl.2017.1472

7. Kim D, et al. Multi-co-training for document classification using various document representations: TF–IDF, LDA, and Doc2Vec. Information Sciences. 2019;477:15–29.

8. Zheng J, et al. Hierarchical neural representation for document classification. Cognitive Computation. 2019;11(2):317–327. DOI:10.1007/s12559-018-9621-6

9. Bodström T, Hämäläinen T. State of the art literature review on network anomaly detection with deep learning. In book: Internet of Things, Smart Spaces, and Next Generation Networks and Systems. Springer, Cham; 2018. P. 64–76. DOI: 10.1007/978-3-030-01168-0_7

10. Datta S, Das S. Near-Bayesian support vector machines for imbalanced data classification with equal or unequal misclassification costs. Neural Networks. 2015;70:39–52. DOI: 10.1016/j.neunet.2015.06.005

11. Irolla P, Dey A. The duplication issue within the Drebin dataset. Journal of Computer Virology and Hacking Techniques. 2018;14(3):245–249. DOI: 10.1007/s11416-018-0316-z

12. Goldberg Y. Neural network methods for natural language processing. Synthesis Lectures on Human Language Technologies. 2017;10(1):1–309. DOI: 10.2200/S00762ED1V01Y201703HLT037

13. Beleites C, et al. Sample size planning for classification models. Analytica chimica acta. 2013;760:25–33. DOI:10.1016/j.aca.2012.11.007

14. Obukhov A, Krasnyanskiy M, Nikolyukin M. Algorithm of adaptation of electronic document management system based on machine learning technology. Progress in Artificial Intelligence. 2020;9:287–303. DOI: 10.1007/s13748-020-00214-2

15. Bazgir O, et al. Representation of features as images with neighborhood dependencies for compatibility with convolutional neural networks. Nature Communications. 2020;11(1):1–13. DOI: 10.1038/s41467-020-18197-y

16. Luo A, et al. A Structural Complexity Metric Method for Complex Information Systems. JSW. 2019;14(7):332-339. DOI: 10.17706/jsw.14.7.332-339

17. Smirnov AV. Metody otsenki i upravleniya kachestvom programmnogo obespecheniya [Methods of software quality assessment and management]. Izvestiya SPbGETU “LETI”. 2019;2:20–25. (In Russ.)

Submitted 29.06.2020
Scheduled in the issue 14.09.2020

About the Author:

Obukhov, Artem D., associate professor of the Automated Decision Support Systems department, Tambov State Technical University (106, Sovetskaya St., Tambov, 392000, RF), Cand.Sci. (Eng.), associate professor, ResearcherID: M-9836-2019, ScopusID: 56104232400, ORCID: http://orcid.org/0000-0002-3450-5213, Obuhov.art@gmail.com

The author has read and approved the final manuscript.

INFORMATION TECHNOLOGY, COMPUTER SCIENCE, AND MANAGEMENT

UDC 519.6 https://doi.org/10.23947/2687-1653-2020-20-4-437-445

Modeling biogeochemical processes in the Azov Sea using statistically processed data on river flow

A. I. Sukhinov[1], Y. V. Belova[1], A. V. Nikitina[2], A. M. Atayan[1]
[1] Don State Technical University (Rostov-on-Don, Russian Federation)
[2] Supercomputers and Neurocomputers Research Center (Taganrog, Russian Federation)

Introduction. This work is aimed at solving the problem of phytoplankton dynamics in the coastal environments using the example of the Azov Sea. This takes into account the transformation of forms of phosphorus, nitrogen and silicon, as well as the aquatic medium motion, the distribution of temperatures and salinities over the sea area. River flow, varying in volume and chemical composition, affects significantly the variability of hydrophysical and biogeochemical parameters of the processes occurring in the coastal environment. This explains the need for statistical processing of the data from long-term observations over the river flow characteristics.

Materials and Methods. The mathematical model of biogeochemical cycles is based on a system of non-stationary equations of the convection–diffusion–reaction of parabolic type with nonlinear functions of sources and lower-order derivatives, to which the corresponding initial and boundary conditions are added. In the course of statistical analysis of the series of long-term observations over river flows, the values of the following indicators were found: skewness coefficient, degree of kurtosis, variance and standard deviation, coefficient of variation, autocorrelation coefficient, Neumann ratio, and Anderson criterion.

Results. The statistical analysis of the series of long-term observations over the hydrochemical indicators of the Don river suggests heterogeneity of the field data. This is due to the stochasticity of nutrient inputs and the volume of freshwater flow to the sea as a result of natural and anthropogenic factors. Field data should be correlated with seasonal changes in the aquatic environment temperature. This paper presents the results of a computational experiment to model the dynamics of phytoplankton populations in summer season, when temperatures are favorable for their reproduction and growth. The proposed mathematical model considers the spatially inhomogeneous distribution and transformation of forms of phosphorus, nitrogen, and silicon, as well as changes in salinity, temperature, and motion of the aquatic environment.

Discussion and Conclusions. The multispecies mathematical model of the dynamics of phytoplankton populations is considered with account for the transformation of forms of phosphorus, nitrogen, and silicon in the coastal environments. The analysis of data from field observations, for which its major statistical parameters are calculated, is carried out. As a result, it is concluded that data of the long-term observations are significantly variable. This is due to two reasons. Random nature of the input of nutrients and the volume of river flow as a result of anthropogenic factors is the first reason. The second reason includes the alternation of relatively high-water and low-water periods for fresh flow over the last 12-15 years. The hydrological regime is changing mainly due to the reduction of the average annual freshwater flow of the Don and partly of the Kuban. This trend is likely to increase due to climate changes, as well as with further regulation of the Don river flow after the Bagaevsky hydroelectric installation start-up. Numerical experiments based on the field data confirmed the predictive validity of the developed models and programs. They can be used to predict change in the composition and abundance (concentrations) in the Azov sea core planktonic populations, which define, on the one hand, food resources, and, on the other hand, the aquatic environment in terms of the ongoing sea salinization.

Keywords: biogeochemical cycles, phytoplankton population, biogenic substance, chemical-biological source, convection–diffusion–reaction equation, field data.

For citation: A. I. Sukhinov, Y. V. Belova, A. V. Nikitina, et al. Modeling biogeochemical processes in the Azov Sea using statistically processed data on river flow. Advanced Engineering Research, 2020, vol. 20, no. 4, pp. 437–445. https://doi.org/10.23947/2687-1653-2020-20-4-437-445

Funding information: the research is done with the financial support from RFFI (project no. 20-01-00421).

Introduction. The sea of Azov is a large estuarine coastal system. It is the shallowest sea in the world. It warms up almost evenly in summer (with temperature differences on average no more than 4 °C). At the same time, it is characterized by a large difference in salinity — from 0% to 12-15%, since river flows provide an influx of fresh water commensurate with the total volume of sea water, and salty Black sea water comes from the Black sea near the Kerch Strait. River runoff affects significantly the biochemical composition of the water body

[1]. Mathematical modeling of biogeochemical processes, which provides performing diagnostic and prognostic calculations of the marine ecosystem dynamics, is considered important. A variable volume and hydrochemical composition of the river runoff affects significantly the parameters of hydrophysical and biological processes occurring in the coastal system. Therefore, it is advisable to conduct a statistical analysis of the data of long-term observations, in particular hydrochemical indicators of runoff of the rivers running into the sea of Azov, and to predict biogeochemical processes on the basis of statistically processed input data.

In the area of hydrodynamics and forecasting of marine systems, the works of Marchuk G. I. [2], Matishov G. G., Sukhinov A. I. [3], Berdnikov S. V., Tyutyunov Yu. V. [4], Yakushev E. V. [5], Ilyichev V. G., and others should be mentioned. The paper presents the results of complexing a mathematical model of biogeochemical cycles and a model of hydrodynamics of the sea of Azov [6–8]. This provides improving the modeling accuracy and considering such factors as hydrodynamic processes in coastal systems, heterogeneous distribution of temperatures, salinities and biogenic substances that affect the development of phytoplankton populations, the transition of biogens from one form to another [9]. It should be noted that numerical models of spatial-three-dimensional hydrophysical processes in coastal systems are the subject of a separate study of the authoring team. They provide considering the dynamically changing geometry of the bottom and coastline, wind stress on the free surface and its elevation, friction on the bottom, Coriolis force, turbulent exchange, evaporation, river runoff, deviation of pressure values in the aquatic environment from the hydrostatic approximation, etc. In this paper, the input data (distribution of the three-dimensional velocity vector, as well as salinity and temperature) are the results of numerical calculations based on the hydrophysical model [10].

Materials and Methods. To describe the model, an initial-boundary value problem is formulated for a system of parabolic equations with lower derivatives and nonlinear right-hand functions:

$$\frac{\partial q_i}{\partial t} + u\frac{\partial q_i}{\partial x} + v\frac{\partial q_i}{\partial y} + w\frac{\partial q_i}{\partial z} = div(k\text{grad}q_i) + R_{q_i}, \quad (1)$$

where q_i — concentration of the *i*-th component [mg/l]; $i \in M$, $M = \{F_1, F_2, F_3, PO_4, POP, DOP, NO_3, NO_2, NH_4, Si\}$; $\{u, v, w\}$ — components of the water flow velocity vector [m/s]; k — turbulent exchange coefficient [m^2/s]; R_{q_i} — function — source of nutrients [mg/(l·s)].

In the equation (1), index i indicates the type of substance (Table 1).

Table 1

Biogenic substances in the model of phytoplankton dynamics

Number	Designation	Name
1	F_1	Green alga *Chlorella vulgaris*
2	F_2	Blue-green alga *Aphanizomenon flos-aquae*
3	F_3	Diatomic alga *Sceletonema costatum*
4	PO_4	Phosphates
5	POP	Weighed organic phosphorus
6	DOP	Dissolved organic phosphorus
7	NO_3	Nitrates
8	NO_2	Nitrites
9	NH_4	Ammonium
10	Si	Dissolved inorganic silicon (silicic acids)

Chemical-biological sources are described by the following equations ($i \in \{1,2,3\}$, where 1 — is ChV , 2 — $AF-A$, 3 — Sc , and $ChV, AF-A, Sc$ — symbolic designations of plankton species):

$$R_{F_i} = C_{F_i}(1 - K_{F_iR})q_{F_i} - K_{F_iD}q_{F_i} - K_{F_iE}q_{F_i},\ i = \overline{1,3},$$

$$R_{POP} = \sum_{i=1}^{3} s_p K_{F_iD} q_{F_i} - K_{PD} q_{POP} - K_{PN} q_{POP},$$

$$R_{DOP} = \sum_{i=1}^{3} s_P K_{F_iE} q_{F_i} + K_{PD} q_{POP} - K_{DN} q_{DOP},$$

$$R_{PO_4} = \sum_{i=1}^{3} s_P C_{F_i} \left(K_{F_iR} - 1\right) q_{Fi} + K_{PN} q_{POP} + K_{DN} q_{DOP},$$

$$R_{NH_4} = \sum_{i=1}^{3} s_N C_{F_1} \left(K_{F_iR} - 1\right) \frac{f_N^{(2)}\left(q_{NH_4}\right)}{f_N\left(q_{NO_3}, q_{NO_2}, q_{NH_4}\right)} q_{F_i} + \sum_{i=1}^{3} S_N \left(K_{F_iD} + K_{F_iE}\right) q_{F_i} - K_{42} q_{NH_4},$$

$$R_{NO_2} = \sum_{i=1}^{3} s_N C_{F_i} (K_{F_iR} - 1) \frac{f_N^{(1)}\left(q_{NO_3}, q_{NO_2}, q_{NH_4}\right)}{f_N\left(q_{NO_3}, q_{NO_2}, q_{NH_4}\right)} \cdot \frac{q_{NO_2}}{q_{NO_2} + q_{NO_3}} q_{F_i} + K_{42} q_{NH_4} - K_{23} q_{NO_2},$$

$$R_{NO_3} = \sum_{i=1}^{3} s_N C_{F_i} \left(K_{F_iR} - 1\right) \frac{f_N^{(1)}\left(q_{NO_3}, q_{NO_2}, q_{NH_4}\right)}{f_N\left(q_{NO_3}, q_{NO_2}, q_{NH_4}\right)} \cdot \frac{q_{NO_3}}{q_{NO_2} + q_{NO_3}} q_{F_i} + K_{23} q_{NO_2},$$

$$R_{Si} = s_{Si} C_{F_3} \left(K_{F_3R} - 1\right) q_{F_3} + s_{Si} K_{F_3D} q_{F_3}.$$

Here, K_{F_iR} — specific respiratory rate of phytoplankton; K_{F_iD} — the specific rate of decay of phytoplankton; K_{F_iE} — specific extinction of phytoplankton; K_{PD} — specific rate of autolysis POP; K_{PN} — phosphatofication coefficient POP; K_{DN} — phosphatofication coefficient DOP; K_{42} — specific rate of ammonia oxidation to nitrites during nitrification; K_{23} — specific rate of oxidation of nitrites to nitrates in the process of nitrification; s_P , s_N , s_{Si} — normalization coefficients between the content of N, P, Si in organic matter [11–12].

The growth rate of phytoplankton is determined from the expressions

$$C_{F_{1,2}} = K_{NF_{1,2}} f_T(T) f_S(S) min\left\{f_P\left(q_{PO_4}\right), f_N\left(q_{NO_3}, q_{NO_2}, q_{NH_4}\right)\right\},$$

$$C_{F_3} = K_{NF_3} f_T(T) f_S(S) min\left\{f_P\left(q_{PO_4}\right), f_N\left(q_{NO_3}, q_{NO_2}, q_{NH_4}\right), f_{Si}\left(q_{Si}\right)\right\},$$

where K_{NF} — maximum specific growth rate of phytoplankton.

Dependences of temperature and salinity:

$$f_T(T) = \exp\left(-\alpha\left(\frac{T - T_{opt}}{T_{opt}}\right)^2\right),\ f_S(S) = \exp\left(-\beta\left(\frac{S - S_{opt}}{S_{opt}}\right)^2\right),$$

where T_{opt} , S_{opt} — temperature and salinity, optimal for this type of phytoplankton; $\alpha > 0$, $\beta > 0$ — coefficient of the interval width of tolerance of phytoplankton to temperature and salinity, respectively.

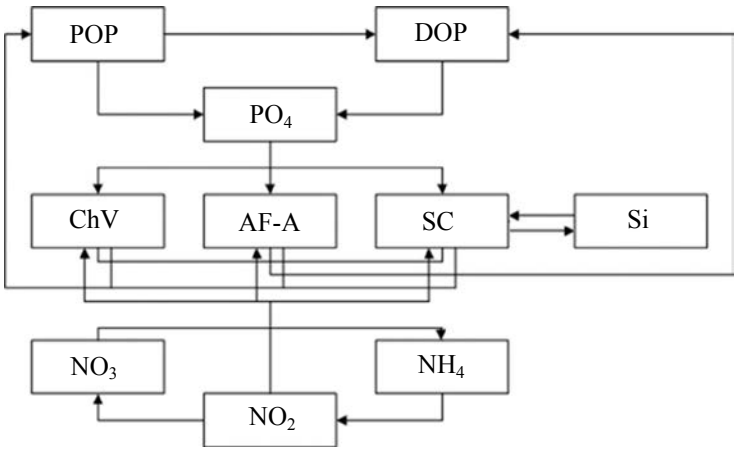

Fig. 1. Model scheme of biogeochemical transformation of phosphorus, nitrogen and silicon forms

Below are the functions that describe the content of biogens.

For phosphorus $f_P\left(q_{PO_4}\right)=\dfrac{q_{PO_4}}{q_{PO_4}+K_{PO_4}}$, where K_{PO_4} — constant of half-saturation with phosphates.

For silicon $f_{Si}\left(q_{Si}\right)=\dfrac{q_{Si}}{q_{Si}+K_{Si}}$, where K_{Si} — constant of half-saturation with silicon.

For nitrogen $f_N\left(q_{NO_3},q_{NO_2},q_{NH_4}\right)=f_N^{(1)}\left(q_{NO_3},q_{NO_2},q_{NH_4}\right)+f_N^{(2)}\left(q_{NH_4}\right)$,

$$f_N^{(1)}(q_{NO_3},q_{NO_2},q_{NH_4})=\frac{(q_{NO_3}+q_{NO_2})\exp(-K_{psi}q_{NH_4})}{K_{NO_3}+(q_{NO_3}+q_{NO_2})},\ f_N^{(2)}(q_{NH_4})=\frac{q_{NH_4}}{K_{NH_4}+q_{NH_4}},$$

where K_{NO_3} — nitrate half-saturation constant;; K_{NH_4} — ammonium half-saturation constant; K_{psi} — inhibition coefficient of ammonia.

Assume that the coefficients included in the expressions for the source functions are positive and independent of time *t*.

For the system (1), an initial-boundary value problem is set in a cylindrical domain G. Let the boundary Σ of the cylindrical region G be a piecewise smooth surface and $\Sigma=\Sigma_H\cup\Sigma_o\cup\sigma$, where Σ_H — the surface of the reservoir bottom, Σ_o — the undisturbed surface of the aquatic medium, σ — lateral (cylindrical) surface.

Let u_n — be the normal component of the velocity vector of the water flow with respect to Σ, vector of the external normal to Σ. For example, for concentrations q_i at the lateral border:

$$q_i=0,\ \text{on}\ \sigma,\ \text{if}\ u_n<0,\ i\in M; \tag{2}$$

$$\frac{\partial q_i}{\partial n}=0,\ \text{on}\ \sigma,\ \text{if}\ u_n\ge 0,\ i\in M; \tag{3}$$

$$\frac{\partial q_i}{\partial z}=0,\ \text{on}\ \Sigma_o\ \text{— water surface},\ i\in M; \tag{4}$$

$$\frac{\partial q_i}{\partial z}=\varepsilon_{1,i}q_i,\ i\in\{F_1,F_2,F_3\},\ \frac{\partial q_i}{\partial z}=\varepsilon_{2,i}q_i;$$

$$i\in\{PO_4,POP,DOP,NO_3,NO_2,NH_4,Si\}\ \text{at the bottom}\ \Sigma_H. \tag{5}$$

Here, $\varepsilon_{1,i},\varepsilon_{2,i}$ — nonnegative constants; $\varepsilon_{1,i}$, $i\in\{F_1,F_2,F_3\}$ take into account the sinking of algae to the bottom and their flooding; $\varepsilon_{2,i}$, $i\in\{PO_4,POP,DOP,NO_3,NO_2,NH_4,Si\}$ take into account the absorption of nutrients by bottom sediments.

For a system of equations, it is required to specify at any time the velocity vector of the water flow, the salinity and temperature field, as well as the initial values of the functions q_i:

$$q_i\left(x,y,z,0\right)=q_{0i}\left(x,y,z\right),\quad \left(x,y,z\right)\in\overline{G},\ t=0,\ i\in M, \tag{6}$$

$$\mathrm{V}\left(x,y,z,0\right)=\mathrm{V}_0\left(x,y,z\right),\ T\left(x,y,z,0\right)=T_0\left(x,y,z\right),\ S\left(x,y,z,0\right)=S_0\left(x,y,z\right).$$

Statistical processing of data from long-term observations on river flows to the sea of Azov. Considerable river runoff relative to the volume of the sea affects significantly the biological and hydrophysical processes occurring in the sea of Azov [13]. A large amount of biogenic substances, including nitrogen, phosphorus and silicon, the main nutrients for phytoplankton, enter the water body from the river flows. In the twentieth century, the main part of the water inflow to the sea of Azov falls on the Don runoff — 63 % (Fig. 2–4)[1].

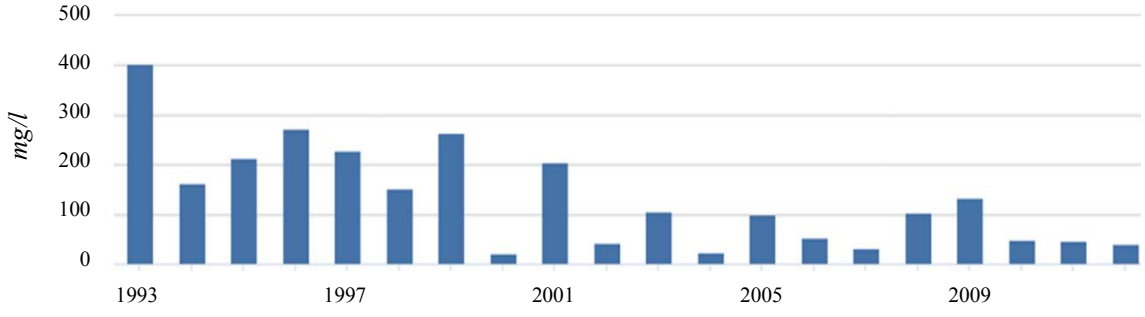

Fig. 2. Series of long-term observations of the Don river runoff (1993–2012): nitrogen concentration (*N-NH*$_4$)

[1] Ecological Atlas. Black and Azov seas. OC “Rosneft”; Arctic scientific center; NIR. Moscow, 2019. 464 p. (In Russ.)

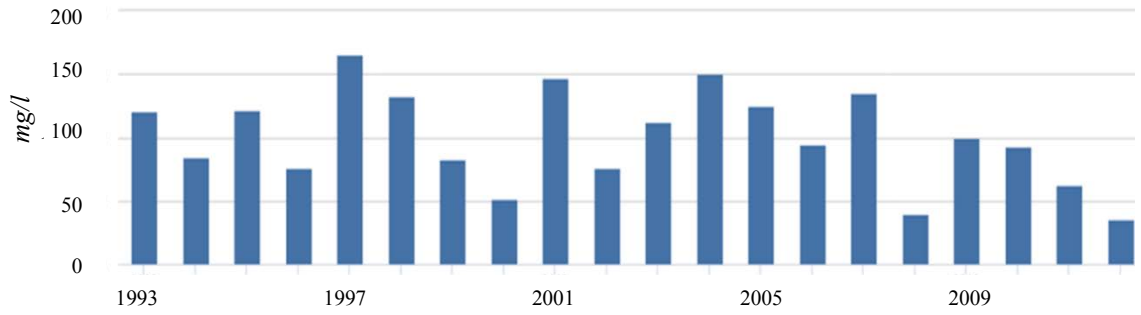

Fig. 3. Series of long-term observations of the Don river runoff (1993–2012): phosphorus concentration (PO_4)

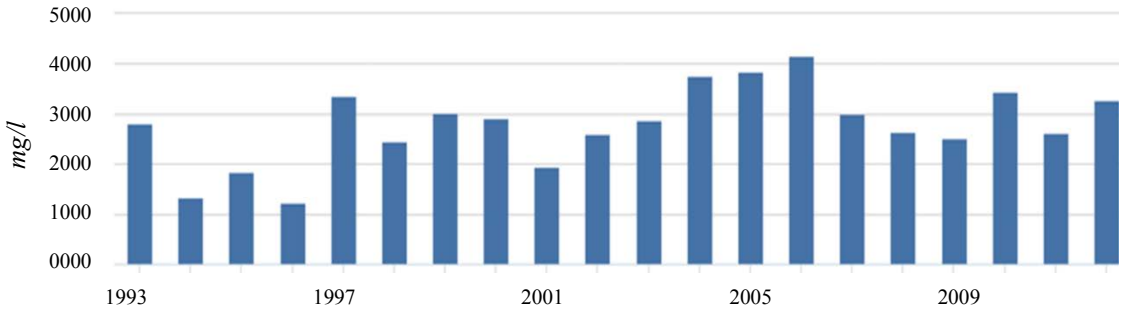

Fig. 4. Series of long-term observations of the Don river runoff (1993–2012): silicon concentration (SiO_4)

Table 2

Results of calculating the statistical parameters of field data

Indicator	***N-NH*$_4$**	***PO*$_4$**	***SiO*$_4$**
Number of values	20	20	20
Maximum value	403.9	165.0	4166.7
Minimum value	20.6	35.4	287.3
Arithmetic average value	132.3	100.1	2648.1
Variance	10362.5	1309.0	868441.9
Standard deviation	101.8	36.2	931.9
Skewness coefficient C_s	0.9	–0.1	–0.7
Kurtosis coefficient C_e	0.2	–0.9	0.2
Coefficient of variation C_v	0.8	0.4	0.4
Ratio C_s/C_v	1.2	–0.3	–2.0
Autocorrelation coefficient	0.3	–0.1	0.1
Neumann ratio	1.1	2.0	1.8

The study on the series of long-term observations of the Don runoff allows us to draw a number of conclusions.

— The nutrient concentrations considered have both positive and negative asymmetries.

— Random variables for nitrogen and silicon are shifted relative to the distribution center, as evidenced by the high value of the asymmetry coefficient.

— Large values of variances and standard deviations were obtained for all biogens.

— The autocorrelation coefficients are small; therefore, a strong nonlinear trend is characteristic of the full-scale data series.

— The variation in all rows is greater than 20 %, so the rows are highly variable.

— For nitrogen, the presence of an autocorrelation relationship according to the Anderson criterion is obvious for the number of values of 20 in the sample, since the autocorrelation coefficient exceeds 0.299 at a confidence level of 5%.

— For nitrogen, the presence of autocorrelation of residues according to the Neumann criterion is obvious at a confidence level of 5% for 20 observations, since the Neumann ratio is less than 1.2.

— Phosphorus and silicon do not show autocorrelation relationships; we reject the hypothesis of autocorrelation of residues.

As a result of statistical analysis of the field data [14], we can conclude that they are highly variable. This is due to the stochastic flow of nutrients from the Don runoff and the significantly changing volume of runoff under the impact of natural and anthropogenic factors. To use field data in the model (1) - (6), it is appropriate to take into account seasonal behavior. Hereafter, when modeling, we will consider the summer period.

Results of numerical experiments. A numerical simulation of the solution to the problem on the dynamics of phytoplankton populations in summer with account for the transformation of phosphorus, nitrogen and silicon forms, is carried out on the example of the sea of Azov. The simulated area corresponds to the physical dimensions of the sea of Azov: length — 355 km, width — 233 km, space step in horizontal directions — 1000 m. Fig. 5 shows a satellite image of the sea of Azov, confirming the compliance of the study results with full-scale data. The image shows clearly the distribution of green and blue-green algae in the Taganrog Bay area, and diatoms — in the central part of the sea.

Fig. 5. Satellite image of the sea of Azov taken with a moderate resolution spectroradiometer (MODIS) on the NASA Aqua satellite on July 31, 2004

В результате вычислительного эксперимента получены сеточные распределения концентраций основных популяций фитопланктона и питательных веществ в Азовском море (рис. 6). Период расчета — 30 суток. Этого достаточно для установления стационарных режимов в задачах динамики фитопланктона.

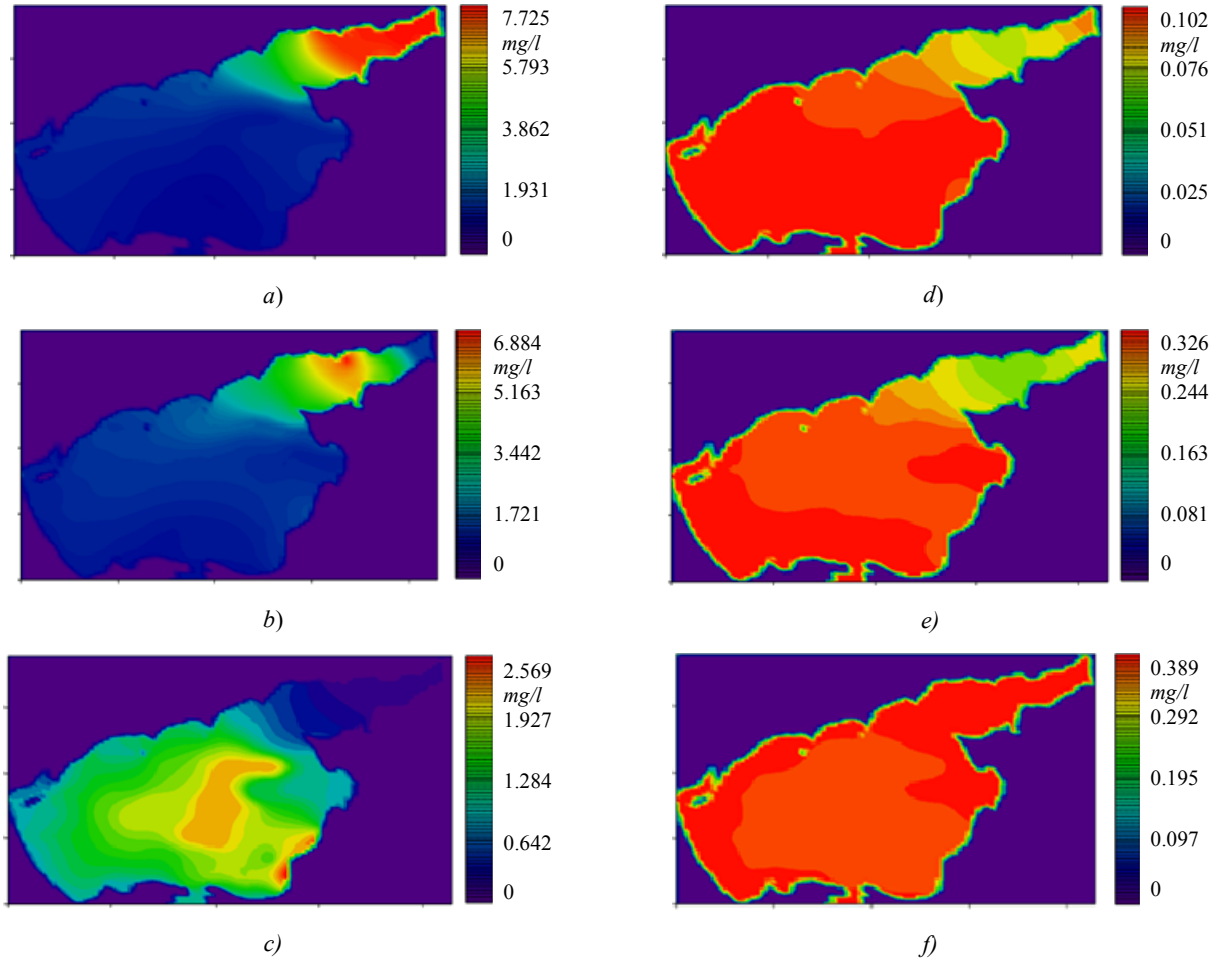

Fig. 6. Distribution of concentrations: *a*) green alga *Chlorella vulgaris*; *b*) blue-green alga *Aphanizomenon flos-aquae*; *c*) diatom *Sceletonema costatum*; *d*) phosphates; *e*) nitrates; *f*) dissolved inorganic silicon

The figures reflect the dynamics of phytoplankton populations, the cycles of phosphorus, nitrogen and silicon. In the process of extinction and decay, phytoplankton releases phosphorus in dissolved and weighed organic forms, then in the process of phosphatofication, they go inorganic — phosphates, which are consumed by phytoplankton. The nitrogen cycle is also described: in the process of vital activity, phytoplankton releases nitrogen in organic form, which decomposes to ammonia. Under the nitrification, ammonium is oxidized to nitrites, and then to nitrates. It is worth noting that phytoplankton consumes all three forms of nitrogen. The consumption and release of silicon by diatoms was stated. Comparison to the simulation results for high-water periods shows that in recent low-water years, the habitats of green and blue-green algae in the Taganrog Bay area have significantly moved (by many kilometers) eastwards, closer to the Don river, a source of fresh water.

Discussion and Conclusions. The paper presents a multi-species mathematical model of the dynamics of phytoplankton populations, form transformations of biogenic substances-phosphorus, nitrogen, and silicon compounds. The model takes into account:

— impact of salinity and temperature on the development of three main types of phytoplankton (green, blue-green and diatomic algae);

— phytoplankton uptake of phosphates and nitrogen forms;

— transition of forms of phosphorus and nitrogen from one to another;

— absorption of silicon by diatoms;

— advective and microturbulent movement of the aquatic environment;

— water flows and sources at the border.

To study the field data, a statistical analysis procedure of long-term series of observations of biogenic substances concentrations (phosphorus, nitrogen, their compounds, etc.) that enter the sea with the Don runoff has been developed and adapted. The statistical analysis of data from long-term observations, in particular hydrochemical indicators of the Don runoff, became the basis for predicting biogeochemical processes with account for the movement of the aquatic environment, the distribution of temperatures and salinity. The of numerical experiment results are consistent with the data of space sensing of the sea of Azov, which confirms the predictive value of the models used and the methods of their numerical implementation. The comparison of the distributions of green and blue-green algae populations in the Taganrog Bay for high-water and low-water periods shows that in recent low-water years, their habitats have significantly moved (by many kilometers) eastwards, closer to the Don river, a source of fresh water.

References

1. Matishov GG, Genyuk SL, Berdnikov SV, et al. Zakonomernosti ekosistemnykh protsessov v Azovskom more [Regularities of ecosystem processes in the sea of Azov]. Moscow: Nauka; 2006. 304 p. (In Russ.)

2. Marchuk GI. Matematicheskoe modelirovanie v probleme okruzhayushchei sredy [Mathematical modeling in the problem of the environment]. Moscow: Nauka; 1982. 319 p. (In Russ.)

3. Sukhinov AI, Nikitina AV, Chistyakov AE, et al. Matematicheskoe modelirovanie uslovii formirovaniya zamorov v melkovodnykh vodoemakh na mnogoprotsessornoi vychislitel'noi sisteme [Mathematical modeling of the formation of suffocation conditions in shallow basins using multiprocessor computing systems]. Numerical Methods and Programming. 2013;14(1):103–112. (In Russ.)

4. Lewis ND, Morozov A, Breckels MN, et al. Multitrophic interactions in the sea: assessing the effect of infochemical-mediated foraging in a 1-D spatial model. Mathematical Modelling of Natural Phenomena. 2013;8(6):25–44.

5. Yakushev EV, Pollehne F, Jost G, et al. Analysis of the water column oxic/anoxic interface in the Black and Baltic seas with a numerical model. Marine Chemistry. 2007;107(3):388–410.

6. Sukhinov AI. Pretsizionnye modeli gidrodinamiki i opyt ikh primeneniya v predskazanii i rekonstruktsii chrezvychainykh situatsii v Azovskom more [Precision models of hydrodynamics and experience of their application in predicting and reconstructing emergency situations in the sea of Azov]. Izvestiya TRTU. 2006;3(58):228–235. (In Russ.)

7. Chistyakov AE, Nikitina AV, Belova YuV, et al. Matematicheskoe modelirovanie gidrodinamicheskikh protsessov melkovodnykh vodoemov s uchetom protsessov perenosa solei i tepla [Mathematical modeling of hydrodynamic processes of shallow water bodies with consideration of salt and heat transfer processes]. In: Proc. VI Int. Conf. and Youth School on Information Technologies and Nanotechnologies (ITNT-2020). Samara: Samara University Publ.; 2020. P. 784–791. (In Russ.)

8. Sukhinov AI, Sukhinov AA. Reconstruction of 2001 ecological disaster in the Azov Sea on the basis of precise hydrophysics models. Parallel Computational Fluid Dynamics 2004. Multidisciplinary Applications. London: Elsevier Science; 2005. P. 231–238. DOI: 10.1016/B978-044452024-1/50030-0

9. Nikitina A, Sukhinov AI, Ugolnitskya GA, et al. Optimal control of sustainable development in biological rehabilitation of the Azov Sea. Mathematical Models and Computer Simulations. 2017;9(1):101–107.

10. Sukhinov AI, Chistyakov AE, Semenyakin AA, et al. Numerical modeling of ecologic situation of the Azov Sea with using schemes of increased order of accuracy on multiprocessor computer system. Computer Research and Modeling. 2016;8(1):151–168.

11. Belova YuV, Atayan AM, Chistyakov AE, et al. Issledovanie statsionarnykh reshenii zadachi dinamiki fitoplanktona s uchetom transformatsii soedinenii fosfora, azota i kremniya [Study on stationary solutions to the problem of phytoplankton dynamics considering transformation of phosphorus, nitrogen and silicon compounds]. Vestnik of DSTU. 2019;19(1):4–12. (In Russ.)

12. Yakushev E, Pakhomova S, Sørenson K, et al. Importance of the different manganese species in the formation of water column redox zones: Observations and modeling. Marine Chemistry. 2009;117:59–70.

13. Sukhinov AI, Nikitina AV, Chistyakov AE, et al. Practical aspects of implementation of the parallel algorithm for solving problem of ctenophore population interaction in the Azov Sea. Bulletin of the South Ural State University. (Computational Mathematics and Software Engineering). 2018;7(3):31–54. DOI: https://doi.org/10.14529/cmse180303

14. Kovalenko SN. Rezul'taty statisticheskoi obrabotki naturnoi informatsii pri biogennom zagryaznenii malykh rek, prinimayushchikh stoki s melioriruemykh sel'skokhozyaistvennykh territorii [Results of statistic processing of natural information when studying biogenic pollution of small rivers receiving runoffs from reclaimed agricultural areas]. Prirodoobustrojstvo. 2009;4:73–77. (In Russ.)

Submitted 11.05.2020
Scheduled in the issue 31.07.2020

About the Authors

Sukhinov, Alexander I., Corresponding Member of RAS, Head of the Mathematics and Computer Sciences Department, Don State Technical University (1, Gagarin sq., Rostov-on-Don, 344003, RF), Dr.Sci. (Phys.-Math.), professor, ResearcherID: I-1091-2016, ScopusID: 8573972700, ORCID: https://orcid.org/0000-0002-5875-1523, sukhinov@gmail.com.

Belova, Yuliya V., teaching assistant of the Mathematics and Computer Sciences Department, Don State Technical University (1, Gagarin sq., Rostov-on-Don, 344003, RF), ResearcherID: L-7893-2016, ScopusID: 57196457293, ORCID: https://orcid.org/0000-0002-2639-7451, yvbelova@yandex.ru.

Nikitina, Alla V., Leading researcher, Supercomputers and Neurocomputers Research Center (106, per. Italyanskiy, Taganrog, Rostov Region, 347900, RF), ResearcherID: H-4941-2017, ScopusID: 57190226179, ORCID: https://orcid.org/0000-0001-7257-962X, nikitina.vm@gmail.com.

Atayan, Asya M., teaching assistant of the Computer and Automated Systems Software Department, Don State Technical University (1, Gagarin sq., Rostov-on-Don, 344003, RF), ScopusID: 57213156282, ORCID: https://orcid.org/0000-0003-4629-1002, atayan24@yandex.ru.

Claimed contributorship

A. I. Sukhinov: academic advising; analysis of the research results; the text revision; correction of the conclusions. Yu. V. Belova: basic concept formulation; research objective and tasks setting; conducting a computational experiment; text preparation. A. V. Nikitina: text preparation; formulation of conclusions. A. M. Atayan: conducting a computational experiment; text preparation.

All authors have read and approved the final manuscript.